Functional Analysis of Plant Mei2-like Proteins

A Thesis Presented in Partial Fulfilment of the Requirements for the Degree of Master of Science in Biochemistry

at

Massey University
Palmerston North, New Zealand

Susanna Chui-Shan Leung
2003

Thesis Abstract

Molecular techniques were used to analyse the function of a novel class of RNA-binding proteins in plants, termed Mei2-like. The biochemical function of this class of proteins is unclear. Although the conserved presence of three RNA recognition motifs (RRMs) in all members of the family suggests the importance of an RNA binding activity, the precise biochemical mechanism by which these proteins act is unknown. Genetic and molecular analyses of the founding member of the family, *Schizosaccharomyces pombe* Mei2p, provide of a conceptual framework for the studies of the plant Mei2-like proteins presented here. Therefore, the aims of this thesis were to 1) study the cellular localisation of Mei2p in plant cells, and 2) deduce the functions of plant *Mei2-like* genes by identifying the protein(s) that physically interact(s) with Mei2-like proteins.

Transient expression of GFP-fused Mei2p in onion epidermal cells was performed to show that Mei2p localised into the nucleus in the presence of meiRNA, a non-coding mRNA. Thus plants seem to share the capacity with *S. pombe* for meiRNA-dependent nuclear localisation of Mei2p. Moreover, intracellular localisation of one of the plant Mei2-like proteins, TERMINAL EAR-Like 2 (TEL2), was studied in onion epidermal cells. The GFP-fused TEL2 localised into the nucleus without co-expression of any special RNA, suggesting that either some RNA species that assist nuclear localisation of TEL2 are already present in onion epidermal cells, or the mechanism of intracellular localisation of TEL2 is different from Mei2p.

The yeast two-hybrid system was utilised to identify protein interactors with TEL2. Six proteins were identified, including the well-studied KORRIGAN

(KOR) protein. Based on the proteins identified, speculation is offered on how these proteins interact with TEL2. Since TEL genes are expressed in the central zone (CZ) of meristems, and mitotic activity of cells in the CZ is low, TEL2 may be involved in controlling cell division in the CZ *via* interactions with these proteins.

Acknowledgements

I would like to thank the following people who helped in this MSc work:

My supervisor, Dr. Bruce Veit, for the guidance and good practices in the lab. Also for sharing knowledge on plant development, molecular biology and critical advice on this thesis.

A. Prof. Michael McManus, for helping on preparing on this thesis and knowledge on protein work.

Dr. Kim Richardson, for assistance on particle bombardment. Dr. Albrecht von Arnim, for a good protocol of particle bombardment. Dr. Helal Ansari, for assistance on the images of the epi-fluorescece microscope. Vernon Trainor, for general help and sharing of experiences in the lab. Chunhong Chen, for experiences on yeast two-hybrid system. Liz Nickless, for assistance on the laser confocal microscope.

People in Bruce's lab: Dan Jeffares, Nena Alvarez, Carmal Gilman, Mo Min, Robert Baker, Suzanne Lambie, and Richard Scott for sharing your skills on molecular biology work.

AgResearch Grasslands Research Centre, for providing an excellence environment for research.

Mathew Chan, for suggestions on my manuscript and encouragement.

My family: my parents, my grandmother and my brother, for love, concern and support. Thank you for being there with me and support me on difficult times.

This research is supported by the Marsden Fund.

Contents

Thesis Abstract i

Acknowledgment iii

List of Figures xii

List of Tables xiv

Gene Nomenclature xv

Abbreviations xvi

Chapter 1 Introduction: Biological and Biochemical Functions of Plant Mei2-Like Proteins

1.1 Overview 1

1.2 Biological significance of RNA-binding proteins 2

1.3 Schizosaccharomyces pombe Mei2 protein 4

1.4 Introduction of Plant Mei2-like genes 7

1.4.1 *Zea mays terminal ear 1* gene 8

1.4.2 The family of *Mei2-like* genes in *Arabidopsis thaliana* 11

1.5 Apical Meristems of Plants 14

1.5.1 Root apical meristem (RAM) 14

1.5.2 Shoot apical meristem (SAM) 15

1.5.3 Surgical studies of the SAM 16

1.5.4 The meristeme d'attente concept and clonal analysis 17

1.6 Genetic Analysis in the SAM of Arabidopsis thaliana 19

1.6.1 *WUSCHEL* and *CLAVATA* 19

1.6.2 *SHOOT MERISTEMLESS* 22

1.6.3 The others genes involved in the development of the meristems 24

1.7 Aims and Hypothesis 26

Chapter 2 General Methods

2.1 Overview 27

2.2 Escherichia coli (E. coli) methods 28

2.2.1 Growth of *E. coli* 28

2.2.2 Preparing of competent cells of *E.coli* 28

2.2.3 Transformation of competent *E.coli DH5α* cells 29

2.2.4 Preparing the electrocompetent *E. coli DH5α* 29

2.2.5 Electroporation 30

2.2.6 Qiaprep Spin Miniprep Kit (Qiagen) 30

2.2.7 Plasmid DNA extraction *via* alkaline lysis/PEG 30

2.2.8 Plasmid isolation using the rapid boiling method (Sambrook *et al.*, 1989) 31

2.2.9 Plasmid isolation by the phenol-chloroform method 32

2.3 General DNA Methods 33

2.3.1 Agarose gel electrophoresis of DNA 33

2.3.2 Quantification of DNA 33

2.3.3 Restriction digestion of plasmid DNA 34

2.3.4 Construction of vectors 35

2.3.5 Polymerase chain reaction (PCR) 36

2.3.6 Sequencing of the constructs 37

2.4 General RNA Methods 38

2.4.1 RNA extraction from *A. thaliana* seedlings 38

2.4.2 Reverse-transcription polymerase chain reaction (RT-PCR) 38

2.5 General Protein Methods 39

2.5.1 Protein extract from *A. thaliana* seedlings 39

2.5.2 Sodium dodecyl sulphate-polyacrylamide gel electrophoresis (SDS-PAGE) 39

2.5.3 Western blot for GFP and GFP-fusion proteins 40

2.6 General Agrobacterium tumefaciens methods 40

2.6.1 Transformation of *A. tumefaciens* by freeze/thaw method 41

2.6.2 Miniprep of plasmid DNA from *A. tumefaciens* 41

2.7 General Methods for the manipulation Arabidopsis thaliana 42

2.7.1 Growth of *Arabidopsis thaliana* 42

2.7.2 Transformation of *A. thaliana* – Floral dip method 42

2.7.3 Screening seeds from transgenic plants 43

2.8 Transient expression in onion epidermal cells 43

2.8.1 Preparation of DNA-coated microcarriers (Sanford *et al.*, 1992) 43

2.8.2 Preparation of onion epidermal cells 44

2.8.3 Transient biolistic assays were performed using the methods of Varagona *et al.*, 1992 and Scott *et al.*, 1999 44

2.9 General Methods on Saccharomyces cerevisiae and the yeast two-hybrid assay 45

2.9.1 Growth of *Saccharomyces cerevisiae* 45

2.9.2 Transformation of yeast with bait plasmid containing

a *TRP1* marker 46

2.9.3 Yeast miniprep methods 46

2.9.4 Conversion of yeast two-hybrid library 47

2.9.5 cDNA library transformation for two-hybrid screen (Agatep *et al.*, 1998) 48

2.9.6 Rescuing the prey vectors from yeast and verifying the constructs 49

Chapter 3 Cellular Localisation of Mei2p in Plant Cells

3.1 Overview 50

3.2 Introduction 51

3.2.1 Subcellular localistion of *S. pombe* Mei2p using GFP as a reporter 51

3.3 Methods 53

3.3.1 Brief introduction to the biolistic particle delivery system 53

3.3.2 Construction of vectors pMGB7, pGMA393 and pMRA7 for transient expression 54

3.4 Results 56

3.4.1 Version of *gfp* used for transient and stable expression 56

3.4.2 Optimisation of transient expression of GFP and its fusion proteins in onion epidermal cells 57

3.4.3 Expression of *mei2::gfp*, *gfp::mei2* and *TEL2::gfp* in onion epidermis 60

3.4.4 Localisation of GFP-fusion of Mei2p in onion

epidermal cells 61

3.4.5 Localisation of GFP-fusion of TEL2 62

3.4.6 Phenotypes of stable expression of GFP-fused Mei2p in plants 68

3.4.7 Transcriptional and translational analysis of stable expression of *35S::mei2::gfp* plants 71

3.4.8 Analysis of *TEL1* expression in *Arabidopsis thaliana* 74

3.5 Discussion 76

3.5.1 Heterologous systems expressing the GFP-fused Mei2p 76

3.5.2 Importance of meiRNA in the GFP-fusion of Mei2p in onion epidermis 77

3.5.3 Localisation of TEL2::GFP and promoter analysis of *TEL1* 78

3.5.4 Stable expression of *35S::mei2::gfp* 79

3.6 Conclusion 83

Chapter 4 Analysis of Protein-Protein Interactions Involving TEL2 Using the Yeast Two-hybrid System

4.1 Overview 84

4.2 Introduction 85

4.2.1 Brief introduction to the yeast two-hybrid system 85

4.3 Methods 88

4.4 Results 90

4.4.1 Bait vectors used in yeast two-hybrid system 90

4.4.2 Checking leaky *HIS3* expression in

bait-transformed PJ69-4α cells 93

4.4.3 Transformation of CD4-22 cDNA library into bait-transformed PJ69-4α 96

4.4.4 Yeast two-hybrid screen 98

4.4.5 Factors affecting transformation of CD4-22 cDNA library into pAS2.1-TEL2ΔN transformed PJ69-4α 103

4.5 Discussion 107

4.5.1 Full length and truncation of *TEL2* affecting growth of PJ69-4α 107

4.5.2 Protein interactions with the RRM3 domain of TEL2 108

(a) KORRIGAN 108

(b) EF-hand calcium-binding protein-like 109

(c) the protein containing lipase domain 111

(d) Ferredoxin precursor isolog 112

(e) Cyanase 112

4.5.3 Speculation of function of TEL2 114

4.5.4 Problems and limitation of the yeast the two-hybrid assay 116

4.6 Conclusion 119

Chapter 5 Summary

5.1 Summary of results 121

5.2 Future directions 123

References 125

Appendices

Appendix 1 Genotypes of yeast strains 145

Appendix 2 Solution pages 146

Appendix 3 Lists of suppliers 154

List of Figures

Figure 1.1 Structure of RRM 4

Figure 1.2 Localisation of GFP-tagged Mei2p expressed in cultured mammalian cells 5

Figure 1.3 Analysis of *te1* mutant phenotype and *te1* expression 9

Figure 1.4 Alignment of maize TE1 protein and *S. pombe* Mei2p 11

Figure 1.5 A maximum parsimony phylogenetic tree showing the relationships of all the complete *Mei2-like* genes 12

Figure 1.6 Histology of the shoot apical meristem (SAM) 16

Figure 1.7 The fate map of the maize meristem obtained by using clonal analysis 19

Figure 1.8 Regulatory loop between *WUS* and *CLV3* 21

Figure 2.1 λ-HindIII ladder 34

Figure 3.1 PDS-1000/He biolistic system 53

Figure 3.2 Constructs used in transient expression assays 55

Figure 3.3 Localisation of GFP in onion epidermal cells after different incubation times after bombardment 59

Figure 3.4 Localisation of Mei2p::GFP in the presence of meiRNA in onion epidermal cells 64

Figure 3.5 Localisation of GFP::Mei2p in the presence of meiRNA in onion epidermal cells 65

Figure 3.6 Localisation of TEL2::GFP in onion epidermal cells 66

Figure 3.7 Localisation of TEL2::GFP in onion epidermal cells by incubating the cells at low temperature 67

Figure 3.8 Detection of fluorescence signal in seedlings transformed with GFP or GFP-fused Mei2p of two weeks-old 70

Figure 3.9 Phenotypes of *35S::mei2::gfp* two week-old seedlings 70

Figure 3.10 Transcriptional and translational analysis of *35S::mei2::GFP* plants 73

Figure 3.11 Analysis of *TEL1* promoter 75

Figure 4.1 Schematic diagram to show the interaction between two fusion proteins (DB-X and AD-Y) in the yeast two hybrid system 87

Figure 4.2 Flow diagram to the yeast two-hybrid procedure 88

Figure 4.3 Plasmid vectors used in the yeast two-hybrid system 89

Figure 4.4 Bait vectors used in the yeast two-hybrid system 91

Figure 4.5 Growth of PJ69-4α cells transformed with different bait vectors 92

Figure 4.6 Growth of bait vector-transformed PJ69-4α cells on different selective media 95

Figure 4.7 Colonies from the yeast two-hybrid screen grown on X-gal indication plates 102

List of Tables

Table 2.1 Filter used in the epi-fluorescence examination 45

Table 3.1 Effects of distance between target tissue and microcarriers on expression of *gfp* (pAVA393) in onion epidermal cells 58

Table 3.2 Effects of incubation time on expression of *gfp* (pAVA393) in onion epidermal cells 59

Table 3.3 Number of onion epidermal cells expressing GFP and GFP-fusion proteins in transient expression assays 61

Table 4.1 Levels of 3-amino-1,2,4-triazol (3-AT) required to suppress leaky *HIS3* expression in PJ69-4α cells transformed with different bait vectors 96

Table 4.2 Transformation efficiency of the CD4-22 cDNA library into bait vector-transformed PJ69-4α cells 97

Table 4.3 Proteins identified in yeast two-hybrid screens 100

Table 4.4 Length of heat shock time affecting transformation efficiency of two strains of yeast 103

Table 4.5 Length of heat shock time for transformation of CD4-22 cDNA library into PJ69-4α 104

Table 4.6 Maintenance of different bait vectors in PJ69-4α 105

Table 4.7 Maintenance of the empty bait vector, pAS2.1, in various yeast strains 106

Gene nomenclature

Arabidopsis thaliana

GENES are capitalised and italicised

PROTEINS are capitalised

gene mutants are in lower case and italicised

Maize

genes are in lower case and italicised

PROTEINS are capitalised

gene mutants are named after the genes, in lower case and italicised

Fission yeast, *Schizosaccharomyces pombe*

genes are in lower case and italicised

Proteins are writtern with the first letter capitalised, and "p" is added after the name of gene, e.g Protein encodes by *mei2* is called Mei2p

Budding yeast, *Saccharomyces cerevisiae*

GENES are capitalised and italicised

gene mutants are in lower case and italicised

Abbreviations

3-AT	3-amino triaziol
BCIP	x-phophate/5-bromo-chloro-indoyl-phosphate
CZ	central zone
EDTA	disodium ethylene diamine tetra acetate
mg	milligram
μg	microgram
ng	nanogram
NBT	4 Nitroblue tetrazolium chloride
NaOAc	sodium acetate
PBS	phosphate buffer saline
PCR	polymerase chain reaction
PZ	peripheral zone
RAM	root apical meristem
RRM	RNA recognition motif
RT-PCR	reverse transcription polymerase chain reaction
RZ	rib zone
SAM	shoot apical meristem
SDS	sodium dedecyl sulphate
TEL	terminal ear 1-like
X-gal	5-bromo-4-chloro-3-indolyl-β-D-galactopyranoside

CHAPTER 1 INTRODUCTION: BIOLOGICAL AND BIOCHEMICAL FUNCTIONS OF PLANT Mei2-LIKE PROTEINS

1.1 Overview

This chapter reviews the diverse function of RNA-binding proteins in the regulation of gene expression. In plants, a family of RNA-binding proteins, termed Mei2-like, may be involved in controlling cell fate. The first member, *Terminal ear 1* (*te1*) functions in maize to limit leaf initiation. Moreover, seven additional members are found in *Arabidopsis thaliana*, but their function in *A. thaliana* is not clear. Genetic and molecular studies of one of the founding member, *Schizosaccharomyces pombe mei2*, are also reviewed in this chapter. Since the *Mei2-like* genes are expressed in the apical meristem, some background information, including the structure, organisation, and genetic analysis of the shoot apical meristem (SAM) will also be provided.

1.2 Biological significance of RNA-binding proteins

In eukaryotes, RNA-binding proteins play important roles in gene expression *via* RNA processing at the post-transcriptional stage. This includes splicing, polyadenylation, transport, localisation and stabilisation. Different types of RNA binding and recognition motifs are found in the RNA-binding proteins, such as the arginine-rich, RGG box (Kiledjian and Dreyfuss, 1992), and the K homology (KH) motif (reviewed by Burd and Dreyfuss, 1994), but the most widely found RNA-binding motifs are the RNA recognition motifs (RRMs).

The following examples illustrate some of the diverse functions of RNA-binding proteins. The *Drosophila* Sex-lethal (Sxl) protein is involved in regulation of sex determination by modulating pre-mRNA splicing and mRNA translation of its own mRNA as well as a downstream *transformer* (*tra*) pre-mRNA. It contains two RRMs, and binds a specific uridine-rich polypyrimidine tract of 3' splice sites in pre-mRNA (Handa *et al.*, 1999). Moreover, RRM also mediates protein-protein interactions that affect specificity and stabilisation in RNA binding (Samuels *et al.*, 1998). For example, the HIV-1 Rev protein regulates the expression of HIV-1 mRNA by exporting incomplete spliced HIV-1 mRNA out of the nucleus (Malim *et al.*, 1989). In humans, the cleavage-polyadenylation specific factor (CPSF) interacts with the cleavage specificity factor (CstF) to participate in polyadenylation of pre-mRNA in a sequence-specific manner (Murthy and Manley, 1992). Polyadenylation can stabilise mRNA and prevent its degradation (Sachs and Wahle, 1993).

A large number of RRM proteins contain one to four RNA-binding motifs (Shamoo *et al.*, 1993) that exhibit RNA binding properties in both specific and

non-specific ways. For example, in the genome of *Arabidopsis thaliana*, 0.8% of genes encode RRM-containing proteins (The *Arabidopsis* Genome Initiative, 2000). The flexible linkers that connect the RRMs may play a critical role in determining the binding affinity for specific RNA sequences. By surveying a range of RRM-containing proteins, the linker sequences were determined to be variable in length, and this, in turn, affects the binding of specific RNAs (Shamoo *et al.*, 1995). The three dimensional structure of RRM was analysed by X-ray crystallography (Nagai *et al.*, 1990) and NMR techniques (Hoffman *et al.*, 1991). Structural analysis shows that the RRM contains four β strands and two α-helices which form an anti-parallel β sheet packed against two perpendicular α-helices (Figure 1.1). The structure is conserved across species (Dreyfuss *et al.*, 1993). It was also found that charged residues and the side chains of aromatic residues interact with RNAs *via* ring-stacking interactions and hydrogen bonds (Oubridge *et al.*, 1994., 1993; Allain *et al.*, 2000; Kranz *et al.*, 1993; Macknight *et al.*, 1997; Nagata *et al.*, 1999). Moreover, the solvent-exposed residues in and near the β-sheet may contribute to RNA binding (Birney *et al.*, 1993; Burd and Dreyfuss, 1994). Apart from RRM domains, the KH domain is another wide spread motif in RNA-binding proteins, and 26 KH domain-containing proteins have been identified in *A. thaliana* (Lorkovic and Brata, 2002).

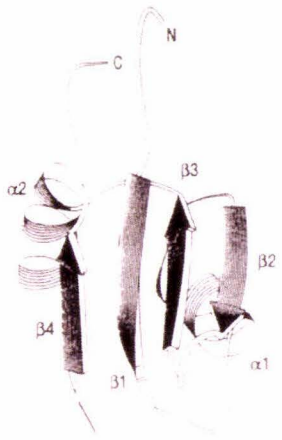

Figure 1.1 Structure of RRM. Each arrow represents a β-strand and the curled ribbons an α-helix. Four β-strands form an anti-parallel β-sheet flanked by 2 α-helices.

1.3 *Schizosaccharomyces pombe* Mei2 protein

In the late 1980s, a gene, *mei2*, which is essential for meiosis in *Schizosaccharomyces pombe*, began to be investigated (Shimoda *et al.*, 1987). Subsequent cloning of *mei2* revealed that the gene encodes an RNA-binding protein of 750 amino acids (Watanabe and Yamamoto, 1994) which contains three RRMs (Yamamoto *et al.*, 1997).

The first two RRMs of Mei2p resemble those of splicesomal proteins, suggesting that Mei2p may be involved in RNA splicing. One of the possible substrates of Mei2p is unspliced *mes1* mRNA, while *mes1* is an essential gene for meiosis II in *S. pombe* (Yamamoto, 1996). More noteworthy is the binding by the RRM3 domain of Mei2p to a non-translated, polyadenylated RNA species, called meiRNA. meiRNA is encoded by the *sme2* locus in *S. pombe*, and is about 0.5 kb in size (Watanabe and Yamamoto, 1994). Binding of meiRNA somehow assists accumulation of Mei2p in the nucleus, as disruption of RRM3 of Mei2p prevents meiRNA binding and accumulation

of Mei2p in the nucleus (Yamashita *et al.*, 1998). This mechanism of RNA-assisted nuclear localisation appears conserved in mammalian COS-7 cells as shown in Figure 1.2 (Yamashita *et al.*, 1998).

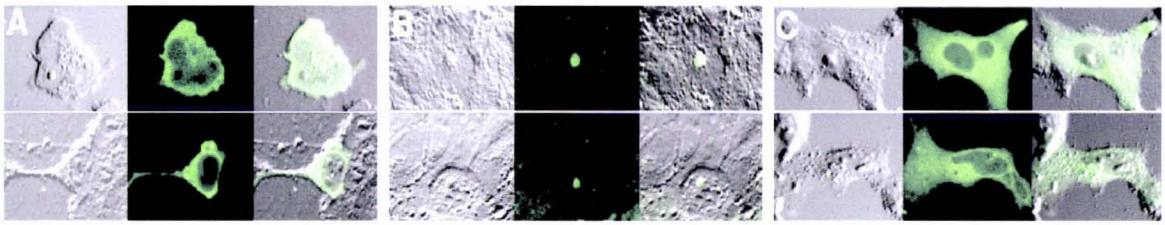

Figure 1.2 Localisation of GFP-tagged Mei2p expressed in cultured mammalian cells. COS-7 cells expressed Mei2p-GFP alone (**A**), co-expression of Mei2p-GFP and meiRNA (**B**), and the disrupted RRM3 of Mei2p in the presence of meiRNA (**C**). Nuclear localisation of GFP-tagged Mei2p only observed in the presence of meiRNA and intact RRM3 of Mei2p, suggesting that binding of meiRNA is essential for Mei2p assembly in the nucleus. The left panels, Nomarski images; the middle panels, GFP fluorescence; the right panels, the merged images. (Source: Yamashita *et al.*, 1998)

The RNA-assisted nuclear transportation of Mei2p was reviewed by Ohno and Mattaj (1999). They proposed four models for this process:

1. meiRNA may associate with other proteins that transport Mei2p from the cytoplasm to the nucleus;
2. binding of meiRNA to Mei2p causes the exposure of the nuclear localisation signal (NLS) of Mei2p which allows Mei2p translocation into the nucleus;
3. Mei2p is imported by the importin-mediated mechanism, and meiRNA assists Mei2p release from the importin in the nucleus;
4. Mei2p is a shuttle protein which moves between the cytoplasm and the nucleus, and binding of meiRNA prevents export of Mei2p from the nucleus.

Recent studies have shown that Mei2p is likely to behave like a shuttle protein that moves backward and forward between the cytoplasm and the nucleus (Sato *et al.*, 2001). When the cells were exposed to a potent inhibitor of exportin 1, leptomycin B (LMB), Mei2p accumulated in the nucleus without meiRNA. This result suggests that meiRNA is not required for the nuclear translocation of Mei2p. However, meiRNA appears necessary for the assembly of Mei2p into a non-translocatable form in the nucleus (Sato *et al.*, 2001).

mei2 is activated by nitrogen starvation and inactivated by cAMP, suggesting that cAMP plays a critical role as a mediating signal for induction of meiosis by nitrogen starvation (Watanabe *et al.*, 1988). *mei2* is also required for pre-meiotic DNA synthesis and initiation of meiosis (Shimoda *et al.*, 1987;

Watanabe and Yamamoto, 1994). Normally, binding of meiRNA to Mei2p is essential for meiosis but not for premeiotic DNA synthesis. However, retention of RNA binding activity is still required for premeiotic DNA synthesis, suggesting that other RNA species may be essential for this process (Watanabe and Yamamoto, 1994).

In addition to the requirement of meiRNA, Mei2p is also sensitive to phosphorylation. Two phosphorylation sites (Ser 438 and Thr 527) between RRM2 and RRM3 of Mei2p are substrates for the Pat1[1] kinase (Shimoda *et al.*, 1987; Watanabe *et al.*, 1997). Phosphorylated Mei2p is inactive and remains in the cytoplasm, causing degradation of Mei2p *via* an ubiquitin-proteasome pathway (Kitamura *et al.*, 2001).

1.4 Introduction of Plant *Mei2-like* genes

Unlike the single *mei2* gene in *S. pombe*, plants appear to have several *Mei2-like* genes. The first member genetically analysed was the *terminal ear 1* (*te1*) of maize. Recent work in *A. thaliana* has revealed additional gene members of this gene family, some of which may have similar functions to *te1*. The analysis of these plant *Mei2-like* genes is described below.

[1] Pat1 kinase is also known as ran1$^+$ protein kinase.

1.4.1 Zea mays terminal ear 1 gene

The sites where leaf primordia arise determine leaf arrangement, or phyllotaxy. The phenotype of the *terminal ear* mutant of maize (*Zea mays L.*) was first described by Matthews *et al.* (1974). The mutants show an irregular pattern of shorter internodes and leaf arrangement, and an abnormal tassel. Shorter internodes of *te1* mutants caused vegetative leaves to overlap, thus enclosing the tassel within overlapping leaves (Figure 1.3 A). The tassel, the male inflorescence of maize, was less branched, or had become feminised in *te1* mutants (Veit *et al.*, 1998; Alvarez, 2002). Generally, the *te1* mutant was shorter than the wild-type plants, with the shorter internodes interspersed with relatively normal internodes along the stem and the number of internodes increased (Veit *et al.*, 1998). Shorter internodes were highly curved (Figure 1.3 B); and on these curved sides of the internodes, the cells were longer, larger and disorganised, suggesting that the cell division pattern is affected in *te1* mutants (Alvarez, 2002). Moreover, the arrangement of leaves was affected with irregular deviations from the normal alternate phyllotaxy, and leaves had double midribs (Figure 1.3 C). The leaf laminas of *te1* mutant were narrower, and more perpendicular with respect to the shoot when compared with wild-type plants.

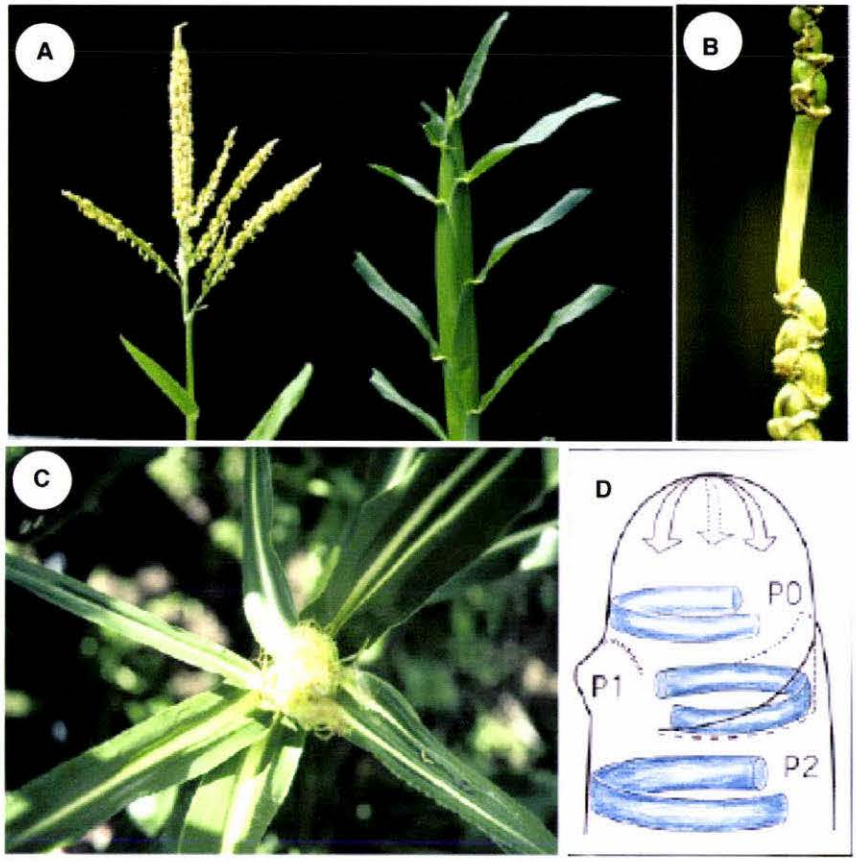

Figure 1.3 Analysis of *te1* mutant phenotype and *te1* expression. (**A**) Comparison of wild-type plant (left) and *te1* mutant (right): the tassel of *te1* mutant is enclosed by overlapping leaves. (**B**) A series of short and curved internodes with a normal internode spread along the stalk of *te1* mutant. (**C**) Top view of *te1* mutant shows irregular deviation from the normal alternate phyllotaxy and leaves with double midribs. (**D**) Schematic diagram shows the expression of *te1* in the shoot apex. *te1* expression is in semi-circular bands opposite to the leaf primordia. (Source: Veit *et al.*, 1998).

Microscope analysis has shown that the vegetative shoot apex of *te1* mutants are smaller and leaf initiation occurs higher upon the apical dome (Alvarez, 2002). *In situ* hybridisation showed that the *te1* gene is expressed opposite to the positions of leaf primordia. Thus *te1* transcripts accumulate in semi-circular bands with gaps over sites where leaves initiate (Figure 1.3 D) (Veit *et al.*, 1998), suggesting that the maize *te1* gene inhibits leaf initiation. Loss of *te1* function results in precocious leaf formation. Furthermore, in the *te1* mutant, a greater number of cells involved in leaf initiation in the vegetative

shoot apex leads to fewer cells available for organogenesis, and this contributes to shorter and irregular internode formation (Veit *et al.*, 1998; Alvarez, 2002).

The predicted TE1 protein showed that *te1* encodes a protein containing three RNA recognition motifs (RRMs): RRM1, RRM2 and RRM3 (Veit *et al.*, 1998), and is highly similar to *Schizosaccharomyces pombe* Mei2 protein (Mei2p), which is also an RNA-binding protein containing three RRMs (Figure 1.4) (Watanabe *et al.*, 1997). Alignment of these two proteins showed that the highest similarity is found in the RRMs, especially RRM3, that has 40% identity (Veit *et al.*, 1998). The Mei2p of *S. pombe* binds a special non-translating RNA, meiRNA at RRM3, to induce nuclear localisation (Yamashita *et al.*, 1998). The conservation of the third RRM in these proteins suggests that TE1 acts as an RNA-binding protein and the mechanism by which TE1 acts may be similar to Mei2p.

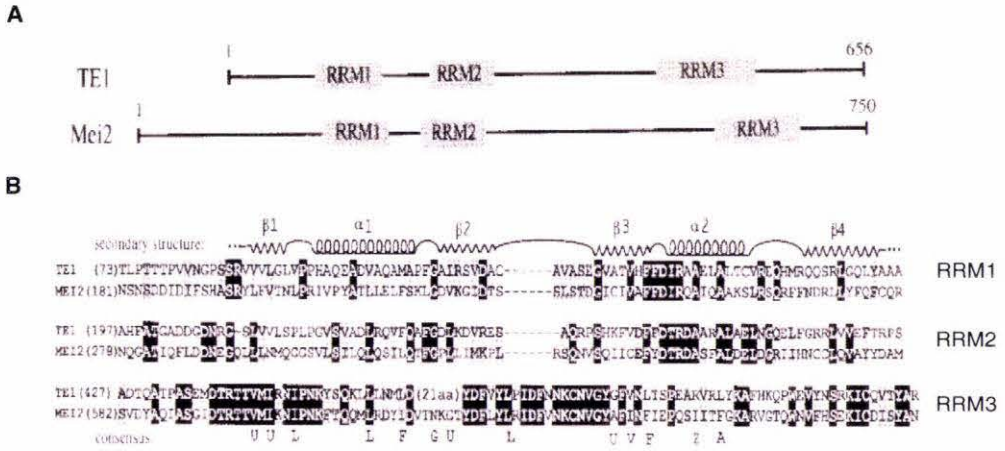

Figure 1.4 Alignment of maize TE1 protein and *S. pombe* Mei2p. (**A**) Both TE1 and Mei2p carry three RRMs. (**B**) High similarities are found in RRMs between TE1 and Mei2p, especially RRM3, which binds to meiRNA in Mei2p. (Source: Veit *et al.*, 1998)

1.4.2 The family of Mei2-like genes in Arabidopsis thaliana

In *A. thaliana*, there are seven genes that show sequence similarity to *mei2* of *S. pombe*, and they are referred to as *Mei2-like* genes (Jeffares, 2001). The highly conserved and unusual RRM3 is the distinctive hallmark of the family (Figure 1.4). All of the genes in this *Mei2-like* family contain three RRMs, and can be grouped into three classes:

1) *TERMINAL EAR 1-Like*: *TEL1* and *TEL2* are two genes present in *A. thaliana* which are most similar to *te1* of Z. *mays*.
2) *A. thaliana Mei2-like*: Five genes are found in *A. thaliana* (*AML1*, *AML2*, *AML3*, *AML4* and *AML5*) which are similar to both *mei2* of S. *pombe* and *te1* of *Z. mays*.
3) *S. pombe mei2*: An outgroup that is not found in plants (Figure 1.5; Jeffares, 2001).

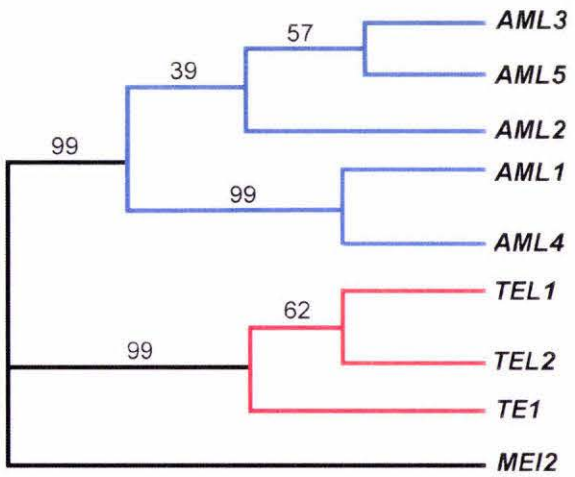

Figure 1.5 A maximum parsimony phylogenetic tree showing the relationships of all the complete *Mei2-like* genes. The *TEL* group (*te1, TEL1* and *TEL2*) and the *AML* group are from *A. thaliana* while *mei2* is from *S. pombe*. Numbers indicate support for clades from 1000 bootstrap replicates. (Jeffares, 2001)

To determine the expression pattern of *Mei2-like* genes in plants, *in situ* hybridisation studies have revealed that both *TEL1* and *TEL2* are expressed strongly in the central zones of the embryonic and vegetative shoot apical meristems (SAMs). *TEL1* is also expressed in the quiescent zone of embryonic and vegetative root apical meristems (RAMs). In addition to the SAM, *Mei2-like* genes are also expressed in the inflorescence and floral meristems, suggesting that *TEL* genes may be involved in defining and/or maintaining stem cells in meristems (Alvarez, 2002). Reverse genetics is another approach that has been used to analyse plant *Mei2-like* genes. Single *tel1* and single *tel2* mutants did not have significant phenotypes, suggesting that *TEL1* and *TEL2* function redundantly in the SAM. This is also supported by the results from *in situ* hybridisation which show that *TEL1* and *TEL2* expression patterns in the SAM overlap (Alvarez, 2002). However, *tel1 tel2* double mutants exhibit the following phenotypes suggesting that *TEL1* and *TEL2* may be involved in the development of the apical meristems:

1) the root/callus phenotype: mass of roots emerge from a seed but the growth is ceased;
2) the immature embryo phenotype: the seedlings are arrested at the heart stage while some of them are arrested at the torpendo stage
3) the cone-shaped phenotype: the seedlings form normal cotyledons, but with either no SAM or fused SAMs;
4) the shoot phenotype: the seedlings have a single cotyledon with multiple shoots growing out.

The seedlings of *tel1 tel2* mutants did not have true roots, except those displaying the root/callus phenotype (Alvarez, 2002).

Although the expression patterns and mutants of *TEL* genes have been studied, the biochemical mechanisms and functions of plant *Mei2-like* genes remain unclear. In *S. pombe*, *mei2* is required in both premeiotic DNA synthesis and meiosis (see section 1.3). As mentioned before, the high similarity between Mei2-like proteins of *A. thaliana* and Mei2p of *S. pombe* is restricted to the C-terminal regions. Overexpression of the C-terminal region of *A. thaliana* AML1 in *S. pombe* could induce meiosis, but not premeiotic DNA synthesis, suggesting that *Mei2-like* genes of plants may be similar enough to *mei2* of *S. pombe* to be able to partially substitute (Hirayama *et al.*, 1997).

1.5 Apical Meristems of Plants

Since the expression of *Mei2-like* genes in the apical meristems may be pertinent to their function, some aspects of apical meristems, including their organisation and cytohistology, are introduced in the following sections.

Plants, unlike animals, produce organs throughout their life, and the body plan of plants is defined post-embryonically. There are two special regions in plants where stem cells are maintained, termed the shoot apical meristem (SAM) and the root apical meristem (RAM). Apical meristems provide pluripotent cells for organogenesis, and are essential for indeterminate growth.

1.5.1 The root apical meristem (RAM)

Roots have a radial organisation. The RAM is at the summit of the root, is covered by the root cap and surrounded by mature derivatives. The quiescent centre (QC) gives rise to all kinds of cells in the root, and so cells in the QC are stem-cell-like. Mitotic activity of the cells in the QC is low because of a prolonged G_1 phase of the mitotic cycle. In roots, stereotyped patterns of cell division occur where initial cells divide along predictable planes to maintain the structure of the root.

1.5.2 Shoot apical meristem (SAM)

The SAM is located at the tip of the shoot. Most of the organs of plants, including leaves, internodes, flowers, can be traced back to the SAM. In terms of structure, the simplest way of describing the SAM is by its "tunica-corpus" organisation. The tunica is the outermost layer of the SAM, and cell division in this tissue is restricted to an anticlinal orientation in which cells divide perpendicular to the surface and so produce a layer of relatively uniform thickness. The corpus is the inner part of the SAM and cell division in the corpus is less restricted such that cell division occurs in all directions (reviewed by Steeves and Sussex, 1989).

Besides the tunica-corpus organisation, the SAM is also organised into cytologically distinct zones. The central region is called the central zone (CZ). The CZ is flanked by peripheral zones (PZ), and the pith rib meristem (RZ) is located underneath the CZ (Figure 1.6 B). The CZ is a region containing undifferentiated cells in which the mitotic activity is much lower than that observed in the PZ and RZ. Within the PZ, cells begin to differentiate, and primordia are initiated in the PZ while the pith in the stem is initiated in the RZ. Once cells are recruited to lateral organ primordia, the fates of cells become further restricted (reviewed by Steeves and Sussex, 1989).

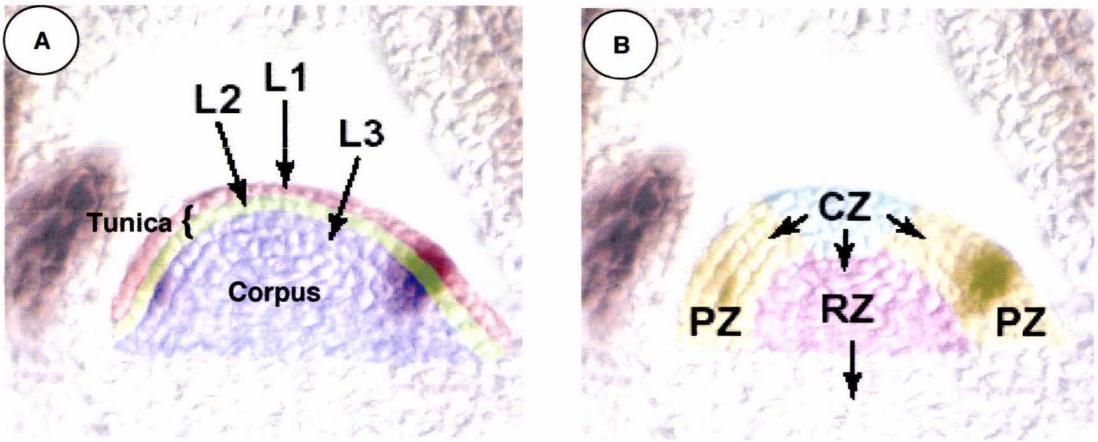

Figure 1.6 Histology of the shoot apical meristem (SAM). (**A)** Three typical cell lineage layers in the SAM: The epidermal layer (L1) and the subepidermal layer (L2) exhibit almost exclusive anticlinal cell division. They are collectively called tunica. The innermost layer (L3) exhibits all orientations of cell division. L3 is also called corpus. (**B**) The zonation of the SAM: the central zone (CZ) is the reservoir of the stem cells. The peripheral zones (PZ) are the place where initiation of organ formation occurs. The rib zone (RZ) is underneath the CZ. Arrows indicate the directions of stem cell division in the CZ. (Source: Bowman and Eshed, 2000)

1.5.3 Surgical studies of the SAM

To analyse the property of the SAM, surgical studies have provided some information. In one experiment, a vertical incision was made that separated leaf primordia from the SAM. The SAM kept growing and initiated leaf primordia, suggesting that it is a relatively autonomous structure. When the SAM was split by vertical incision into two halves, each half reorganised completely and gave rise to organs. These results provide further evidence for the autonomy of the SAM (Wardlaw, 1949).

However, the maintenance of the SAM may also require exogeneous nutrients and hormones. In other excision studies, an explant comprising the SAM plus two pairs of leaf primordia and young expanding leaves was sufficient to give rise to a plant without added hormones (Ball, 1946). However, when the terminus of the SAM was excised, the SAM could not

complete development unless indoleacetic acid (IAA) was added (Smith and Murashige, 1970) These results suggest that hormones are required for the SAM to complete development, and that *in vivo*, these hormones may be provided by expanded leaves (Shabde and Murashige, 1977)

1.5.4 The méristeme d'attente concept and clonal analysis

In the early 1950s, Buvat and colleagues proposed the 'méristeme d'attente' concept. This theory proposed that the méristeme d'attente, the region at the summit of the apex, has little or no mitotic activity, and thus it does not have any function in the development of the vegetative shoot, including organogenesis. 'The anneau initial', which is next to the méristeme d'attente, is an important region in the development of the shoot and gives rise the leaf primordia. Therefore, the méristeme d'attente is a "waiting" meristem throughout vegetative development but will give rise to most of the reproductive structures (review in Steeves and Sussex, 1989).

Clonal analysis is a useful technique that provides more information on the development of the SAM In this method, individual cells in the shoot apex are marked and so the fate of a particular cell can be traced during differentiation and growth. Visible, heritable markers are used, such as ploidy levels, anthocyanin or chlorophyll pigmentation. Cell lineage patterns can be determined during development and are typically designated as L1, L2 and L3 (Figure 1.6 A) Both L1 and L2 layers undergo anticlinal cell division while cell division in L3 layers is less orientated (Satina *et al.*, 1940). Therefore, L1 and L2 are in the tunica, and L3 is in the corpus (Figure 1.6 A). Clonal analysis

reveals that the cells of the L1 layer give rise to the epidermis, the cells of the L2 layer usually give rise to the sub-epidermis, and the cells of the L3 layer give rise to the remaining internal cell types.

Poethig *et al.* (1986) used clonal analysis to study the fate of cells in the SAM of *Zea mays* L. and determined that the cells in the peripheral region of the SAM gave rise to the lower nodes, while the cells in the central part gave rise to the upper nodes. McDaniel and Poethig (1988) studied clones of the developing shoot and constructed a fate map of the SAM (Figure 1.7). Generally, cell fate is influenced by the position. Single-internode sectors predominate in the internodes at the lower part of the mature plant while multiple-internodes sectors are present in the middle and the upper part of the plant. The results suggested that cells in the basal part of the meristem have more limited fates while the cells at the apex have more variability.

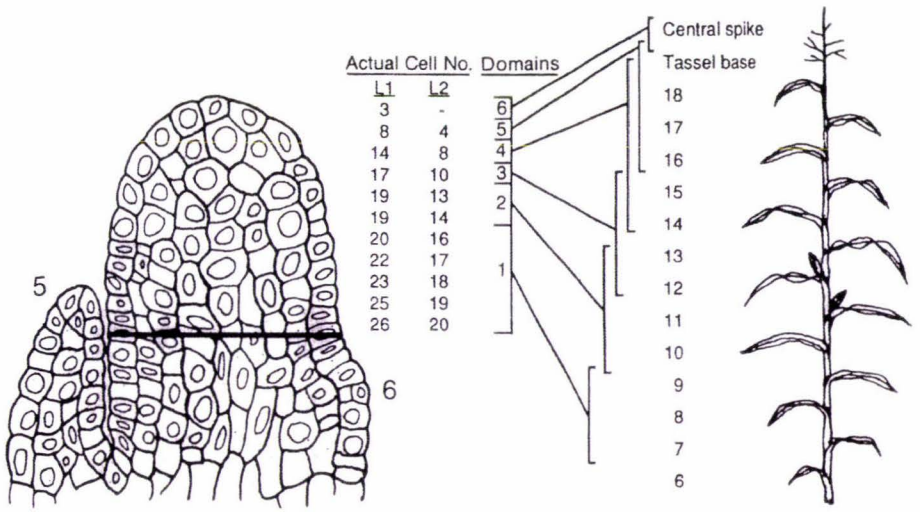

Figure 1.7 The fate map of the maize meristem obtained by using clonal analysis. The number of cells in L1 and L2 layers was estimated by counting cells in serial cross sections and in median longitudinal sections of three meristems. The numbers 5 and 6 indicate primordia which produced leaves 5 and 6. The portion of the mature corn plant (2.2m tall) which was produced by the meristem proper is shown on the right (except leaf 5). (Source: McDaniel and Poethig, 1988).

1.6 Genetic Analysis in the SAM of *Arabidopsis thaliana*

In the recent years, another approach has been used to study the SAM. That is the isolation of mutants that are impaired in meristem activity. This approach provides information about the expression of specific genes needed to regulate and maintain the SAM, to determine which genes control cell differentiation, and allow cells in different zones to recognise their 'identities'.

1.6.1 WUSCHEL and CLAVATA

The *WUSCHEL* (*WUS*) gene encodes a homeodomain protein which acts as a transcriptional regulator (Mayer *et al.*, 1998). *WUS* is required for specification and maintenance of both the shoot and floral meristems (Laux *et*

al., 1996). Furthermore, *WUS* expression is sufficient to induce meristem cell identity (Schoof *et al.*, 2000). *wus* mutants exhibited a flat structure in place of the vegetative SAM, in which defective shoot and floral meristems are initiated repetitively but terminate prematurely. Moreover, mutant flowers lack stamens and carpels (Laux *et al.*, 1996).

WUS expression is observed in the four inner cells at the 16-cell stage during early embryogenesis. In embryogenesis, the SAM does not appear until the transition stage, and *WUS* expression in the inner cells of the apex appears to specify the SAM in the embryo. In late embryogenesis, *WUS* expression is limited to the L3 layer. In the vegetative SAM, *WUS* expression is underneath the stem cells (L1 - L3) but not in the stem cells. However, *WUS* appears to function as a regulator of stem cell fate, suggesting that *WUS* must act in a non cell-autonomous manner to affect stem cell fate of neighbour cells (Mayer *et al.*, 1998).

There are three loci termed *CLAVATA* (*CLV*) (*CLV1*, *CLV2*, and *CLV3*), that encode gene products that act in the same signalling pathway and are specific regulators of the shoot apical and floral meristems (Clark *et al.*, 1995; Fletcher *et al.*, 1999; Brand *et al.*, 2000). *CLV1* encodes a leucine-rich repeat transmembrane receptor serine/threonine kinase, while *CLV2* encodes a leucine-rich receptor like protein. CLV1 and CLV2 forms a heterodimer, and CLV3 is a protein ligand of the CLV1/CLV2 heterodimer that binds to the extracellular domain of the heterodimer (reviewed by Clark, 2001). In mutants of *clv1*, *clv2* and *clv3*, accumulation of undifferentiated cells in the apex is observed, resulting in an enlarged SAM. This suggests that *CLV* genes are

involved in differentiation of the cells in the SAM (Fletcher *et al.*, 1999; Schoof *et al.*, 2000). What is proposed is that CLV3 forms a complex with CLV1 and CLV2 which represses *WUS* expression. Thus a regulatory loop between *WUS* and *CLV* is established that controls the size of the stem cell population (Figure 1.8) (Schoof *et al.*, 2000; Brand *et al.*, 2000).

Another gene, *SHEPHERD* (*SHD*) is required for the formation of the *CLV* complex (Ishiguro *et al.*, 2002). *shd* mutants are similar in phenotype to *clv* mutants, while *shd clv* double mutants are indistinguishable from the *clv* single mutant, suggesting that *SHD* and *CLV* act in the same pathway (Ishiguro *et al.*, 2002). Finally, *POLTERGEIST* (*POL*) is another regulator in the SAM that acts downstream of *CLV* loci and redundantly with *WUS* (Yu *et al.*, 2000).

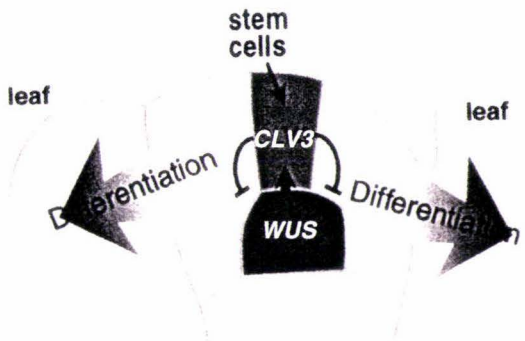

Figure 1.8 Regulatory loop between *WUS* and *CLV3*. *WUS* is expressed underneath the central zone and upregualtes *CLV3* expression. CLV3 forms a complex with CLV1 and CLV2 (not shown in the diagram) and represses *WUS* expression. Moreover, *CLV3* promotes stem cells differentiation. (Source: Schoof *et al.*, 2000)

Besides CLV, AGAMOUS (AG) is another protein interacting with WUS to regulate stem cell population in the floral meristem (Lohmann *et al.*, 2001). Initially, WUS is an activator of *AG* transcription, the later stages of floral development, *AG* represses *WUS* expression, so acting as a negative feedback loop. Thus the same mechanism of maintaining stem cell population occurs in both shoot and floral meristems (Lenhard *et al.*, 2001; Lohmann *et al.*, 2001).

1.6.2 SHOOT MERISTEMLESS

The *SHOOT MERISTEMLESS* (*STM*) encodes a homeodomain protein (Long *et al.*, 1996) that is involved in the maintenance of undifferentiated cells in the SAM and the floral meristem. It is an orthologue of maize *knotted-1* (*kn1*) (Endrizzi *et al.*, 1996; Vollbrechet *et al.*, 1991), which, in maize, is expressed in the SAM, but it is not expressed in organs such as leaves and flowers (Smith *et al.*, 1992; Jackson *et al.*, 1994). *kn1* maintains cells in an undifferentiated state within the central zone (Kerstetter *et al.*, 1997), and also maintains the function and the normal size of the SAM (Vollbrecht *et al.*, 2000).

STM expression is found in both the CZ and the PZ (Endrizzi *et al.*, 1996), and seedlings of *stm* mutants are blocked in the formation of SAM at the torpedo stage. Therefore, they lack SAMs, suggesting that *STM* is involved in the formation of SAM during embryogenesis (Barton and Poethig, 1993). Moreover, the spacing of cotyledons in the embryo is also affected in the *stm*

mutant, indicating that expression of *STM* in the PZ is involved in separation of organs (Endrizzi *et al.*, 1996).

Beside *STM*, *CUP-SHAPED COTYLEDON 1* and *2* (*CUC1* and *CUC2*) are also involved in the formation of the SAM and separation of cotyledons (Aida *et al.*, 1999). Both *CUC1* and *CUC2* act upstream of *STM* and are redundantly required for *STM* expression, while *STM* is required for spatial expression of *CUC2* in cotyledon separation (Aida *et al.*, 1999). Recent studies have shown that *PIN-FORMED1* (*PIN1*) and *MONOPTEROS* (*MP*), which encode a transporter for auxin and a transcription factor respectively, mediate auxin signalling, and regulate *CUC* gene expression, thereby controlling pattern formation in the SAM (Aida *et al.*, 2002).

Homoeostasis of the stem cell population in the SAM can be maintained by feedback regulation. Besides the *CLV/WUS* feedback loop, *CLV3* expression is also regulated by *STM* (Brand *et al.*, 2002). Clark *et al.* (1996) have shown that *STM* and *CLV* act on the same set of downstream genes in a competitive but opposing way since *stm* and *clv* mutations can suppress the phenotypes of each other. Actually, *WUS*, by itself, only regulates *CLV3* expression in the embryonic shoot meristem. Co-expression of *WUS* and *STM* is required to activate *CLV3* expression in the vegetative SAM (Brand *et al.*, 2002).

WUS and *STM* perform complementary roles in cell differentiation (Lenhard *et al.*, 2002) and trigger organogenesis (Gallois *et al.*, 2002). Ectopic expression of *WUS* and *STM* activate different downstream genes which converge in the suppression of the differentiation in the SAM (Lenhard *et al.*, 2002).

Furthermore, ectopic expression of *STM* activates a set of genes in the periphery of the SAM (Gallois *et al.*, 2002).

1.6.3 Other genes involved in the development of the meristems

The *PINHEAD/ZWILLE* (*PNH/ZLL*) gene encodes a translation factor (Lynn *et al.*, 1999), that is responsible for establishment of the central-peripheral organisation of the embryonic SAM, which also limits differentiation in the peripheral zone, and maintains undifferentiated stem cells in the central zone (Moussian *et al.*, 1998). Recent studies have shown the involvement of *PNH* in axis determinacy in the embryo. By altering *PNH* expression from the central zone to the peripheral zone, a shift from determinate cotyledon axis to an indeterminate state, results suggesting that *PNH* is able to change cell fate (Newman *et al.*, 2002).

The expression pattern of *PNH* overlaps with that of *ARGONAUTE1* (*AGO1*) and PNH and AGO1 have a high degree of similarity. Mutation of either gene caused similar defects in the primary and axillary SAMs, suggesting that *PNH* and *AGO1* act together in regulating gene expression in the embryonic SAM *via* mRNA translation (Bohmert *et al.*, 1998; Lynn *et al.*, 1999). *AGO1* is required in post-translational gene silencing in plants (Fagard *et al.*, 2000). By alignment, it is similar to QDE-2 of *Neurospora*, which is responsible for quelling (transgene-induced gene silencing) in fungi, and RDE-1 of *Caenorhabditis elegans*, which is required for RNA interference in animals. These results suggest that the product of *AGO1* is a novel class of regulator

of gene expression *via* silencing and is conserved among species (Fagard *et al.*, 2000).

MGOUN1 (*MGO1*) and *MGOUN2* (*MGO2*) are involved in primordia initiation in the SAM (Laufs *et al.*, 1998). *mgo* mutants exhibit reduction of organs and enlarged meristems, indicating that *MGO* genes are required in the modification of the correct number of cells participating in organ formation (Laufs *et al.*, 1998). Moreover, fragmentation of the SAM observed in *mgo* mutants, differs from the SAM in *clv* mutants, suggesting that *MGO* and *CLV* play different roles in primordium initiation (Laufs *et al.*, 1998).

AINTEGUMENTA (*ANT*) is another gene which is involved in initiation of primordia (Mizukami and Fischer, 2000). Previous studies have shown that *ANT* regulates cell division in the integuments during ovule development, and is required for floral organ growth (Elliot *et al.*, 1996). However, its function is different from that of *MGO* genes. *ANT* maintains the meristematic competence of cells during organogenesis, and therefore *ANT* upregulates cell proliferation. This suggestion is supported by the observation that cells of organs ectopically expressing *ANT* show neoplastic activity (Mizukami and Fischer, 2000).

FASCIATA genes (*FAS1* and *FAS2*) encode the subunits of the *A. thaliana* counterpart of chromatin assembly factor-1 (CAF-1). Since *fas* mutants disturbed the maintenance of *WUS* expression in the SAM and *SCARECROW* (*SCR*) expression in the RAM, *FAS* is required for stable gene

expressions in both SAM and RAM *via* chromatin assembly during DNA replication (Kaya *et al.*, 2001).

1.7 Hypotheses and Aims

Hypothesis I:	The meiRNA that assists accumulation of Mei2 protein in the nucleus is conserved between *S. pombe* and plant cells.
Aim:	Transient expression of GFP-tagged Mei2 protein and meiRNA into onion epidermal cells will be used to prove/disprove this hypothesis.
Hypothesis II:	Predicted TEL proteins of *A. thaliana* carry three RRMs that are highly similar to those found in Mei2p of *S. pombe*. One possible function of Mei2 protein is involvement in RNA splicing, and so TEL has may have a similar function.
Aim:	A yeast two-hybrid system will be utilised to identify the potential interactors of TEL2. Based on the biochemical properties of those identified interactors, functions of *TEL* genes will be deduced.

CHAPTER 2 GENERAL METHODS

2.1 Overview

This chapter describes methods used in this project, including the culture of strains of *Escherichia coli* and *Agrobacterium tumefaciens*, plant transformation methods, as well as molecular biology methods. The yeast two-hybrid system is utilised to identify potential protein-protein interactions, and the methods used are also described in this chapter.

2.2 *Escherichia coli* (*E. coli*) Methods

The following methods were used to prepare plasmid vectors for cloning and amplifying plasmid DNA in *E. coli*.

2.2.1 Growth of E. coli

To purify plasmids, *E. coli* was grown in liquid Luria broth (LB) medium containing an appropriate antibiotic at 37°C overnight with shaking (200 – 220 rpm). Glycerol stocks were prepared by mixing 0.85 mL of stationary-phase liquid bacterial culture with 0.15 mL of sterile glycerol, then freezing the suspension in liquid nitrogen, followed by storage at –70°C.

2.2.2 Preparation of competent cells of E.coli

A 5 mL culture of *E. coli* (strain DH5α; GibcoBRL) was prepared as described in section 2.2.1, except that no antibiotics were added to the LB medium. A 0.5 mL aliquot was then inoculated into 50 mL of pre-warmed SOC medium (see Appendix 2) (1:100 dilution) to give an OD_{600} reading of 0.02. The bacterial culture was incubated at 30°C with shaking (200 – 220 rpm) until the cells reached the early- to the mid-log phase at which point the OD_{600} reading was 0.5 - 0.7. At this stage, the bacterial cells were harvested by centrifugation at 3000 x g for 15 minutes at 4°C, cells were then washed with RF1 solution (see Appendix 2) containing 15% (v/v) glycerol and were collected by centrifugation as described previously. Finally, cells were resuspended in RF2 solution (see Appendix 2) containing 15% (v/v) glycerol,

and aliquots of these competent cells were quick-frozen in liquid nitrogen and stored at –70°C

2.2.3 Transformation of competent E.coli DH5α cells

An aliquot (50 μL) of chemically competent cells (section 2.2.2) was thawed on ice and was mixed with 2 μL of plasmid DNA or ligation mix (section 2.3.4). The mixture was incubated on ice for 10 minutes, then heat-shocked at 42°C for 20 seconds before 0.5 mL of LB medium was added to the cell mixture. The cells were then incubated at 37°C for 1 hour with shaking (220 rpm), and 250 μL of the cell mixture was then plated onto solid LB medium containing an appropriate antibiotic, and incubated at 37°C for at least 18 hours.

2.2.4 Preparing of electrocompetent E. coli DH5α

A 10 mL culture of *E. coli* was grown at 37°C overnight with shaking (220 rpm) in a non-selective LB medium, and a 5 mL aliquot was inoculated into 500 mL (1:100 dilution) of pre-warmed LB medium. The bacterial culture was incubated at 37°C with shaking (200 – 220 rpm) until the cells reached the early- to mid-log phase, after which they were harvested by centrifugation at 3000 x g for 15 minutes at 4°C. Cells were washed three times with sterile 10% (v/v) glycerol and then resuspended finally in sterile 10% (v/v) glycerol, before being quick-frozen in liquid nitrogen, and stored at –70°C.

2.2.5 Electroporation

An aliquot (40 μL) of electrocompetent cells was thawed on ice. The cells were mixed with 1 – 2 μL of plasmid DNA and then the mixture was incubated on ice for 1 minute before being transferred into a chilled 0.2 cm cuvette. The MicroPulser (BioRad) was set at "Ec2", the cuvette placed in the chamber slide and the cells were electroporated by pressing the "PULSE" button once One mL of SOC medium was then added immediately and the cells incubated at 37°C for 45 minutes with shaking (220 rpm). Aliquots (250 μL) of cell mixture were then plated onto solid LB medium containing an appropriate antibiotic, and plates were incubated at 37°C for at least 18 hours.

2.2.6 Qiaprep Spin Miniprep Kit (Qiagen)

This miniprep kit was used for extracting plasmid DNA for cloning or for obtaining new constructs after intermediate cloning steps in *E. coli*. The protocol is based on alkaline lysis of bacterial cells and absorption of plasmid DNA onto a silica membrane. Purified DNA samples were resuspended in 50 μL of 10 mM Tris.HCl (pH 8.5) and stored at –20°C.

2.2.7 Plasmid DNA extraction via alkaline lysis/PEG

A 10 mL culture of *E. coli* was prepared by incubating cells in LB containing an appropriate antibiotic at 37°C for at least 18 hours. The cells were collected by centrifugation at 3000 x g for 15 minutes at 4°C, and then lysed

by the addition of 300 μL of 0.2 M NaOH and 1% (w/v) SDS. The lysate was neutralised by addition of 300 μL of 3M potassium acetate (pH 4.8) and RNA degraded by the addition of 5 μL of 10 mg/mL RNaseA for 20 minutes at 37°C. The clear lysate were then extracted twice with chloroform. Plasmid DNA was precipitated from the upper aqueous phase of the lysate by addition of an equal volume of isopropanol, and the DNA pelleted by centrifugation at 10,000 x g for 10 minutes at 20°C. The DNA pellet was washed with 70% (v/v) ethanol, dried and then resuspended in sterile MQ water. Plasmid DNA was re-precipitated by addition of 40 μL of 13% (w/v) PEG 8000, and DNA collected by centrifugation at 10,000 x g for 20 minutes at 4°C. DNA was washed with 70% (v/v) ethanol, and resuspended in 25 μL of 10mM Tris.HCl (pH 8.5).

2.2.8 Plasmid isolation using the rapid boiling method (Sambrook et al., 1989)

The rapid boiling method was used to screen colonies to detect inserts of interest after cloning. This protocol was based on Sambrook *et al.* (1989) with some modifications. Colonies of interest were picked and restreaked onto selective LB plates. The plates were incubated at 37°C for at least 18 hours, after which the cells were picked up using sterile toothpicks and then resuspended in 350 μL of STET buffer (see Appendix 2). Bacterial cells were lysed by the addition of 25μL of 10 mg/mL lyticase (Roche) in 10 mM Tris.HCl (pH 8.5). The lysis reaction was incubated at 37°C for 15 minutes, boiled for 1 minute, and then cell debris collected by centrifugation at 10,000 x g for 10 minutes at 20°C. DNA in the supernatant was precipitated by the addition of 1

volume of isopropanol and 1/10 volume of 3 M sodium acetate (pH 5.2), the precipitate collected by centrifugation at 10,000 x g for minutes at 20°C, and the pellet washed with 70% (v/v) ethanol. After centrifugation, the DNA pellet was dried and then resuspended in 30 μL of 10 mM Tris.HCl (pH 8.5). The DNA samples were then analysed by restriction digestion (section 2.3.3).

2.2.9 Plamid isolation by the phenol-chloroform method

This method was a faster way to screen colonies for inserts of interest, and is based on gel electrophoresis of crude preps containing undigested plasmid. However, the size of insert must be greater than 10% of the total size of plasmid vector to discern any difference by agarose gel electrophoresis. A 0.5 mL aliquot of a 5 mL bacterial culture prepared in selective liquid LB medium was collected by centrifugation at 3000 x g for 5 minutes at 20°C, and all but 50 μL of LB medium was removed. The pelleted cells were resuspended in the 50 μL of LB medium and 50 μL of phenol:chloroform:isoamyl alcohol (25:24:1) added. The mixture was vortexed, centrifuged at 12,000 x g for 10 minutes and 10 μL of the aqueous (upper) phase was removed for gel analysis (see section 2.3.1). A small sample of an empty vector was also run on the gel. The clone was identified by comparing the shift in size of the supercoiled DNA with the empty vector. The remaining bacterial culture could then be used for plasmid isolation using the Qiaprep Spin Miniprep Kit (see section 2.2.6).

2.3 General DNA Methods

2.3.1 Agarose gel electrophoresis of DNA

DNA fragments were separated according their size using agarose gel electrophoresis. Separation was through 0.8% - 1.2% agarose, depending upon the size of DNA fragments, using 1 x TAE (40 mM Tris-acetate and 1 mM EDTA, pH 8.0) as running buffer, at 100 V. Molecular weight markers [usually the 1kb-plus ladder (Invitrogen) or the λ-*Hin*d III ladder (Figure 2.1)] were applied to determine the sizes of the unknown DNA fragments. On the conclusion of electrophoresis, the gel was stained with a 10 μg/mL solution of ethidium bromide, and DNA fragments were visualised under UV exposure and the image captured using a BioRad Transilluminator with an attached digital camera and analysed by Quantity One software (BioRad)

2.3.2 Quantification of DNA

The amount of DNA can be quantified using the following methods:

(1) Agarose gel electrophoresis: A 211 ng aliqout of a *Hin*d III digestion of λ DNA was separated through an agarose gel as described in section 2.3.1. The digest contained several bands which occur in different amounts according to a stoichiometry that is related to the size of each bands (Figure 2.1). The DNA sample could be quantified by comparing the intensities of the unknown bands with the bands of the λ-*Hin*d III ladder.

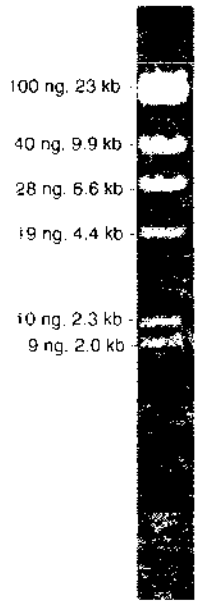

Figure 2.1 The λ-*Hind* III ladder. 211 ng of λ DNA is digested by *Hind* III to give 7 fragments. The amount of each fragment is calculated according to the size of fragment relative to the size of λ DNA. The fragment of 0.56 kb is not shown clearly on the gel since the amount of the fragment (2.5 ng) cannot be detected on the gel.

(2) Spectrophotometry: DNA was diluted with water, placed into quartz cuvettes, and absorbance readings at 260nm (A_{260}) and 280nm (A_{280}) were recorded. The ratio of A_{260}/A_{280} indicated the purity of DNA samples. The concentration of DNA samples are determined according to the formula

Concentration of DNA (ng/μL) = A_{260} x 40 x Dilution Factor

(3) Dot quantification method: The DNA standards and DNA samples were mixed with a 1 μg/μL solution of ethidium bromide and illuminated with UV. The amount of DNA in the samples was quantified by comparing the intensities of the unknown samples with the DNA standards.

2.3.3 Restriction digestion of plasmid DNA

A single digestion was performed in a total volume of 10 μL, that contained the appropriate restriction enzyme (5 U – 10 U), 1 x reaction buffer (supplied

with the restriction enzymes) and 100 ng – 400 ng of plasmid DNA. A double digestion was completed in a final volume of 20 μL. The reaction mixture contained the same amount of plasmid DNA and concentrations of reaction buffer but two restriction enzymes were used (5 U – 10 U of each). Usually, the digestion was incubated at 37°C for two hours unless specified. DNA fragments were separated and visualised using agarose gel electrophoresis (section 2.3.1).

2.3.4 Construction of vectors

Vectors were constructed using the following steps:

(1) Gel purification of the insert: restriction enzymes were used to remove the DNA insert of interest from its original plasmid (section 2.3.3). Approximately 1 μg of plasmid DNA was used in restriction digestions, and on completion, the restriction enzymes were heat-inactivated at 65°C for 20 minutes, unless specified. The DNA fragments were separated by agarose gel electrophoresis [1% (w/v) agarose in 1 x TAE, section 2.3.1] and the DNA fragment of interest was excised from the gel, and purified using the Concert Rapid Gel Extraction System (GibcoBRL) or Qiaquick Gel Extraction Kit (Qiagen).

(2) Digestion of the cloning vector: the cloning vector was digested with restriction enzymes (section 2.3.3), and the digestion monitored by agarose gel electrophoresis (section 2.3.1). When the digestions were complete, thermosensitive alkaline phosphatase (2 U) (GibcoBRL) was

added and incubated at 65°C for 15 minutes, thus preventing ligation between linearised cloning vectors.

(3) Ligation: the insert (provided in (1)) is ligated into the cloning vector (provided in (2)) at a ratio of

$$\frac{\text{Amount of insert (ng) x Size of insert (kb)}}{\text{Amount of vector (ng) x Size of vector (kb)}} = \frac{3}{1}$$

The ligation was set up in a total volume of 20 μL which contained 1 μL of T4 DNA ligase (1 U – 5 U, Roche or Invitrogen), 1 x ligation reaction buffer, the appropriate amount of insert and cloning vector. The ligation reaction was incubated at 25°C overnight, and the construct was amplified by transformation into *E. coli* (see section 2.2.3).

2.3.5 Polymerase chain reaction (PCR)

Each PCR consisted of 5 – 10 ng of template, 2 mM $MgCl_2$, 0.8 mM dNTPs, 0.4 μM each of forward primer and reverse primer, 2 U Taq polymerase (Invitrogen) and 1 x PCR buffer provided. Sterile MQ water was used to make up the final volume to 25 μL. A typical PCR programme consisted of the following steps and was carried out using an I-cycler (BioRad):

(1) 95°C for 5 minutes

(2) 30 cycles of (a) 95°C for 30 seconds

(b) annealing temperature for 30 seconds

(c) extension time at 72°C based on the rate of 1 kb/minute

(3) 72°C for 4 minutes

PCR products were analysed by separating 10 μL of each reaction through a 1.2% (w/v) agarose gel (section 2.3.1).

2.3.6 Sequencing of the constructs

For sequencing plasmid DNA, a DYEnamic ET Terminator Cycle Sequencing Kit (Amersham Pharmacia Biotech) was used. The reaction, in a final volume of 20 μL, contained 200 – 400 ng of template (the construct), 2 pmol of primer and sequencing reagent. The following cycling programme was performed for 25 cycles: 95°C, 20 seconds; 50°C, 15 seconds; 60°C, 1 minute. The cycling programme is performed using an I-cycler (BioRad), and on conclusion, the product was purified by precipitation with the addition of 80 μL of 95% (v/v) ethanol and 2 μL of 1.5 M sodium acetate/250 mM EDTA (pH 8.5). The DNA pellet was resuspended in 10 μL formamide, and an ABI PRISM 3100 Genetic Analyzer (Applied Biosystems) was used for sequencing the DNA.

2.4 General RNA Methods

To ensure an RNase free environment was maintained during manipulations, all glassware, mortars and pestles, and forceps used for RNA extraction were baked at 180°C for 8 hours. MQ water was autoclaved twice for 45 minutes at 121°C and 15 lb/sq in of pressure.

2.4.1 RNA extraction from A. thaliana seedlings

Transformed seedlings were selected on 1 x Murashige and Skoog (MS) medium (see Appendix 2) with appropriate antibiotics (see section 2.7.3). Seedlings were quick frozen in liquid nitrogen and were ground using a mortar and a pestle. A Qiagen Plant RNeasy Minikit (Qiagen) was used to extract RNA following the manufacturer's instructions.

2.4.2 Reverse-transcription polymerase chain reaction (RT-PCR)

The ThermoScript RT-PCR system (Invitrogen) was used for cDNA synthesis, according to the manufacturer's instructions. The Oligo$(dT)_{20}$ primer supplied with the kit was used as the primer for synthesis of cDNA at a final concentration of 5 μM. The synthesis of cDNA was carried out at 55°C for 1 hour, and reactions were terminated at 85°C for 5 minutes. RNase H (1 μL, supplied in the kit) was then added, the reaction continued for 20 minutes at 37°C to remove the remaining RNAs, and then cDNAs were used as templates for amplification using PCR (refer to section 2.3.5).

2.5 General Protein Methods

Proteins were subjected to western analysis to demonstrate translation of transgenes in plants.

2.5.1 Protein extraction of A. thaliana seedlings

Proteins were extracted from seedlings by firstly grinding plants in liquid nitrogen with a mortar and a pestle, suspending the ground plant tissues in extraction buffer comprising 0.1 M Tris.HCl (pH 8.0), 50 mM EDTA, 0.1% (v/v) 2-mercaptoethanol, and 1 mM PMSF. The suspension was spun at 14,000 rpm for 5 minutes at 4^0C, and the supernatant removed into a fresh tube without disturbing the pellet.

2.5.2 Sodium dodecyl sulphate-polyacrylamide gel electrophoresis (SDS-PAGE)

An acrylamide/bis-acrylamide mix (40%, Sigma) was adjusted to 7.5% or 10% for use as the resolving gel, and 5% acrylamide/bis-acrylamide was used for the stacking gel. SDS-PAGE was run at 75 V for 25 minutes as proteins separated through the stacking gel and 150 V for 1 hour as proteins separated through the resolving gel. At the conclusion of electrophoresis, the separated proteins were visualised by Coomaisse Blue staining, and then under visible light.

2.5.3 Western blot for GFP and GFP-fusion proteins

After SDS-PAGE (section 2.5.2), proteins were transferred to PVDF membrane using the Semi-Dry Protein Transfer system (Bio-Rad) at 15 V for 20 to 30 minutes. The membrane was blocked with 5% (w/v) non-fat milk powder in 1 x phosphate buffer saline (PBS) containing 0.2% (v/v) Tween-20 (PBST) buffer, followed by incubation with the primary antibody, anti-GFP (Roche) at a 1:1000 dilution in 1 x PBS, for 1 hour at 25°C. The membrane was washed in 1x PBST buffer twice, and the secondary antibody, anti-mouse IgG alkaline phosphatase conjugate (Sigma) at a 1:30000 dilution in 1 x PBS, was added, and the blot incubated for 1 hour at 25°C. After washing, developing reagent [0.1 M Tris.HCl (pH9.5), 0.1 M NaCl, 5 mM $MgCl_2$, 0.33 mg/mL NBT solution, 0.165 mg/mL BCIP solution] was added and the membrane incubated at 25°C overnight (Bollag *et al.*, 1996). At the conclusion of the development, the membrane was washed thoroughly in MQ water.

2.6 General *Agrobacterium tumefaciens* Methods

Agrobacterium tumefaciens-mediated transfer was used to introduce genes into plants. *A. tumefaciens* is a soil-dwelling bacterium that causes the "crown gall" diseases (Howe, 1995). Plasmid vectors designed for transformation into plants contain a transfer DNA (T-DNA) region, that consists of foreign DNA, a selectable marker gene and left and right borders. During the infection process, the T-DNA is transferred from *A. tumefaciens* into the plant nucleus, where it is integrated into the plant genome (Howe, 1995).

2.6.1 Transformation of A. tumefaciens by the freeze/thaw method

An aliquot (250 μL) of competent *A. tumefaciens* cells was thawed on ice, and then mixed with 10 μL of miniprep plasmid DNA. The cell mixture was left on ice for 5 minutes, frozen in liquid nitrogen for 5 minutes, and then placed in the 37°C water bath for 5 minutes. LB medium (1 mL) was then added, the cells incubated at room temperature (25°C) for 2 - 4 hours with shaking (200 rpm). The cells were then briefly pelleted, plated on the solid selective LB medium with appropriate antibiotics, and incubated for 2 days at 28°C.

2.6.2 Miniprep of plasmid DNA from A. tumefaciens

This protocol was based on alkaline lysis of bacteria (Sambrook *et al*, 1989) with some modifications. A 5 mL culture of *A. tumefaciens* was grown in the selective LB or YEB medium (refer to Appendix 2) at 28°C for 2 days with shaking (220 rpm), and 2 mL of culture was used in the miniprep. Cells were collected by centrifugation at 3000 x g for 10 minutes at 18°C, washed with 1 mL of 1 M NaCl, centrifuged as before, and the bacterial cells resuspended in 250 μL of Solution I (50 mM glucose; 10 mM EDTA, pH 8.0; 25 mM Tris.HCl, pH 8.0). These were then lysed by the addition of 250 μL of Solution II [0.2 M NaOH and 1% (w/v) SDS]. The lysate was then neutralised with the addition of 300 μL of Solution III (3 M potassium acetate, pH 4.8), and the plasmid DNA was precipitated from the clear lysate by the addition of 2 volumes of 100 % ethanol. The precipitated DNA was collected by centrifugation at 10,000 x g for 10 minutes at 20°C, the DNA pellet washed with 70% (v/v)

ethanol, dried, and then resuspended in 20 μL of 10 mM Tris.HCl (pH 8.5). Plasmid DNA was amplified by transformation into *E. coli* (section 2.2.3) since growth of *A. tumefaciens* was slower than *E. coli* and the amount of plasmid DNA obtained from *A. tumefaciens* was not enough for manipulation. After amplification in *E. coli*, the plasmid DNA was analysed by restriction digestions (see section 2.3.3).

2.7 General Methods for the Manipulation of *Arabidopsis thaliana*

2.7.1 Growth of Arabidopsis thaliana

Arabidopsis thaliana (ecotype Columbia) is grown under long day conditions at 25°C in the containment glasshouses located at Massey University and AgResearch Grasslands Research Centre.

2.7.2 Transformation of A. thaliana – Floral dip method

Transformation of *A. thaliana* was achieved using the floral dip method (Clough and Bent, 1998) with some modifications. A preculture of *A. tumefaciens* was prepared by inoculating 10 mL of YEB containing appropriate antibiotics with a single colony from a petri dish. A 2 mL aliquot of this preculture was then inoculated into 500 mL (1:250 dilution) of YEB medium with appropriate antibiotics and grown at 28°C for approximately 24 hours, or until an OD_{600} at least 0.6 was reached. The culture was then centrifuged at 7000 rpm for 15 minutes at 4°C, and the cells resuspended in

150 mL of infiltration medium [0.5 x MS with 5% (w/v) sucrose, see Appendix 2] containing 10 μg/L of BAP. The plants were dipped in this *A. tumefaciens* culture containing 500 μL per litre of the surfactant Silwet L-77, and transformed plants were covered for 1 day to prevent dehydration. After this time, plants were grown in the containment glasshouse under long day conditions at 25°C.

2.7.3 Screening seeds from transgenic plants

Siliques were harvested when the plants had finished flowering and these structures were yellow. The siliques were dried at 37°C for 1 week, the seeds were harvested, and then washed sequentially with 80% (v/v) ethanol, then 1% (v/v) bleach and then sterile MQ water. The sterilised seeds were then sown on germination medium containing 0.5 x MS and the appropriate antibiotics for selection. The sown seeds were stratified at 4°C for 2 days, and then incubated at 25°C under long day conditions.

2.8 Transient Expression in Onion Epidermal Cells

2.8.1 Preparation of DNA-coated microcarriers (Sanford et al.,1992)

Microcarriers (60 mg of tungsten particles, Bio-Rad) were washed with 70% (v/v) ethanol and water, resuspended in 1 mL of 50% (v/v) glycerol to give a concentration to 60 mg/mL. A 50 μL (3 mg) aliquot of tungsten particles was then coated with 3.75 – 5 μg of DNA (0.75 – 1 μg/μL), with the addition of

50 μL of 2.5 M $CaCl_2$ and 20 μL of 0.1 M spermidine (Sigma-Aldrich). The DNA-coated tungsten particles were then washed with 70% (v/v) and 100% ethanol before being resuspended in 48 μL of 100% ethanol to produce enough material for 6 bombardments.

2.8.2 Preparation of onion epidermal cells

Freshly picked onions were preferred. Onion bulbs could be also purchased from a supermarket, but only onions with growing shoots were chosen to ensure the bulbs were still alive. The onion bulb was soaked in 0.5 X MS medium for 2 days, so as to allow the onion epidermal cells to receive nutrients. After this time, the outermost and innermost leaves of onions were discarded. The epidermis was peeled off from one leaf of the inner side, and was spread out on a petri plate containing 1 X MS medium. These epidermal peels were used within one hour of removal from the leaves.

2.8.3 Transient biolistic assays were performed using the methods of Varagona et al., 1992 and Scott et al., 1999

For each bombardment, 6 μL of DNA-coated microcarrier suspension was spread onto a macrocarrier (Bio-Rad). The target onion epidermal peel container within the petri dish was placed onto the second shelf from the bottom (6 cm from the microcarriers). Rupture disks of 1100 psi (Bio-Rad) were used, and a vacuum was pulled to 28 inches of Hg. The "Fire" switch was pressed continuously until the rupture disk burst, and the transformed epidermis was incubated at 25°C for 13 to 14 hours in the dark after

bombardment. After this time, the epidermis was stained with 20 μg/mL of DAPI for 10 minutes in the dark to visualise nuclei (McLean *et al.*, 1990). GFP and GFP-fusion proteins were observed under the Leica UV stereomicroscope and the Nikon Microphot-SA microscope (with the epi-fluorescence system attached) or the Leica TCS 4d confocal laser scanning microscope using the following filters (Table 2.1).

Table 2.1 Filters used in the epi-fluorescence examination

Purpose	Excitation (nm)	Emission (nm)
GFP	480	515
DAPI	395	455

2.9 General Methods on *Saccharomyces cerevisiae* and the Yeast Two-Hybrid Assay

The yeast strain PJ69-4α was used in the yeast two-hybrid assay. The genotype of PJ69-4α is: *MATα trp1-901 leu2-3,112 ura3-52 his3-200 gal4Δ gal80Δ GAL2-ADE2 LYS::GAL1-HIS3 met2::GAL7-lacZ.*

2.9.1 Growth of Saccharomyces cerevisiae

Saccharomyces cerevisiae, a budding yeast, was grown at 30^{0}C and the stationary phase was reached after 48 hours incubation. Non-transformed yeast strains were grown in YPD medium (see Appendix 2), and transformed yeast cells were grown in the synthetic complete (SC) and drop-out medium (Appendix 2) which was the minimal medium for yeast growth.

2.9.2 Transformation of yeast with bait plasmid containing a TRP1 marker (http://www.umanitoba.ca/faculties/medicine/biochem/gietz/Quick.html)

This method was used for transforming the bait vector into the host cells. The bait vector contained a *TRP1* marker, and so yeast strains transformed with the bait vector could be selected on medium lacking tryptophan.

Non-transformed cells were scraped off from the YPD plates, and incubated in 100 mM lithium acetate (LiAc) for 5 minutes at 30°C, and 100 ng – 5 μg of plasmid DNA was transformed into these cells using 33% (w/v) PEG 3350, 100 mM LiAc and 100 μg of carrier DNA. The cells were mixed with the above components and incubated at 42°C for 20 minutes. The transformed yeast was then grown on SC-Trp medium at 30°C for 2 to 4 days.

2.9.3 Yeast miniprep methods

Cultures (2 mL) were prepared by growing yeast cells at 30°C for 2 days in liquid minimal medium. Alternatively, yeast cells were harvested by scrapping freshly grown plates. Cells were suspended in 1 mL of SCE solution (Appendix 2) and lysed in 200 μL of Solution I (1 μL/mL 2-mercaptoethanol, 0.5 mg/mL lyticase) and 400 μL of Solution II [1% (w/v) SDS, 0.2 M NaCl]. The lysate was neutralised with 300 μL of precooled 2.7 M potassium acetate (pH 4.8), and the plasmid DNA was precipitated from the clear lysate by the addition of 0.6 volumes of isopropanol. The precipitated DNA was collected by centrifugation at 10,000 x g for 10 minutes at 20°C, the DNA pellet was

washed with 70% (v/v) ethanol, dried, and then suspended in 20 μL of 10 mM Tris.Cl (pH 8.5). Plasmid DNA was amplified by transformation into *E. coli* using electroporation (section 2.2.5) and was analysed by restriction digestions (section 2.3.3).

2.9.4 Conversion of yeast two-hybrid library

A CD4-22 cDNA library was constructed by Kim *et al.* (1997). cDNA was generated from mRNA isolated from 3 day-old etiolated seedlings of *A. thaliana*, and the inserts cloned into λ-ACT. The size of inserts ranged from 0.6 kb to 2.5 kb with a mean size of 1kb. The cDNA library was amplified in the *E. coli* strain LE392 to a titre of 1.18 x 10^9 pfu/mL. The λ phage library was converted to a plasmid cDNA library by infecting the *E. coli* strain BNN132 with 20 μL of undiluted λ phage cDNA library in the presence of 10 mM $MgCl_2$. The λ-ACT with inserts were converted to pACT (see Figure 4.2 for the map of pACT), and the infected cells were grown on solid LB medium containing 2% (w/v) glucose and 100 μg/mL ampicilin at 37°C at least 18 hours. Cells were pooled, and grown in 1 L of TB medium with 100 mg/mL ampicilin at 37°C for 4.5 hours. After incubation, the TB medium was removed, and the cells were resuspended in 250 mL of STE buffer (see Appendix 2). The plasmid cDNA library was extracted by using Qiagen Plasmid Maxiprep Kit (Qiagen), using the protocol supplied with the product. The CD4-22 plasmid cDNA library was resuspended in 500 μL of 10 mM Tris.HCl (pH 8.5). The concentration was determined by spectrophotometry to be 0.83 μg/μL (see section 2.3.2).

2.9.5 cDNA library transformation for two-hybrid screen (Agatep et al., 1998)

A pre-culture was prepared by inoculating bait-transformed PJ69-4α cells into 100 mL of SC-Trp medium and incubating overnight at 30^{0}C. Next day, the cell titre of the culture was determined by an OD_{660} reading, as 7.5 x 10^8 cells was required to inoculate 150 mL of 2 x YPAD medium (Appendix 2) This culture was incubated for 3 - 5 hours at 30^{0}C until the cell titre had increased four-fold. At this point, the cells were centrifuged at 3000 x g for 10 minutes at 18^{0}C and incubated in 3 mL 100 mM lithium acetate for 15 minutes at 30^{0}C, and transformed with 30 μg of library plasmid DNA using 33% (w/v) PEG 3350, 100 mM LiAc and 3 mg of carrier DNA The cells and the above components were incubated for 30 minutes at 30^{0}C, the cells were then heat-shocked for 40 minutes at 42^{0}C with mixing by inversion for 15 seconds after every 5 minutes. The cells were then collected by centrifugation as described previously, and resuspended in 20 mL of sterile MQ water. Cells were plated on SC-Trp-Leu-His medium, and incubated for 3 – 14 days at 30^{0}C since *HIS3* was one of the reporter genes used in two-hybrid screen.

Colonies that appeared on SC-Trp-Leu-His were restreaked onto "X-gal indicator" plates (Appendix 2) containing 40 mg/L of 5-bromo-4-chloro-3 indolyl-β-D-galactoside (X-gal) since the *lacZ* gene was another reporter gene.

2.9.6 Rescuing the prey vectors from yeast and verifying the constructs

The vectors of "blue" colonies that appeared on the X-gal indicator plates were rescued by using the yeast miniprep method (see section 4.2.3). After amplification in *E. coli*, plasmid DNA was extracted using the alkaline lysis/PEG method (section 2.2.7). The prey vectors were verified by sequencing (section 2.3.5) using the pACT.Gal4ad.F1 forward primer. The sequences obtained were analysed by BLASTn and BLASTx searches available on the TAIR website (http://www.tair.org).

CHAPTER 3 CELLULAR LOCALISATION OF Mei2p IN PLANT CELLS

3.1 Overview

Since the meiRNA-assisted nuclear localisation mechanism of Mei2p appears well conserved in mammalian COS-7 cells (Yamashita *et al.*, 1998), it was of interest to investigate whether plants also posses this mechanism. Transient expression of GFP-fused Mei2p in onion epidermal cells was performed to show that Mei2p localised into the nucleus in the presence of meiRNA. However, the localisation pattern was not as clear as in mammalian cells. Transient expression of *TEL2::gfp* in onion epidermis also showed nuclear localisation without co-expression of any special RNA. This suggests that either some RNA species which assist with nuclear localisation of TEL2 are already present in onion epidermal cells, or that the mechanism of intracellular localisation of TEL2 is different from that of Mei2p. In plant lines with stable expression of *mei2::gfp*, no special phenotype was observed and no fluorescence signal was detected in any examined plant lines. RT-PCR analysis showed that transcripts of *mei2::gfp* were present in two lines but the GFP-fusion of Mei2p could not be detected by western analysis, suggesting that the GFP-tagged Mei2p might be degraded in plant cells.

3.2 Introduction

3.2.1 Subcellular localistion of S. pombe Mei2p using GFP as a reporter

Subcellular localisation of proteins is important in biological processes, and proteins carry specific sequences that direct this localisation. However, the localisation of *Schizosaccharomyces pombe* Mei2p depends upon binding of a specific non-translated mRNA, meiRNA (Yamashita et al., 1998). Nuclear localisation is required for Mei2p functioning in meiosis, and Yamamoto and colleagues established this localisation of Mei2p by tagging Mei2p with green fluorescent protein (GFP).

GFP is derived from *Aequorea victoria*, jellyfish, and the cDNA of *gfp* was cloned by Prasher *et al.* (1992). GFP contains 238 residues that produces a molecular weight of 27 – 30 kDa. The chromophore of GFP is formed by cyclisation and oxidation of Ser65, Tyr66 and Gly67 (reviewed by Gerdes and Kaether, 1996). Structural studies have revealed that GFP consists of an 11-stranded β-barrel threaded by an α-helix which runs through the cylinder. The chromophore is attached to the α-helix, and so it is buried in the cylinder (Tsien, 1998). The fusion of GFP with other proteins typically does not alter the fluorescence emitted by GFP, and due to this robust fluorescence signal, GFP is widely used in cell biology. Examples include studying subcellular localisation of the GFP-tagged proteins, and promoter analysis (reviewed by Geredes and Kaether, 1996; Leffel *et al.*, 1997).

Although wild-type *gfp* is expressed well in bacteria and yeast, it is not expressed well in plants, especially *A. thaliana*. Low expression of GFP is

attributed to missplicing of *gfp* transcripts in *A. thaliana* since a cryptic intron is present, resulting in the deletion of 84 nucleotides (Haseloff *et al.*, 1997). Therefore, the codon usage of wild-type *gfp* has been modified to destroy the cryptic intron, and this form of *gfp* is known as *mgfp4* (Haseloff *et al.*, 1997).

Binding of meiRNA is essential for nuclear localisation of Mei2p, but disruption of RRM3 prevents nuclear localisation of Mei2p even if meiRNA is present. This suggests that an intact RRM3 domain of Mei2p is required for meiRNA binding. The GFP-fused Mei2p localises into the nucleus in the presence of meiRNA and forms "a dot" in the nucleus. Moreover, transformation with both *mei2::gfp* and *gfp::mei2* could rescue the *mei2* mutation of *S. pombe*, indicating that the GFP did not affect the function of Mei2p in *S. pombe*. The RNA-assisted nuclear localisation mechanism of Mei2p appears to be conserved in mammalian COS-7 cells, suggesting that a similar RNA-assisted nuclear localisation system may be present in mammalian cells to regulate meiosis (Yamashita *et al.*, 1998).

To investigate whether meiRNA-assisted nuclear localisation of Mei2p is conserved in plant cells, Mei2p was fused with GFP and transiently expressed in onion epidermal cells. To make the GFP-fusion of Mei2p, mGFP4 was used to prevent missplicing of *gfp* mRNA in plant cells.

3.3 Methods

3.3.1 Brief introduction to the biolistic particle delivery system

In the biolistic experiments, the biolistic PDS-1000/He system (Bio-Rad) was used. Plasmid DNA was coated on tungsten microcarriers, and these were accelerated by the pressure of helium, which determines the particle velocity. Rupture disks designed to burst at a particular pressure of helium are used to achieve consistent particle velocities. The target cells "receive" DNA-coated microcarriers under vacuum (Figure 3.1).

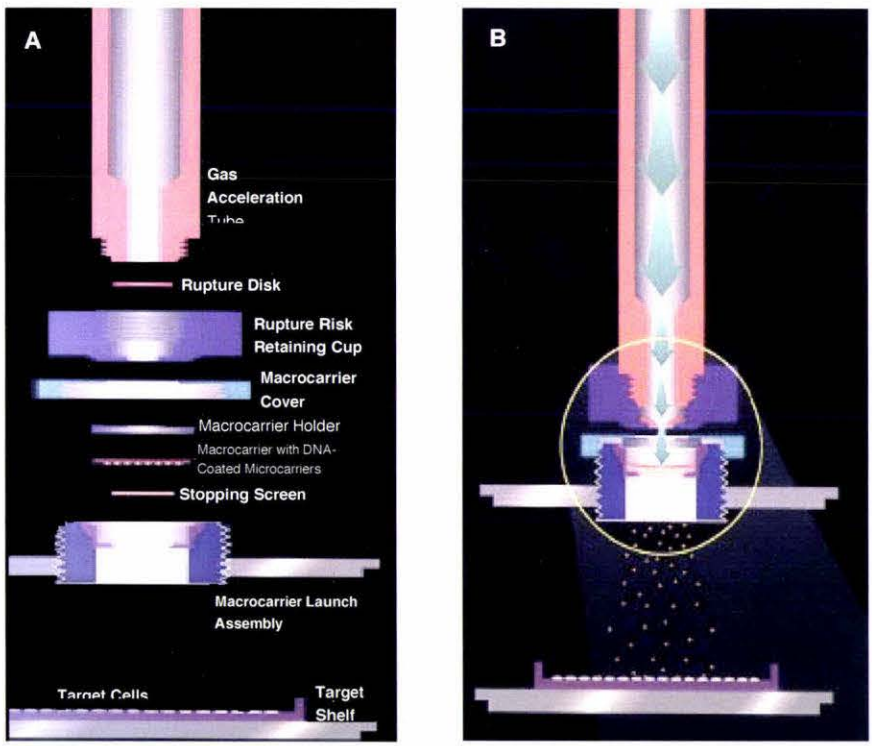

Figure 3.1 PDS-1000/He biolistic system. (**A**) Schematic diagram shows various parts inside the vacuum chamber. (**B**) DNA-coated microcarriers are accelerated by the pressure of helium and are delivered into target cells. (Source: http://www.bio-rad.com/webmaster/pdfs/Bulletin_1700.pdf)

3.3.2 Construction of vectors pMGB7, pGMA393 and pMRA7 for transient expression

A *mei2* cDNA of *S. pombe* was cloned as either an in-frame N-terminal or C-terminal fusion with green fluorescence protein (GFP) in pMGB7 and pGMA393 respectively. All GFP-tagged proteins were constructed in the cloning cassette pAVA393 (von Arnim *et al.*, 1998). *S. pombe sme2* encoding meiRNA was cloned in pMRA7. Overexpression of all GFP-fusion proteins and *sme2* was under the control of the 35S constitutive promoter from cauliflower mosaic virus (CaMV).

To construct pMGB7, a *Hind* III-*Sal* I fragment containing the open reading frame (ORF) of *mei2* was removed from pGFT81 (obtained courtesy of M. Yamamoto). The plasmid pBAV392 (obtained courtesy of V Trainor) containing *gfp* was digested with *Hind* III and *Xho* I to remove the 35S promoter. The *Hind* III-*Sal* I fragment of *mei2* from pGFT81 was then cloned into pBAV392 in frame with *gfp*. Next, the *mei2::gfp* fragment was removed by *Hind* III and *Sma* I and subcloned into pART7 (Gleave, 1992) at a *Hind* III and (blunted) *Xba* I site to make pMGB7.

To construct pGMA393, the *Nde* I (blunted)-*Spe* I fragment containing *mei2* was removed from pRST81 (obtained courtesy of M. Yamamoto), and cloned into pAVA393 at the *Bgl* II (blunted)-*Xba* I sites. Both pMGB7 and pGMA393 were sequenced to confirm that the correct reading frame was maintained.

To construct pMRA7, an *Eco* RV-*Bam* HI fragment containing the ORF of *sme2* was removed from pUC119-sme2 (obtained courtesy of M. Yamamoto) and cloned into pART7 at *Sma* I and *Bam* HI sites.

A cDNA of *TEL2* has been cloned as an in-frame N-terminal fusion of GFP in pVT42 (obtained courtesy of V. Trainor). The constructs used in transient expression assays are shown in Figure 3.2.

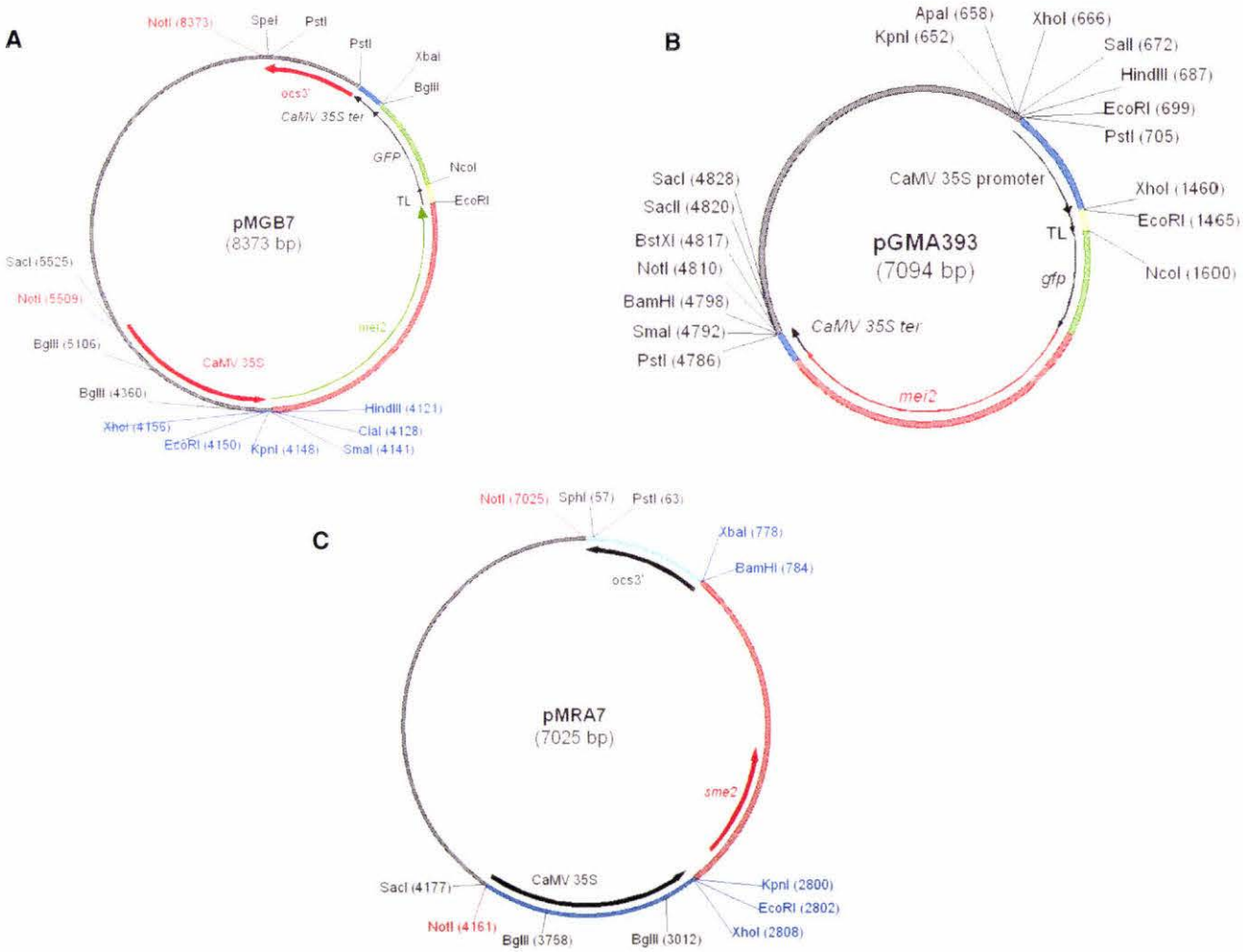

Figure 3.2 Constructs used in transient expression assays. Mei2p was fused with GFP as N-terminal and C-terminal fusion in pMGB7 (**A**) and pGMA393 (**B**), respectively. Both GFP-tagged Mei2p were cloned in pAVA393 cloning cassette as in-frame fusion to GFP. Expression of GFP-fused Mei2p and *sme2* (encoding meiRNA) (**C**) is under the control of the constitutive CaMV 35S promoter.

3.4 Results

3.4.1 Version of gfp used for transient and stable expression

The pGFT81 and pRST81 palsmids were supplied by the Japanese collaborator, M. Yamamoto, and comprise *mei2* fused with the *gfp*-S65T mutant (Heim *et al.*, 1995) as a C-terminal or N-terminal fusion respectively Since these GFP-fusions are under the control of the *nmt1* promoter of *S. pombe*, they were cloned into pART7 to put each gene under the control of the constitutive CaMV 35S promoter which allowed expression in plant cells. However, no GFP fluorescence signal was detected in transient expression experiments with *mei2::gfp*, or with co-expression of *mei2::gfp* and *sme2* (encoding meiRNA) in onion epidermal cells. These results suggest that the Mei2p-GFP(S65T) fusion can be expressed in *S. pombe*, but not in plant cells

One possible explanation is the presence of a cryptic intron in *gfp* transcripts. Haseloff *et al.* (1997) pointed out that wild-type *gfp* contains a cryptic intron that is excised efficiently in plant cells, resulting in a non-functional, truncated transcript. To overcome this problem, the codon usage of *gfp* has been altered to retain the intron, and so *mgfp4* was created (Haseloff *et al.*, 1997). The plasmid pAVA393 contains *mgfp4* in a cloning cassette, and makes it possible to construct both N- and C-terminal fusions with GFP (von Arnim *et al.*, 1998).

To direct expression of the GFP-fused Mei2p, *mei2* was fused with *mgfp4* in pAVA393 either as the N-terminal or the C-terminal fusion to make pMGB7

and pGMA393 respectively. These constructs were then used in transient expression assays in onion epidermal cells

3.4.2 Optimisation of transient expression of GFP and its fusion proteins in onion epidermal cells

In the transient expression assays, several factors affecting expression of introduced DNA were considered, including incubation time for transcription and translation, and distance between target tissues and accelerated particles. The plasmid pAVA393 containing *mgfp4* under the control of the constitutive promoter CaMV 35S, was used as a positive control and for optimisation of the assay

The distance between target tissue and microcarriers was another factor that affected the expression of *gfp* in onion epidermal cells. In these experiments, the frequency of expression of *gfp* in onion epidermal cells was around three-fold higher when onion epidermis was placed 6 cm below the microcarriers when compared with 3 cm below the microcarriers. Results are summarised in Table 3.1

Table 3.1 Effects of distance between target tissue and microcarriers on expression of *gfp* (pAVA393) in onion epidermal cells

Experiment	Distance between tissue and microcarriers (cm)	Number of cells expressing *gfp*	
1	3	19	
2	3	8	***Average***
3	3	23	16.7 ± 6.3
4	6	60	
5	6	40	
6	6	38	46 ± 9.9

The incubation time also affected expression of *gfp* and *gfp*-fused proteins. A 24-hour incubation increased expression of *gfp* around 1.5-fold when compared with a 7-hour incubation (Table 3.2). In a separate experiment, when localisation of GFP was observed 14 hours after bombardment, GFP was found in both the cytoplasm and the nucleus (Figure 3.3 A). However, a larger proportion of GFP fluorescence was observed in the nucleus after 24 hours of incubation (Figure 3.3 B). These results are in agreement with the observations of Sheen *et al.* (1995), who showed that the majority of GFP located into the nucleus when GFP was expressed in maize mesophyll protoplasts.

Table 3.2 Effects of incubation time on expression of *gfp* (pAVA393) in onion epidermal cells

	Number of cells expressing *gfp*		
Experiment	**7hr after bombardment**	**24hr after bombardment**	**Increase in number of cells expressing**
1	16	28	12
2	20	37	17
3	24	34	10
Average	20	33	13

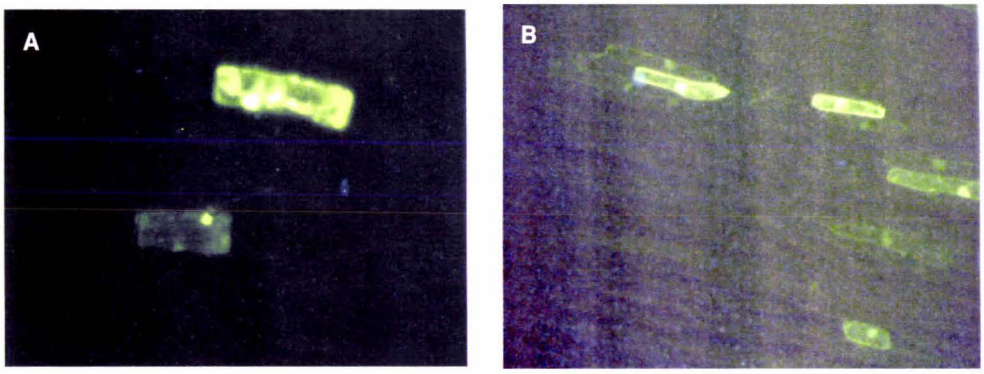

Figure 3.3 Localisation of GFP in onion epidermal cells after different incubation times after bombardment. The onion epidermis was bombarded by the plasmid pAVA393 coated microcarriers and incubated for 14 hours (**A**) and 24 hours (**B**).

3.4.3 Expression of mei2::gfp, gfp::mei2 and TEL2::gfp in onion epidermial cells

It is known that the Mei2p of *S. pombe* binds to meiRNA and accumulates in the nucleus and this pattern is conserved in mammalian cells (Yamashita *et al.*, 1998). To determine whether this localisation of Mei2p is also conserved in plant cells, GFP-tagged Mei2p and meiRNA were transiently co-expressed in onion epidermal cells.

Initially, for expression of pMGB7 in onion epidermal cells, no fluorescence signal was detected. The *mei2* gene was cloned in the cloning cassette of pAVA393, and a translation enhancer (TL) in the cloning cassette facilitates the expression of *gfp* and the gene fused with *gfp* (von Arnim *et al.*, 1998). In pMGB7, the TL was in between *mei2* and *gfp*, and so this arrangement may decrease the efficiency of translation of *mei2::gfp* transcripts (Figure 3.2 A). Therefore, pGMA393 was also constructed as a C-terminal fusion of GFP::Mei2p with the TL in front of *gfp::mei2* (Figure 3.2 B). Moreover, the different forms of GFP-fusions (i.e. the N-terminal and the C-terminal fusions) may behave differently in the cells, thus justifying the use of both forms.

The results of transient expression assays in onion epidermal cells are summarised in Table 3.3. The expression levels and the number of transformation events showed no difference between pMGB7 and pGMA393, indicating that the position of the TL did not influence transient expression of GFP-fused Mei2p in onion epidermal cells. No expression of GFP-tagged Mei2p was observed in the absence of meiRNA. A few cells expressing

Mei2p::GFP were observed in the presence of meiRNA, with signal observed in 8 cells expressing *mei2::gfp* and 9 cells expressing *gfp::mei2*. The frequency of expression of *TEL2::gfp* was higher than expression of *mei2::gfp* or *gfp::mei2* with 79 positive cells observed in *TEL2::gfp* expression assay to give a frequency that was around 10-fold higher when compared with *mei2::gfp* and *gfp::mei2* constructs in the presence of meiRNA. The frequency of expression of *gfp* alone achieved the highest expression rate which was 4-fold higher than *TEL2::gfp* expression and 40-fold higher than *mei2::gfp* and *gfp::mei2* expression (in the presence of meiRNA).

Table 3.3 Number of onion epidermal cells expressing GFP and GFP-fusion proteins in transient expression assays

Description	Total number of cells expressing GFP	Number of plates	Average number of cells expressing GFP per plates
Mei2p::GFP	0	8	0
Mei2p::GFP + meiRNA	8	8	1.0
GFP::Mei2p	0	8	0
GFP::Mei2p + meiRNA	9	8	1.1
TEL2::GFP	79	7	11.3
GFP only	92	2	46.0

3.4.4 Localisation of GFP-fusion of Mei2p in onion epidermal cells

The distribution of fluorescence of the N- and C-terminal GFP-fused Mei2p (with meiRNA) coincided with the position of the nucleus as determined by DAPI staining (Figure 3.4 A, C; Figure 3.5 A, C). In the stereomicroscope images, a clear 'dot' formation was observed in both *mei2::gfp* (Figure 3.4 E,

F) and *gfp::mei2* (Figure 3.5 E, F) constructs in the presence of meiRNA. Although there was no DAPI staining to locate the nucleus in these experiments, from the size and the shape of the dot, it could be deduced that GFP fluorescence was concentrated in the nucleus. The expression of Mei2p::GFP and expression of GFP::Mei2p in onion epidermal cells exhibited a similar distribution of GFP fluorescence.

Compared with the distribution of fluorescence of *35S::gfp* (Figure 3.4 G, 3.5 G), the GFP-tagged Mei2p was more concentrated in the nucleus while GFP was distributed evenly through the cell. However, nuclear localisation of GFP-tagged Mei2p in onion epidermal cells was not as clear as that in mammalian COS-7 cells (Figure 1.2 B; Yamashita *et al.*, 1998). In the mammalian cells, the GFP-fused Mei2p localises into the nucleus in the presence of meiRNA.

3.4.5 Localisation of GFP-fusion of TEL2

Since the RRMs of TEL2 resemble the RRMs of Mei2p (Jeffares, 2001), it was of interest to investigate whether TEL2 localises to the nuclei of onion epidermal cells. Transient expression of *TEL2::gfp* in onion epidermal cells showed that fluorescence of *TEL2::gfp* was mostly distributed in the nucleus (Figure 3.6 A, C) as determined by DAPI staining (Figure 3.6 B, D). When compared with the *35S::gfp*, in which fluorescence is distributed evenly in the cell (Figure 3.6 G), *TEL2::gfp* is localised in the nucleus without co-transformation with any special RNA species. However, TEL2::GFP formed inclusion bodies (Figure 3.6 A, C, indicated by arrows; Figure 3.6 E, F) in the

cytoplasm that affected the pattern of localisation of TEL2::GFP observed in onion epidermal cells.

Another protocol was used that tried to minimise the formation of inclusion bodies in the cytoplasm of onion epidermal cells. After particle bombardment, the samples of onion epidermis were incubated at low temperature (8 – 10^{0}C) for four to seven days, and after this treatment, the number of inclusion bodies in the cytoplasm was greatly minimised. In these treated tissues, fluorescence of TEL2::GFP was concentrated in the nucleus (Figure 3.7 A, C) as determined by DAPI staining (Figure 3.7 B, D). From the images of the UV stereomicroscope, fluorescence of TEL2::GFP also concentrated as 'a dot' (Figure 3.7 E, F), and by its shape and size, it could be deduced that fluorescence of TEL2::GFP was mainly distributed in the nucleus. Therefore, minimising formation of inclusion bodies aided observation of nuclear localisation of TEL2::GFP.

In summary, the mechanism of RNA-assisted nuclear localisation of the GFP-fused Mei2p appears conserved in onion epidermal cells. The *TEL2::gfp* fusion also localised into the nucleus without co-expression of special RNA species. The level of expression of *TEL2::gfp* in onion epidermal cells was much higher than that of the GFP-fused Mei2p.

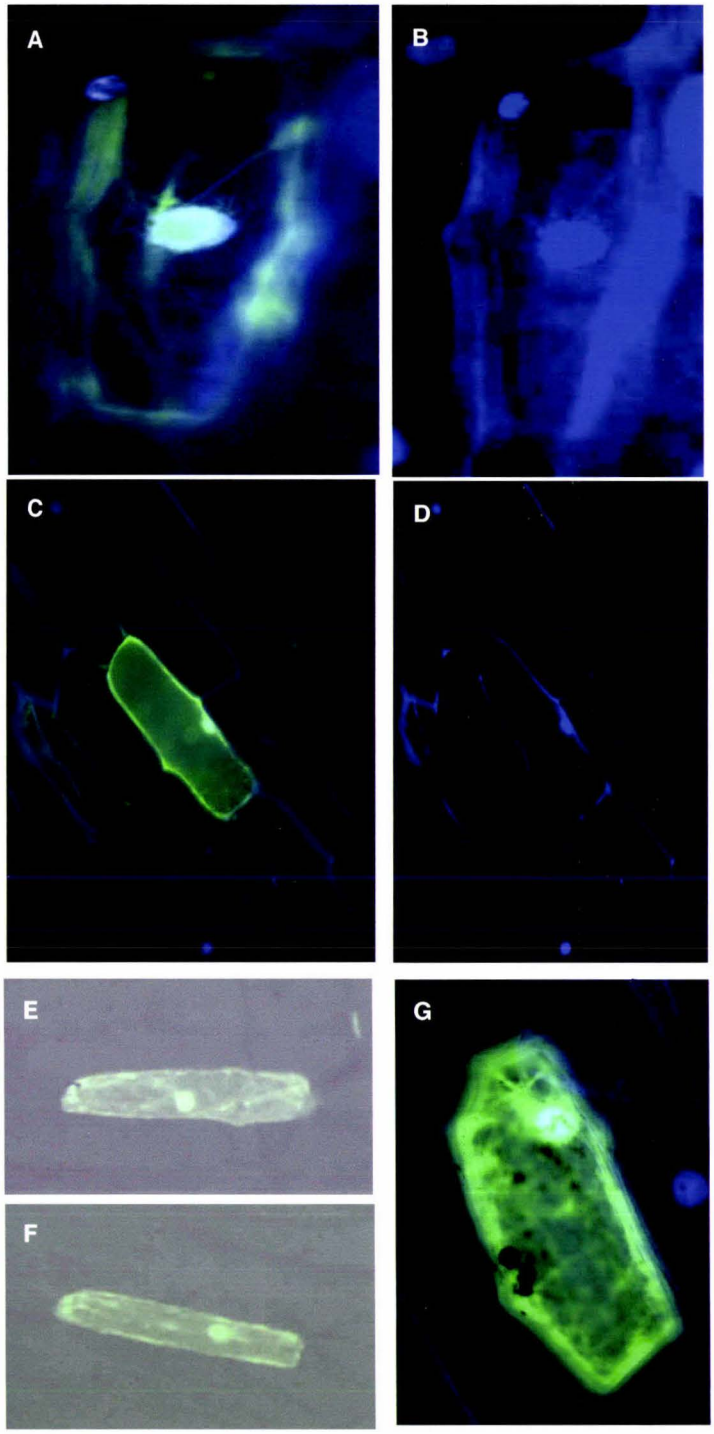

Figure 3.4 Localisation of Mei2p::GFP in the presence of meiRNA in onion epidermal cells. (**A**) and (**C**) are merged images of GFP and DAPI staining while (**B**) and (**D**) are images of DAPI staining. The images represent two independent events observed. (**E**) and (**F**) are UV stereomicroscope images and they represent another two independent events. GFP signal was concentrated as "a dot". Since there was no DAPI staining in (**E**) and (**F**), the position of nucleus could not be indicated. (**G**) The merged image of the 35S::GFP positive control.

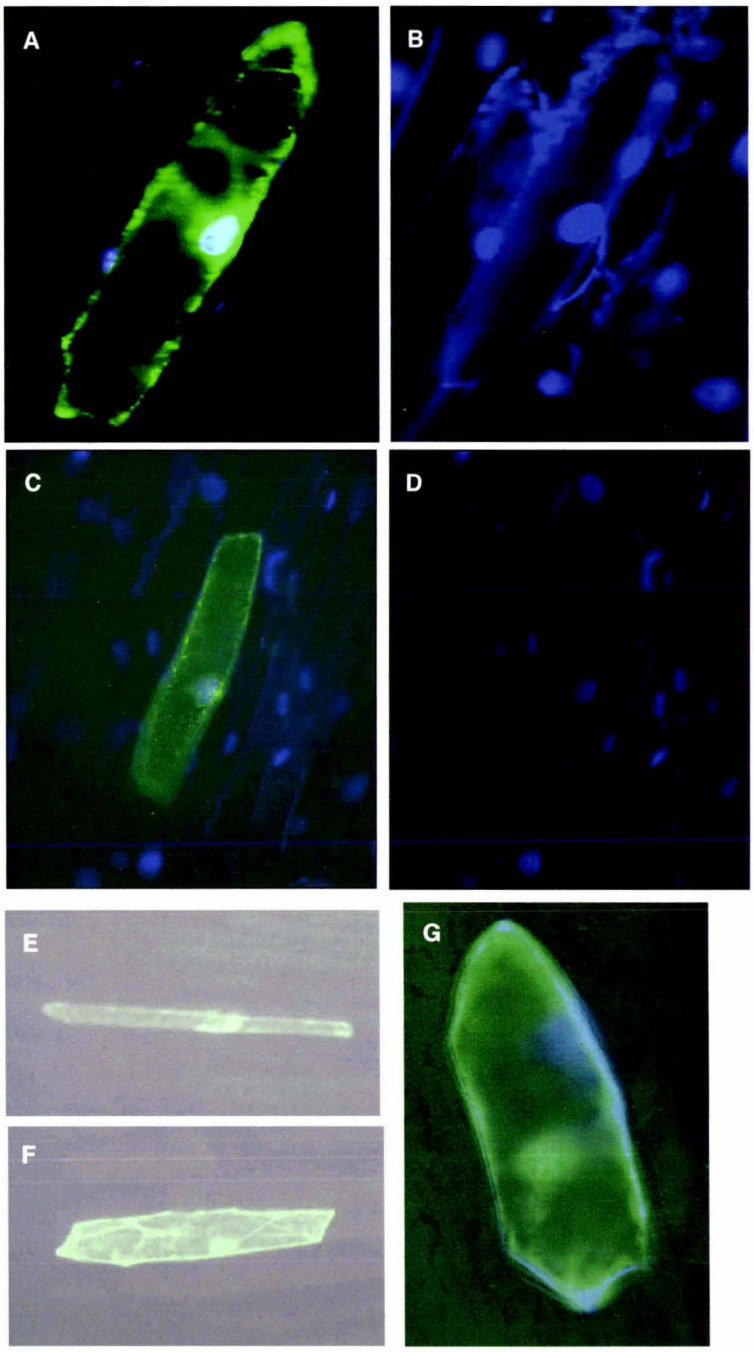

Figure 3.5 Localisation of GFP::Mei2p in the presence of meiRNA in onion epidermal cells. (**A**) and (**C**) are the merged images of GFP and DAPI staining. (**B**) and (**D**) are images of DAPI staining. Strong signal from DAPI staining affected GFP signal in (**A**). (**E**) and (**F**) are the images from the UV stereomicroscope that represent another two independent events observed. GFP-fused Mei2p were concentrated as a dot. (**G**) The merged images of the 35S::GFP positive control, showing the relatively uniform distribution of GFP.

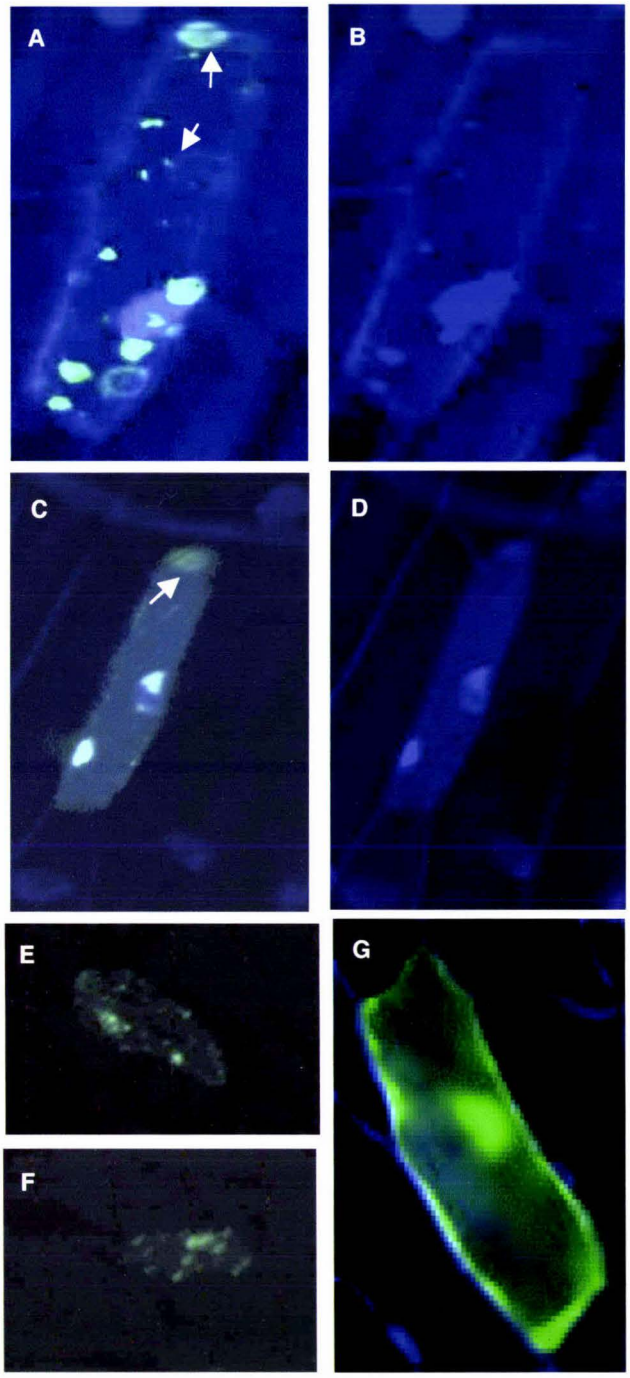

Figure 3.6 Localisation of TEL2::GFP in onion epidermal cells. (**A**) and (**C**) are merged images of GFP and DAPI staining. (**B**) and (**D**) are images of DAPI staining. (**E**) and (**F**) are the images from the UV stereomicroscpe and they represent another two independent events observed. TEL2::GFP localises into the nucleus without co-transformation of any RNA species in onion epidermal cells. Arrows indicate inclusion bodies in the cytoplasm. (**G**) The merged images of the 35S::GFP positive control.

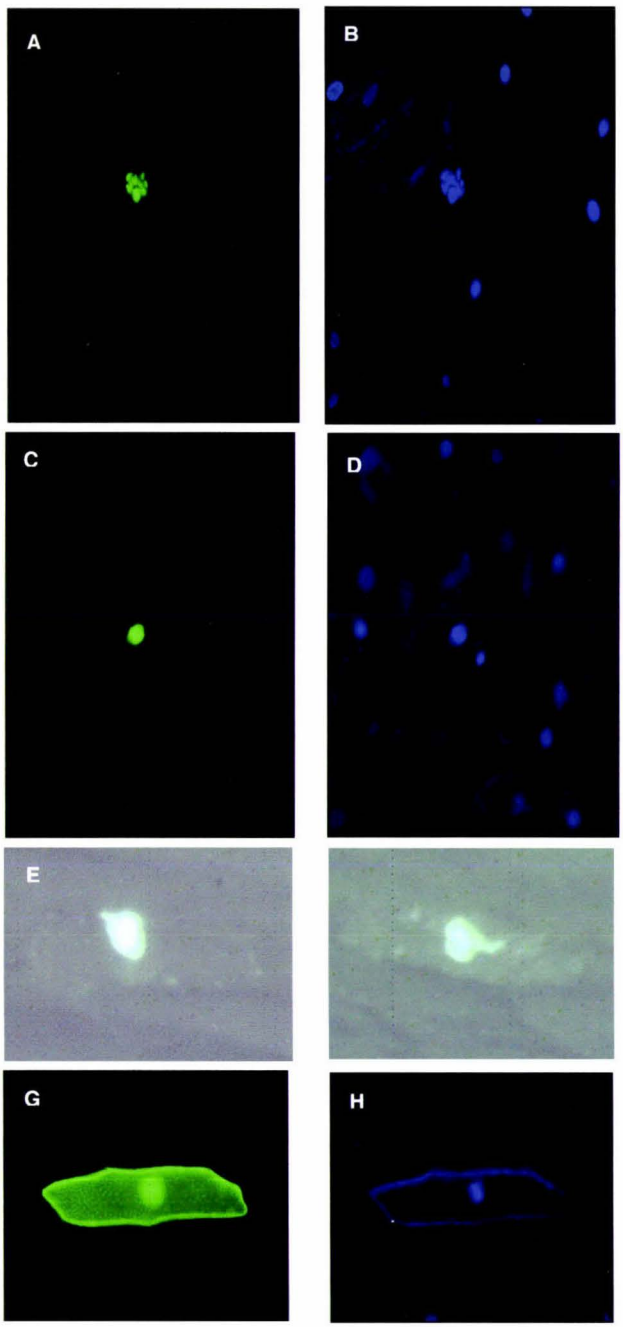

Figure 3.7 Localisation of TEL2::GFP in onion epidermal cells by incubating the cells at low temperature. After particle bombardment, the samples of onion epidermis were incubated at 8-10^{0}C for 6 days. Formation of Inclusion bodies in cytoplasm was minimised. (**A**) and (**C**) are images of GFP. (**B**) and (**D**) are images of DAPI staining. (**E**) and (**F**) are the images from the UV stereomicroscope and they represent another two independent events observed. TEL2::GFP localised into the nucleus without co-transformation of any RNA species in onion epidermal cells. (**G**) The image of GFP of the 35S::GFP positive control in onion epidermis and (**H**) the image of DAPI staining .

3.4.6 Phenotypes of stable expression of GFP-fused Mei2p in plants

In transient expression assays, no GFP fluorescence was detected when only *gfp*-fused *mei2* was expressed in onion epidermis. These results suggested that GFP-fused Mei2p might be degraded in onion epidermal cells (see Discussion, section 3.5.2). To determine whether expression of *mei2* might be dependent on the presence of meiRNA, the stable expression of *35S::mei2::gfp* was investigated.

Transgenic plants putatively expressing *35S::mei2::gfp* were selected by growing on kanamycin (50 µg/mL) as the kanamycin resistance gene was selectable. There were six plant lines with stable expression of *35S::mei2::gfp*, and three of these (Lines 1, 6 and 7) were selected because they grew well on the selection medium. No fluorescence was detected in these three lines even though the expression of *mei2::gfp* was driven by the constitutive CaMV 35S promoter (Figure 3.8 A, B and C). A fluorescence signal was detected from two seedlings (out of 30 seedlings) in the line where GFP alone was overexpressed (*35S::gfp* Line 14) (Figure 3.8 E).

The *35S::mei2::gfp* plants did not exhibit any special phenotype although the plant lines expressed the kanamycin resistance gene. Seedlings with overexpression of *mei2::gfp* (Lines 1, 6 and 7; Figure 3.9 A, B and C) were similar to the seedlings transformed with the empty vector (pART27) (Figure 3.9 E). The leaves did not show any difference between the transgenic seedlings, those transformed with pART27 or those from wild-type seedlings (Figure 3.9 F).

In the six-week old plants, those constitutively expressing *gfp* (*35S::gfp*) were shorter when compared with *35S::mei2::gfp* and those transformed with pART27. These plants were also less bushy (data not shown). However, seedlings of plants transformed with *35S::gfp* (Figure 3.9 D) did not show any phenotypic differences when compared with seedlings of wild-type plants (Figure 3.9 F).

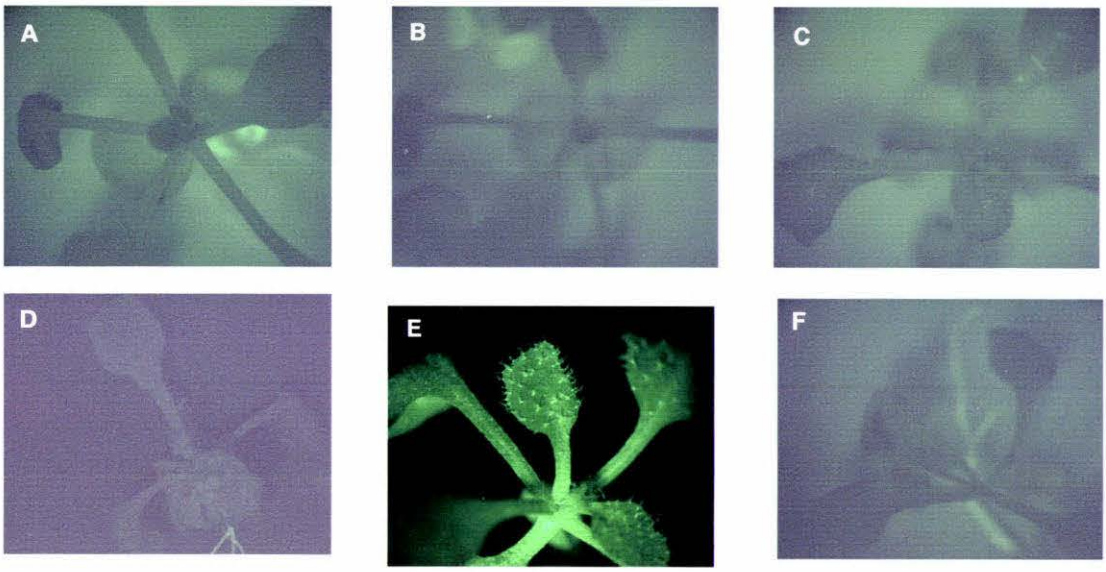

Figure 3.8 Detection of fluorescence signal in seedlings transformed with GFP or GFP-fused Mei2p of two weeks-old. No fluorescence signal was detected in the seedlings of *35S::mei2::gfp* lines, Line 1 (**A**), Line 6 (**B**) and Line 7 (**C**). Fluorescence signal was detected in the *35S::gfp* Line 14, (**E**) but not in the empty vector Line 9 (**D**) and the wild-type seedlings (**F**).

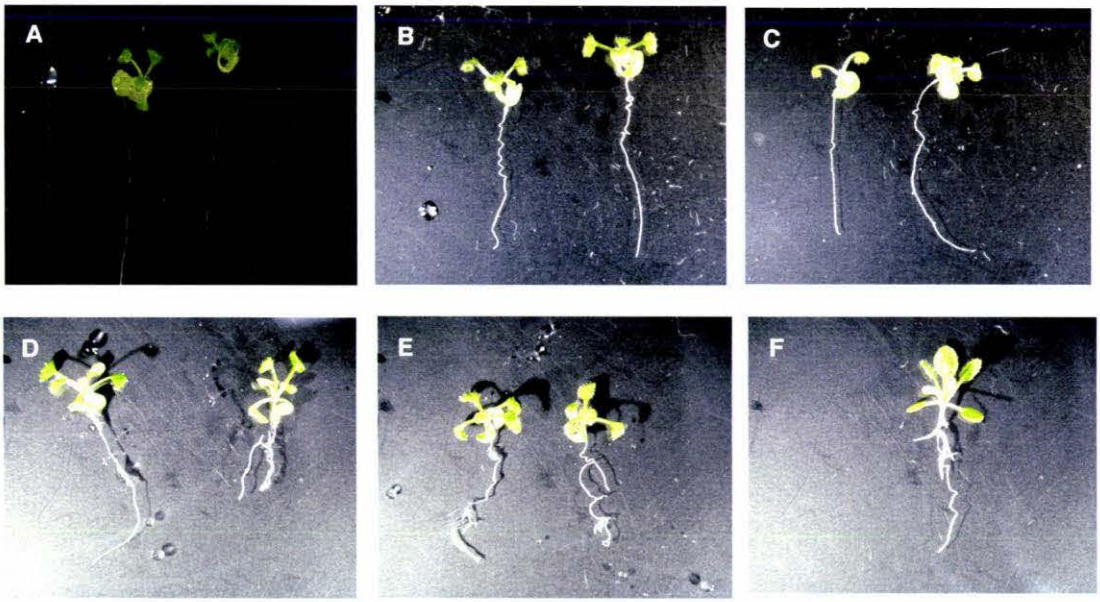

Figure 3.9 Phenotypes of *35S::mei2::gfp* two-week old seedlings. Three lines (**A**, **B** and **C**) of *35S::mei2::gfp* seedlings were selected, Lines 1 (**A**), 6 (**B**) and 7 (**C**). These seedlings did not exhibit any special phenotypes when compared with seedlings of *35S::gfp* Line 14 (**D**), the empty vector Line 9 (**E**) and the wild-type (**F**).

3.4.7 Transcriptional and translational analysis of stable expression of 35S::mei2::gfp plants

Since no GFP fluorescence signal was detected in plants transformed with *35S::mei2::gfp*, the level of transcription and translation of the transgene was analysed. Reverse-transcription-dependent PCR (RT-PCR) assays were used for transcriptional analysis, while western blots were used for translational analysis.

For RT-PCR, the primers were designed to amplify a 0.8 kb region of the *mei2* gene. The results of experiments with *35S::mei2::gfp* plants (Lines 1, 6 and 7) showed that *mei2::gfp* transcripts were only detected in Lines 1 and 6 but not in Line 7 despite the later showing growth in selective medium (50 μg/mL kanamycin in 0.5 x MS) (Figure 3.10 A). As expected, no *mei2* transcripts were detected in lines transformed with pART27 (Figure 3.10 A).

Since the predicted size of Mei2p is around 95 kDa, while GFP is 28 kDa (von Arnim *et al.*, 1998), the GFP-fusion protein of Mei2p should then be *ca.* 123 kDa. In western analysis, 10% acrylamide and 7.5 % acrylamide gels were used in SDS-PAGE (Figure 3.10 B, C, D and E). Since the GFP-tagged Mei2p is a large protein compared with GFP, 7.5% acrylamide gel provided better resolution for the larger proteins (e.g. GFP-tagged Mei2p). However small proteins like GFP could not be resolved under these condition (Figure 3.10 C).

On the western blots of these gels, one band was present in the protein sample extract of Line 14 of the *35S::gfp* transformed plants (Line 14) (Figure 3.10 D, E). This indicates that GFP was present in Line 14 of the GFP overexpressing plants, although only weak signal was detected under the UV stereomicroscope. No GFP-fused Mei2p was detected in the western blot of the *35S::mei2::gfp* transformed lines although transcripts of *mei2::gfp* were detected in Lines 1 and 6 using RT-PCR (Figure 3.10 D, E). Non-specific binding of antibodies to the plant proteins occurred, especially when the amount of protein loaded was increased (Figure 3.10 C, E). The most abundant protein in plants is Rubisco, a protein involved in photosynthesis (Lawlor, 2001), and the large subunit of this protein is around 55 kDa in size. The protein sample of *35S::gfp* spilled out to adjacent lanes when it was loaded. The bands of the same protein size of GFP (28 kDa) occurred in the other lanes which were not loaded with the protein sample of *35S:gfp* line (Figure 3.10 B, C).

In summary, the transcripts of *mei2::gfp* were detected in Lines 1 and 6 of *35S::mei2::gfp* plants by using RT-PCR. However, in western blot analysis, no Mei2p::GFP protein could be detected in those two lines.

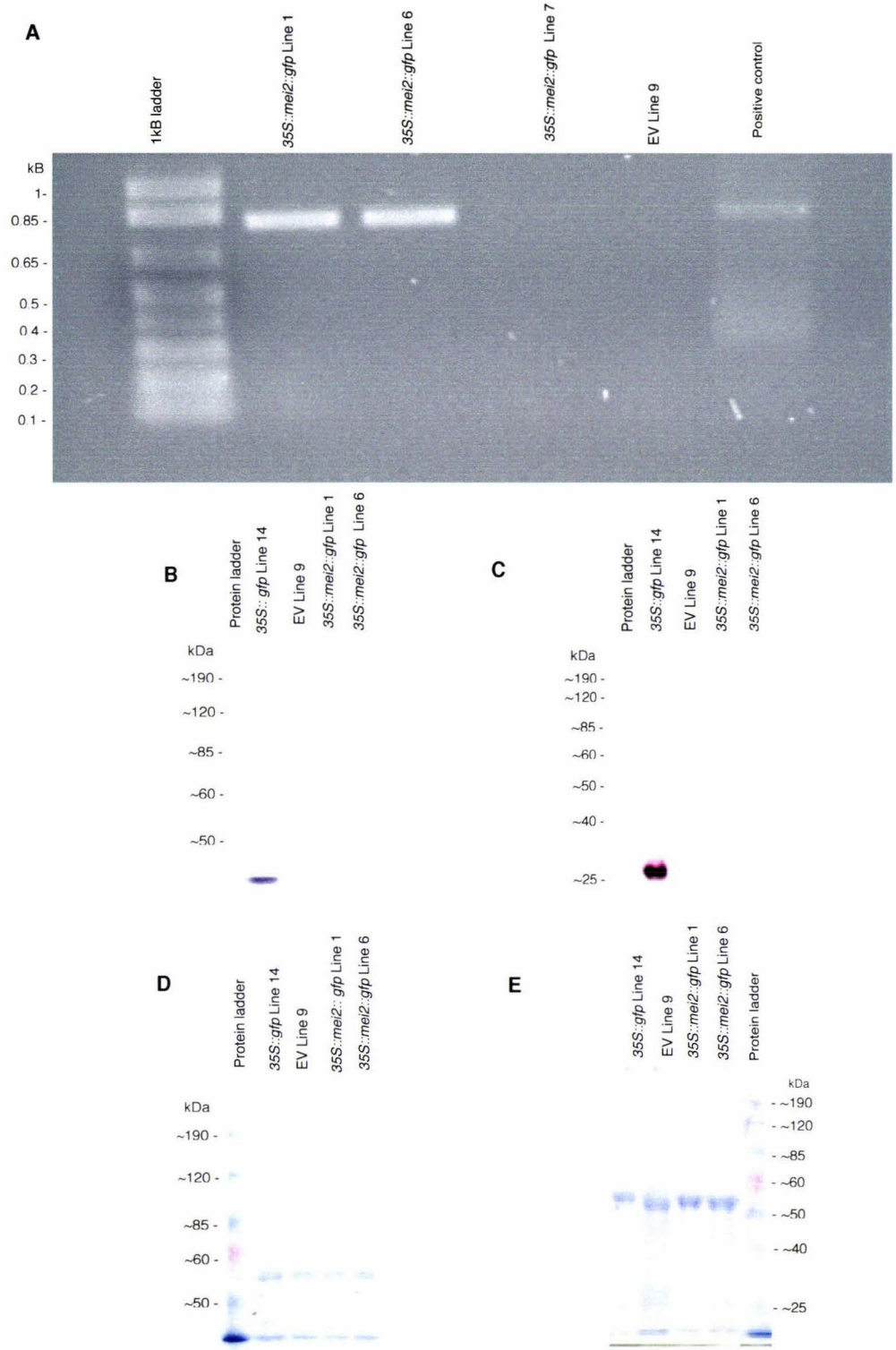

Figure 3.10 Transcriptional and translational analysis of *35S::mei2::GFP* plants. (**A**) RT-PCR showed the presence of *mei2::GFP* transcripts in Lines 1 and 6, but not in Line 7. The positive control was pMGB7 (refer to Figure 3.2 A) which contains the *mei2* gene. The presence of Mei2p::GFP in Lines 1 and 6 was analysed by the western blotting (**B**, **C**) by using anti-GFP as a primary antibody and anti-mouse IgG alkaline phosphatase conjugate as a secondary antibody. However, no Mei2p::GFP was detected in these two lines although the transcripts were present. Constitutive expression of GFP was detected in western blots (**B**, **C**). Coomaisse blue staining (**D**, **E**) showed the amount of proteins loaded for SDS-PAGE using a 7.5% (**B, D**) and a 10% (**C**, **E**) acrylamide gel.

3.4.8 Analysis of TEL1 expression in Arabidopsis thaliana

Previous work with *A. thaliana* using *in situ* hybridisation has showed that *TEL1* is expressed in the vegetative and embryonic SAM and the RAM (Alvarez, 2002). Based on this observation, the regulation of transcription of *TEL1* was investigated using GFP as a reporter gene. This is not related to subcellular localisation of Mei2-like proteins, rather, GFP was used as a reporter to show expression of *TEL1*. To do this, TEL1 promoter was fused with mGFP4-ER (Haseloff *et al.*, 1997; http://www.plantsci.cam.ac.uk/Haseloff/microscopy/gfpFrameset.html) and was transformed into *A. thaliana*.

Previous research had shown that *TEL1* expression is localised in the quiescent zone of the RAM using *in situ* hybridisation (Alvarez, 2002). Thus it would be expected that fluorescence of GFP should be detected at the tip of a root. In this thesis, two lines (Lines 2 and 9) out of fifty lines in total, showed fluorescence at the tip of root (Figure 3.11 A, B), confirming that expression of *TEL1* is active at the RAM. In comparison, in a plant line transformed with *35S::gfp*, the fluorescence signal was strong throughout the root (Figure 3.11 C). The root of the wild-type plant did not displaying any fluorescence (Figure 3.11 D).

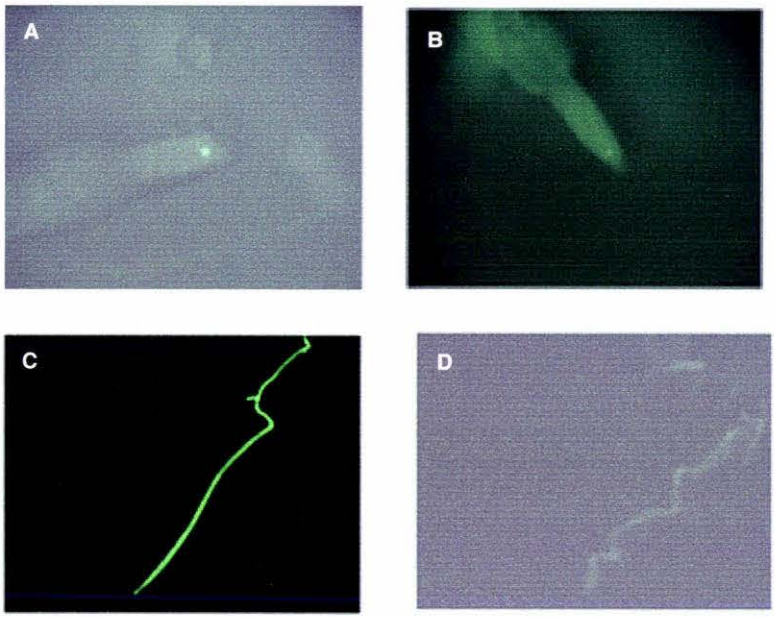

Figure 3.11 Analysis of the *TEL1* promoter. The *TEL1* promoter was fused with mGFP-ER and transformed into *A. thaliana*. Line 2 (**A**) and Line 9 (**B**) showed that fluorescence of GFP was detected at the tips of the roots. Compared to the root of *35S::gfp* plant line (**C**), the GFP fluorescence was more intense and was distributed evenly throughout the root. No fluorescence was detected in the root of the wild-type plant (**D**).

3.5 Discussion

3.5.1 Heterologous systems expressing the GFP-fused Mei2p

In *S. pombe*, Mei2p binds to its specific ligand, meiRNA, via RRM3, and targets the assembly to the nucleus (Yamashita *et al.*, 1998; Sato *et al.*, 2001). This mechanism of nuclear localisation is conserved in mammalian COS-7 cells (Yamashita *et al.*, 1998). To investigate whether the RNA-assisted transport of *S. pombe* Mei2p is conserved in plant cells, transient expression assays in onion epidermal cells were performed.

Compared with the distribution of GFP alone in the cells, GFP-tagged Mei2p was more concentrated in the nuclei of onion epidermal cells while GFP was distributed evenly in the cytoplasm (Figures 3.4, 3.5). However, nuclear localisation of Mei2p in the presence of meiRNA was not as clear as that observed in COS-7 cells. The results suggest that the localisation mechanism of Mei2p may not be as efficient in plant cells. Since the localisation behaviour of Mei2p was not well conserved in onion epidermal cells, transportation of RNA-binding proteins in plants may differ from that observed in fission yeast.

Another point that should be noted is the stoichiometric difference of expression of the Mei2p-GFP and meiRNA. The transcripts of *mei2::gfp* (and *gfp::mei2*) can be translated more than once, and so the expression of *mei2::gfp* is 'amplified'. For the expression of *sme2* (encoding meiRNA), the transcripts function directly in nuclear localisation of Mei2p. Therefore, the

amount of the GFP-fused Mei2p in the cell could be significantly greater than meiRNA. If one meiRNA was required to induce nuclear localisation of one Mei2p, then Mei2p-GFP would be in excess and might remain in the cytoplasm. Experimental support for this hypothesis could be obtained by comparing the populations of RNA transcripts of *mei2::gfp* and meiRNA. However, this would assume that the *mei2::gfp* mRNAs were in excess, and they would also be translated with equal efficiency.

In *S. pombe*, Mei2p moves between the cytoplasm and the nucleus, and meiRNA assists in the assembly of Mei2p in the nucleus (Sato *et al.*, 2001). Apart from meiRNA, other proteins in the nucleus may participate in the retention of Mei2p in the nucleus. However, those protein partners or similar proteins may not be present in onion epidermal cells, and so accumulation of Mei2p in the nucleus will not occur.

3.5.2 Importance of meiRNA in the GFP-fusion of Mei2p in onion epidermis

In transient expression assays of both *mei2::gfp* and *gfp::mei2*, no fluorescent signals were observed in the absence of meiRNA. It is unclear why there was no expression of Mei2p::GFP in the absence of meiRNA. One possible explanation is the GFP-tagged Mei2p might give low levels of fluorescent signals, which, combined with a diffusion effect of expression in the cytoplasm, might be below the detection limit. By contrast, Mei2p-GFP fusion binding of meiRNA might concentrate the proteins to the nucleus and enhance the fluorescent signal. Alternatively, the GFP-fused Mei2p might not be stable in the cytoplasm and so is degraded rapidly. Binding of meiRNA

may stabilise the proteins, allowing nuclear localisation of Mei2p and preventing its degradation in the cytoplasm.

3.5.3 Localisation of TEL2::GFP and promoter analysis of TEL1

TEL2, one member of the Mei2-like protein family in plants, carries three RRMs that are similar to those in Mei2p of *S. pombe* (Jeffares, 2001). Given the high similarity between the RRM domains of TEL2 and Mei2p, it is conceivable that intracellular localisation of TEL2 might be mediated by similar mechanisms to Mei2p of *S. pombe*. Transient expression of *TEL2::gfp* in onion epidermal cells showed that TEL2::GFP localised into the nucleus without co-expression of any RNA species. However, it is possible that the RNA species responsible for nuclear localisation of TEL2 are already present in onion epidermis, or, there could be fundamental differences in the mechanisms of intracellular localisation of RNA-binding proteins in plant cells from those observed in *S. pombe*.

In transient expression assays using *TEL2::gfp*, some inclusion bodies were formed in the cytoplasm. However, formation of inclusion bodies can be minimised by incubating the bombarded onion epidermal tissues at low temperature for several days. Minimising the formation of inclusion bodies allowed the nuclear localisation of TEL2::GFP to be clearly shown.

In *S. pombe*, *mei2* is possibly involved in RNA splicing, as one of the potential target RNA is unspliced *mes1* mRNA (Yamamoto, 1996). This splicing step would be essential for meiosis since *mes1* is a key gene in this process. In

support of this hypothesis, the first RRMs of Mei2p resemble those of splicesomal proteins (Yamamoto, 1996). The RRMs of TEL2 and Mei2p are highly similar, suggesting that TEL2 may also function in RNA splicing. However, it is not clear how this potential function of TEL2 is related to its pattern of intracellullar localisation.

Previous genetic studies showed that *TEL* genes are expressed in the SAM and the RAM in both vegetative and embryonic stages (Alvarez, 2002). In this thesis, the TEL1 promoter-driven GFP expression was detected at the tip of the root, suggesting that *TEL1* is actively expressed in the vegetative RAM. The results are similar to those of Alvarez (2002). Further experiments are required to show whether TEL proteins localise to the nucleus of the cells in the meristems, as GFP-tagged TEL protein can be stably expressed in *A. thaliana*. The localisation pattern of the GFP-fused TEL proteins in the meristems of *A. thaliana* can be observed under high magnification using an UV epi-fluorescence microscope.

3.5.4 Stable expression of 35S::mei2::gfp

Since no GFP fluorescence was detected in the onion epidermal cells transformed with either *mei2::gfp* or *gfp::mei2*, this would suggest that Mei2p-GFP may not be stable in plant cells without meiRNA, or meiRNA may be required for expression of *mei2*. Stable expression of *mei2::gfp* was driven by the constitutive CaMV 35S promoter, and so, theoretically, the expression of *mei2::gfp* should occur in all parts of the plants, and strong fluorescence was expected to be observed using the UV stereomicroscope.

In the GFP overexpression lines (*35S::GFP*), easily observable GFP expression was detected in only two lines out of 30 seedlings in the T2 generation. There are many possible explanations for this.

The first is that gene suppression may occur mediated through silencing of multiple copies of the transgene, or through position-effect-silencing of a single copy insertion. Alternatively, GFP is from *Aequorea victoria*, and so is a foreign protein in plants and may not be well expressed. Further, Haseloff (http://www.plantsci.cam.ac.uk/Haseloff/GFP/plantrans.html) has pointed out that regeneration can be decreased from plants strongly expressing GFP, as the protein may be slightly toxic to the plant cells.

GFP fluorescence was detected in three lines of the *35S::mei2::gfp* transformed plants. Since GFP itself might be slightly toxic to the plant cells and Mei2p is from *S. pombe*, the fusion of GFP and Mei2p might be more toxic or unstable in plants. In the *35S::mei2::gfp* plant lines, no obvious phenotypes were observed. They were similar in appearance to the plants containing an empty vector line (pART27) and to wild-type plants. Further, the size of the *35S::mei2::gfp* plants was normal. Although *mei2* is essential for meiosis in *S. pombe* (Watanabe and Yamamoto, 1994), the 'normal' phenotype of the *35S::mei2::gfp* plants suggests that *mei2* may not function in the same way in plant cells, as the cell cycle does not appear to be affected by the expression of *35S::mei2::gfp*.

The *35S::gfp* plants were smaller in size and less bushy when compared with the *35S::mei2::gfp* plants, and the plants containing the empty vector.

Mei2p::GFP might not affect the growth and regeneration of these plants because it is possible that Mei2p::GFP is degraded in plant cells. To address the expression of *mei2::gfp* in plants, RT-PCR was used for transcriptional analysis while western blotting was used for translational analysis. The results of RT-PCR showed that *mei2::gfp* transcripts were present in Lines 1 and 6 of the *35S::mei2::gfp* transformed plants but not in Line 7, even though all three lines grew in selective medium. The results of western blots showed that Mei2p::GFP was not observed in Lines 1 and 6 despite the presence of transcripts being detected by RT-PCR. The results suggested that Mei2p::GFP protein might not be stable in the transgenic plant background.

The other point to be noted is that in transient expression experiments, thousands of copies of *35S::mei2::gfp* were present in onion epidermal cells, but only a few cells expressed *mei2::gfp*. If, in the stable expression experiment, only one or a few copies of *35S::mei2::gfp* gene integrated in the *A. thaliana* genome, the expression rate would be much lower than that observed in the transient expression assay. Thus the fluorescent signal might not be detectable.

The *sme2* gene of *S. pombe* (encoding meiRNA) was not co-transformed into plants, but transcripts of *mei2::gfp* were present in Lines 1 and 6 of the *35S::mei2::gfp* transformed plants. Thus meiRNA might not be required for the expression of *mei2::gfp* in plant cells. In transient expression of *35S::mei2::gfp* in onion epidermal cells, no GFP signal was detected in the absence of meiRNA but the signal was detected in the presence of meiRNA. These results suggest that meiRNA may be required to prevent the

degradation of Mei2p::GFP in plant cells. Therefore, co-expression of *mei2::gfp* and *sme2* in plants may stabilise Mei2p::GFP sufficiently to permit detection of the fluorescent signal. Since both Mei2p and GFP are foreign proteins in plants and Mei2p::GFP is not functional, Mei2p::GFP may be degraded. Moreover, those foreign proteins may be toxic, and so degradation can overcome this problem. Therefore, inducible expression of *mei2::gfp* can be used to reduce any toxicity that may be caused by overexpression of *mei2::gfp* using the constitutive 35S CaMV promoter.

GFP was detected in the *35S::gfp* plants by western blots. The GFP signal of this *35S::gfp* plant line is not strong when observed under the UV stereomicroscope, but the band corresponded to GFP in the western blot was intense. This suggests that western blotting can serve as an alternate method to check the presence of GFP when the signal of GFP is not strong enough to be observed under the UV stereomicroscope.

3.6 Conclusions

In transient expression assays using onion epidermal cells, expression of *mei2::gfp* and *gfp::mei2* alone was not observed. The GFP signal of GFP-fusions of Mei2p could only be detected when meiRNA was also expressed. These results suggest that meiRNA may be required to stabilise the GFP-tagged Mei2p, and it is also possible that the GFP-fused Mei2p diffuses throughout the cytoplasm, and so is below the limit of detection. The meiRNA-assisted nuclear localisation mechanism of Mei2p of *S. pombe* is conserved in mammalian cells, but the nuclear localisation of Mei2p in plant cells is not as clear. In transient expression assays of *TEL2::gfp* into onion epidermis, TEL2::GFP protein could localise into the nucleus without co-expression of any RNA species. This suggests that either there are some RNA species present in the onion epidermal cells that assisted the nuclear localisation of TEL2, or that the mechanism of nuclear localisation of TEL2 is different from that of Mei2p.

In the stable expression experiments, plants transformed with *35S::mei2::gfp* did not exhibit any special phenotypes. They were similar to the plants containing the empty vector (pART27) and the wild-type plants. Moreover, no GFP fluorescence signal was detected under the UV stereomicroscope. RT-PCR detected transcripts of *mei2::gfp* in Line 1 and Line 6. However, western blot analysis did not detect the presence of the GFP-fusion of Mei2p in those two lines. This suggests that GFP::Mei2p might be degraded in plants since both Mei2p and GFP are foreign proteins

CHAPTER 4 ANALYSIS OF PROTEIN-PROTEIN INTERACTIONS INVOLVING TEL2 USING THE YEAST TWO-HYBRID SYSTEM

4.1 Overview

Although genetic studies suggest that *TEL* genes are involved in developmental regulation, the biochemical mechanism by which they act is unknown To address this question, the yeast two-hybrid system was exploited to identify potential protein partners of TEL2. Six proteins were identified in this assay, including the well-studied protein KORRIGAN. Based on the putative functions of protein interactors, speculation is offered on how any of these proteins may interact with TEL2 to control cell division in the central zone of the meristem.

4.2 Introduction

4.2.1 Brief introduction to the yeast two-hybrid system

Several *Mei2-like* genes are expressed in the SAM, suggesting that these genes are involved in development during plant growth (Alvarez, 2002). However, the biochemical mechanism by which these proteins function is not clear. For Mei2p of *S. pombe*, more biochemical information is available. Mei2p binds to a specific non-translated mRNA, meiRNA, *via* RRM3 (Watanabe and Yamamoto, 1994) and this binding is essential for localisation of Mei2p into the nucleus (Sato *et al.*, 2001). Although this data suggests that Mei2p activity requires RNA binding for localisation to the nucleus, the precise mechanism is unclear. Finally, localisation of Mei2p to the nucleus is essential for its meiosis-promoting activity.

Since the first two RRMs of Mei2-like proteins resemble those present in RNA splicing factors, one model is that Mei2-like proteins may regulate splicing. To test this hypothesis, the yeast two-hybrid assay was utilised to identify potential protein partners of Mei2-like proteins.

The two-hybrid system in yeast was created to study protein-protein interactions, utilising of the properties of the GAL4 protein of the yeast *Saccharomyces cerevisiae*. GAL4 consists of two functional domains: a N-terminal region that contains a DNA-binding domain (DB), which binds to specific DNA sequences (UAS_G), and a C-terminal domain that contains an activation domain (AD) which activates transcription (Figure 4.1). In the two-

hybrid system, the DB and the AD of GAL4 are split into separate proteins and each fused with another protein to create two hybrid proteins. The protein of interest is fused to the DB (DB-X), to form 'a bait' in the two-hybrid assay. A library of cDNA encoding potential protein partners is fused with the AD (AD-Y) to create prey proteins in the assay (Fields and Song, 1989). If a DB-X protein physically interacts with any of the AD-Y proteins, the interaction essentially reconstitutes the activity of the GAL4 transcriptional activator. Binding of this complex to a target promoter of GAL4 will then activate the expression of the associated gene (Vidal *et al.*, 1996a; Robinson and Brasch, 1998). Under different selective media for yeast growth, the phenotypes of yeast can show the interaction between two proteins of interest.

In this thesis, TEL2, one of the members of Mei2-like family, was selected to be a bait in the yeast two-hybrid system As mentioned above, interaction of the DB-TEL2 protein with any with its prey protein should activate the expression of the reporter genes, *HIS3* and *lacZ*. Activation of *HIS3* allows the *his3* mutant yeast strain to grow on a medium lacking histidine. The *lacZ* gene encodes β-galactosidase which cleaves an artificial substrate [5-bromo-4-chloro-3-indolyl-β-D-galactoside (X-gal)] to release a blue dye. Thus the interaction between the bait and the prey can be confirmed by screening blue colonies on the X-gal indication medium

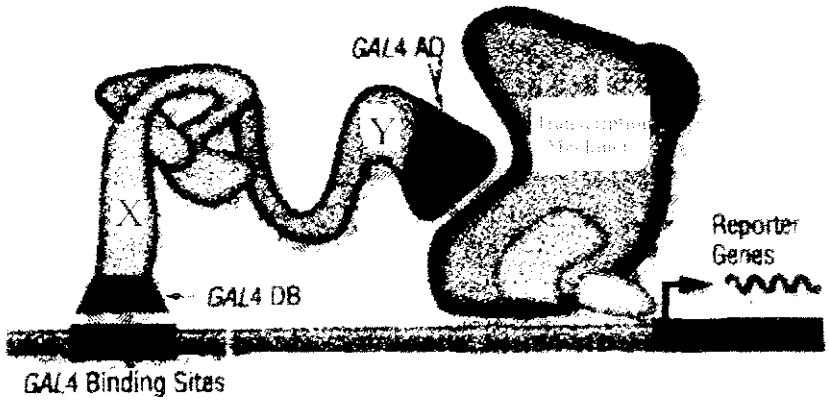

Figure 4.1 Schematic diagram to show the interaction between two fusion proteins (DB-X and AD-Y) in the yeast two hybrid system. DB-X binds to DNA at a specific GAL4 binding site while AD-Y interacts with the transcription machinery via the GAL4 activation domain. Transcription of the reporter gene is then activated (Life Technologies Bulletin)

4.3 Methods

Detailed protocols are described in Chapter 2. Procedures for the yeast two-hybrid assay are summarised in Figure 4.2.

Figure 4.2 Flow diagram of the yeast two-hybrid procedure.

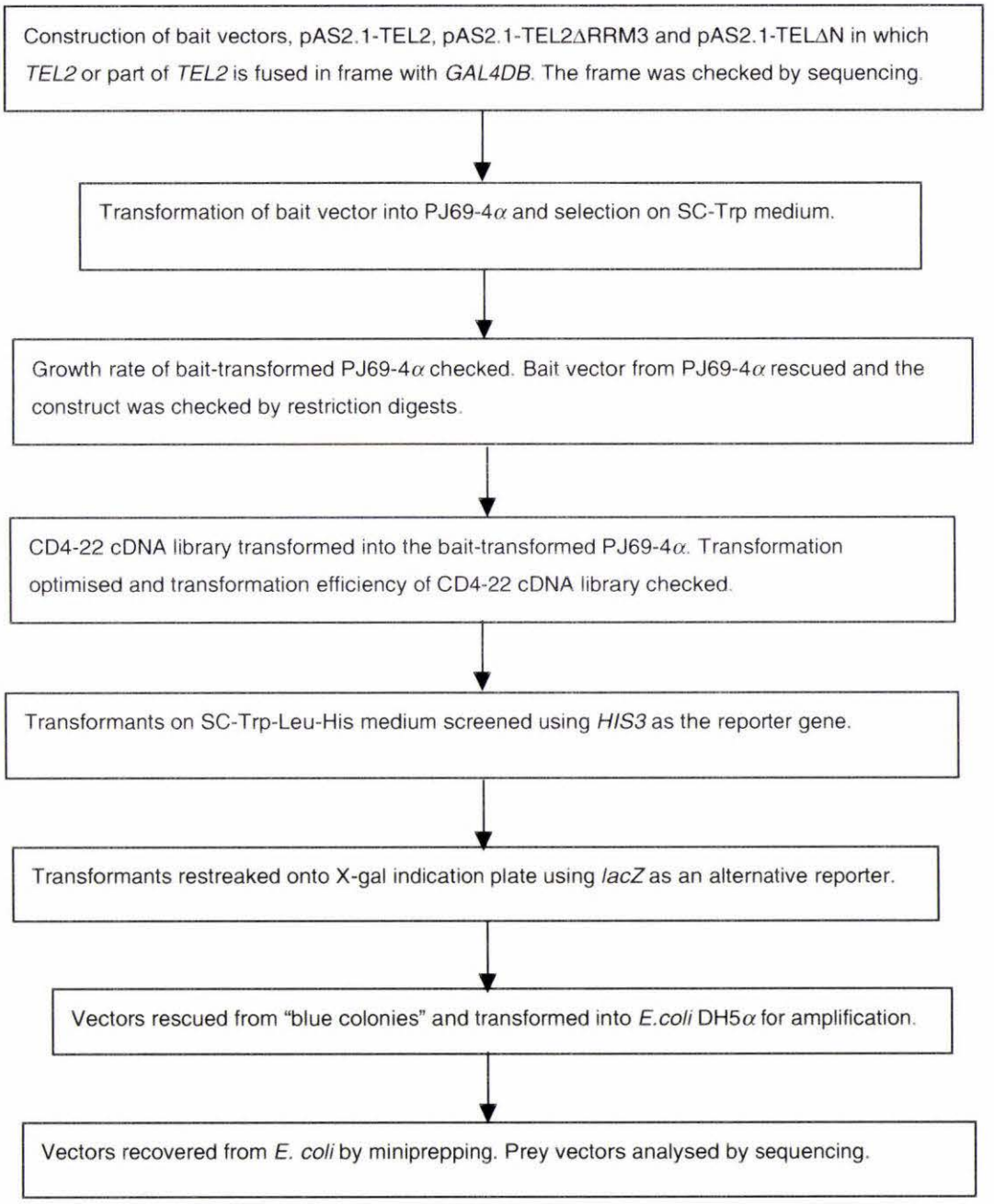

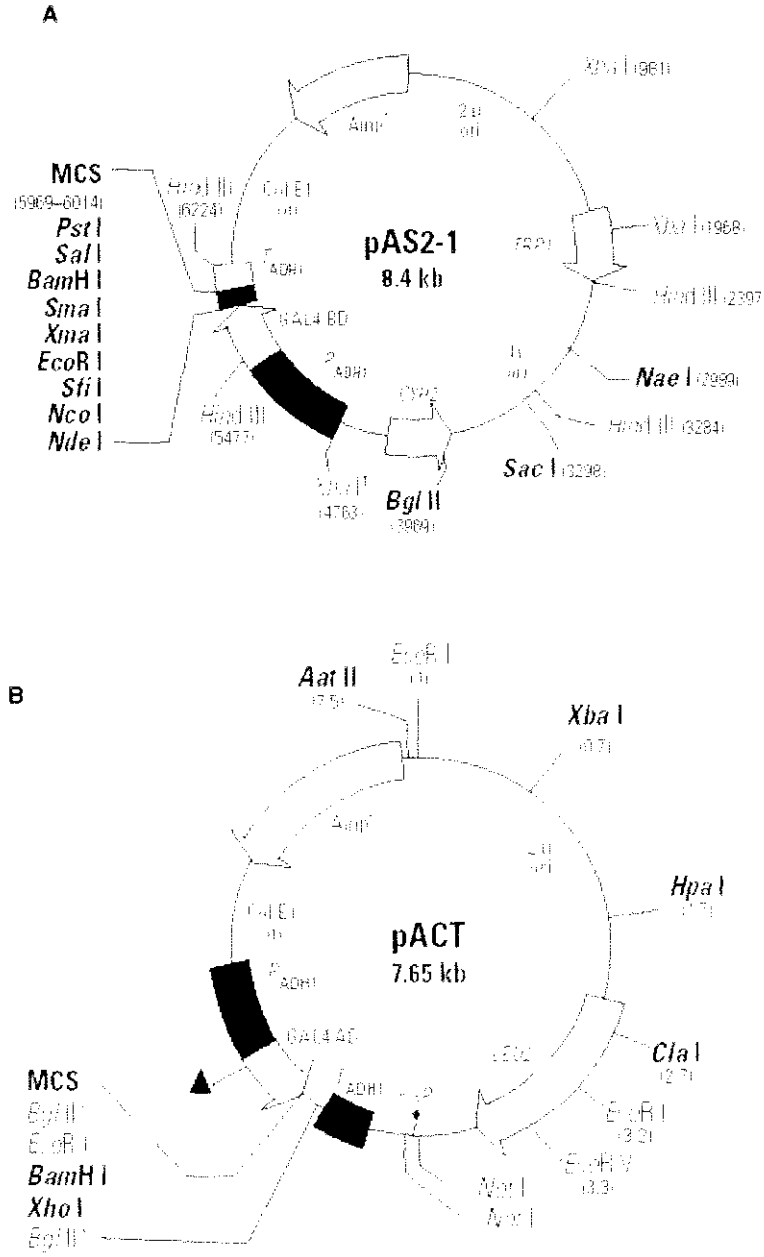

Figure 4.3 Plasmid vectors used in the yeast two-hybrid system. (**A**) pAS2.1, which contains the GAL4 DNA binding domain (GAL4DB), is the vector used for construction of the bait. The *TRP1* gene allows for selection in Trp⁻ auxotrophic yeast strain. (**B**) pACT, which contains the GAL4 activation domain (GAL4AD), is the vector used for construction of the prey. The *LEU2* gene allows for selection in Leu⁻ auxotrophic yeast strain.

4.4 Results

4.4.1 Bait vectors used in yeast two-hybrid system

To construct a bait vector, full length *TEL2* was fused in-frame with the GAL4 DNA binding domain (GAL4DB) of pAS2.1 to create pAS2.1-TEL2 (Figure 4.4 A). The growth rate was checked before transforming a CD4-22 cDNA library (refer to Figure 4.2). However, when compared to empty vector of pAS2.1, the full length of TEL2 and GAL4DB fusion transformants showed a retarded growth rate in PJ69-4α cells (Figure 4.5). In these experiments, the PJ69-4α cells transformed with pAS2.1-TEL2 did not exhibit any growth until 11 hours, whereas, PJ69-4α cells transformed with empty pAS2.1 started to grow after 7 hours (Figure 4.5). These results indicate that expression of full length *TEL2* suppressed the growth of PJ69-4α cells despite the fact that there are no *TEL2* or *mei2* orthologues in *S. cerevisiae*.

Since full length *TEL2* suppressed the growth of the PJ69-4α cells, the use of truncations of *TEL2* was investigated. Truncation of the N-terminal half of *TEL2* (the region containing RRMs 1 and 2), designed *TEL2ΔN*, and truncation of C-terminal half (the region containing RRM3), designed *TEL2ΔRRM3*, were fused with the GAL4DB and transformed into PJ69-4α. In growth experiments, the lag periods of these transformed PJ69-4α cells were shorter compared to that of full length *TEL2* (Figure 4.5). The lag periods of the truncated *TEL2* transformants were around 8 hours, which was similar to PJ69-4α cells transformed with empty pAS2.1, whose lag period was slightly

less than 8 hours (Figure 4.5). Thus the growth rates of *TEL2ΔN* and *TEL3ΔRRM3* transformants were similar to the empty pAS2.1 (Figure 4.5), indicating that neither the N-terminus nor the C-terminus of TEL2 affected the growth of PJ69-4α cells when compared with full length *TEL2*. However, the growth rates of PJ69-4α cells transformed with pAS2.1-TELΔN and those transformed pAS2.1-TEL2ΔRRM3 were still slower than that of transformants containing the empty pAS2.1 (Figure 4.5).

In summary, full length *TEL2* transformatins retarded the growth of PJ69-4α, although the cause of reduced growth rate was not determined in this study. Truncation of *TEL2* appears to ameliorate the reduced growth to some degree.

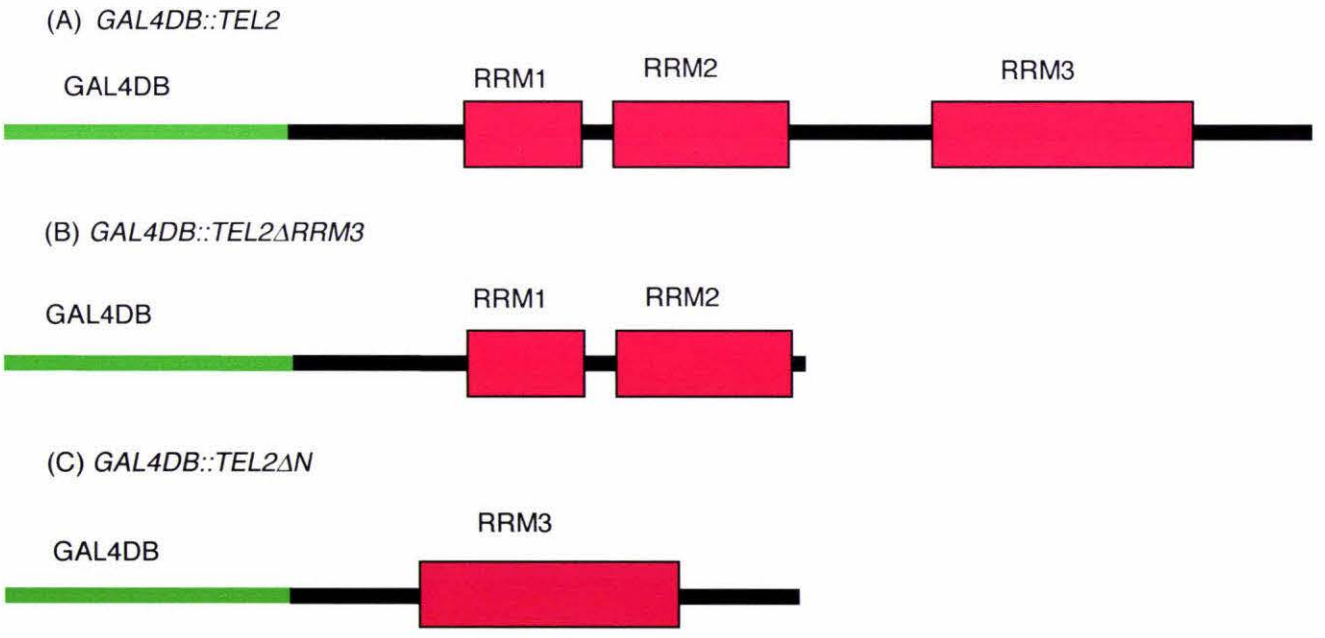

Figure 4.4 Bait vectors used in the yeast two-hybrid system. TEL2 carries three RNA recognition motifs (RRMs): RRM1, RRM2 and RRM3. Full length *TEL2* (~1.7 kb), and C- and N-terminal truncations of *TEL2* (~ 0.75 kb each) were fused to *S. cerevisiae* GAL4 DNA binding domain (GAL4DB) as pAS2.1-TEL2 **(A)**, pAS2.1-TEL2ΔRRM3 **(B)** and pAS2.1-TEL2ΔN **(C)**, respectively.

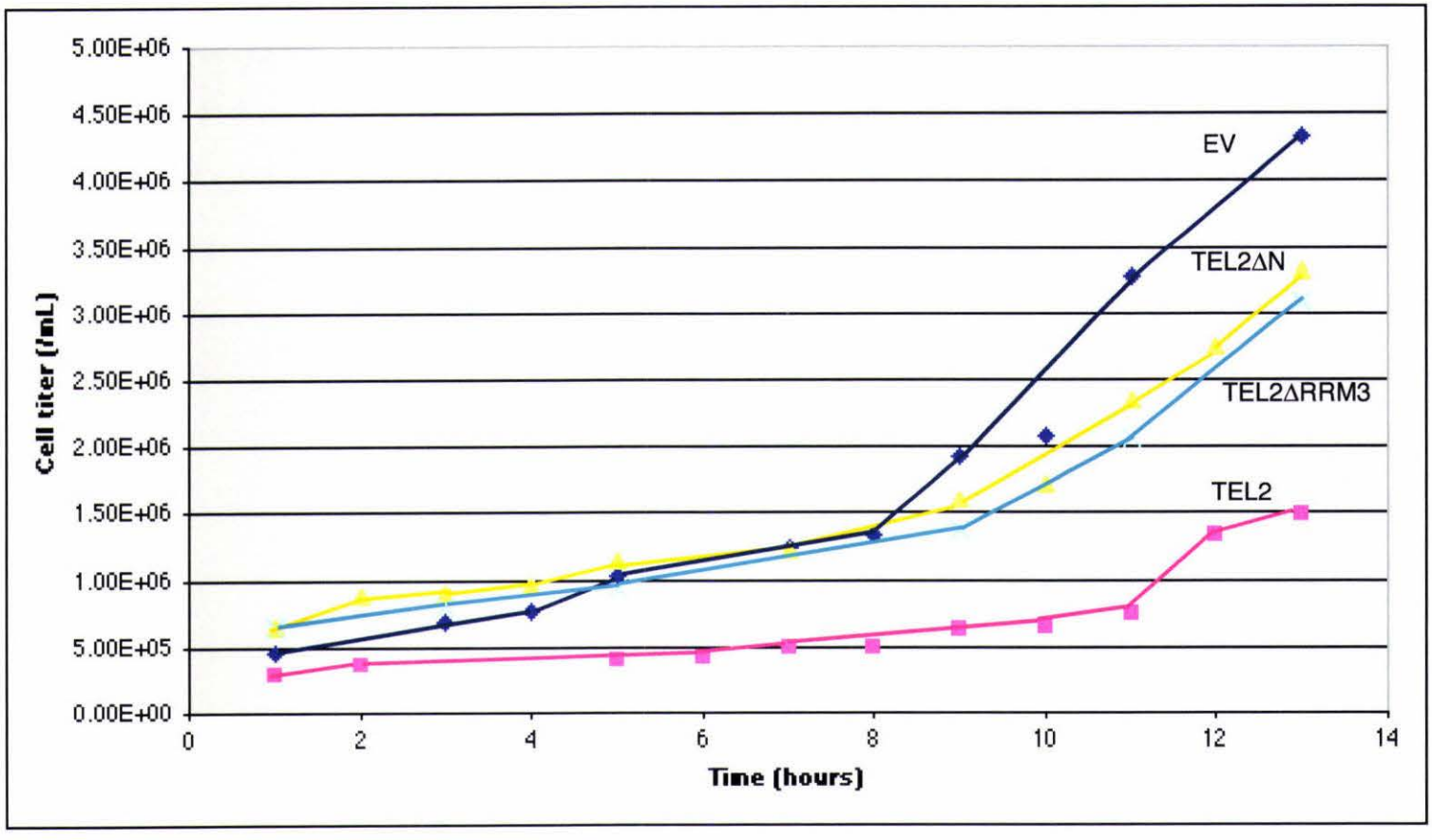

Figure 4.5 Growth of PJ69-4α cells transformed with different bait vectors. The cells were grown in SC-Trp media overnight, then cells were pelleted and inoculated into 2 x YPAD media. The cells were taken and the cell titers were determined over time. Keys: TEL2 is pAS2.1-TEL2; TEL2ΔRRM3 is pAS2.1-TEL2ΔRRM3; TEL2ΔN is pAS2.1-TEL2ΔN; EV is empty vector of pAS2.1.

4.4.2 Checking leaky HIS3 expression in bait-transformed PJ69-4α cells

The *HIS3* gene is one of the common reporter genes used with the yeast two-hybrid procedure to show protein-protein interactions with the protein of interest. The expression of *HIS3* is activated when the bait protein interacts with the prey protein. However, *HIS3* expression is sometimes leaky which means that *HIS3* expression may occur in yeast host cells transformed with the bait vector only, resulting in growth in cells in which no bait-prey interaction occurs. This leaky *HIS3* expression can be suppressed by 3-amino-1,2,4-triazol (3-AT) since 3-AT is a competitive inhibitor of the enzyme encoded by *HIS3* (Vidal *et al.*, 1996b).

After transformation of bait vectors into PJ69-4α, expression of *HIS3* and *LEU2* (a selectable marker for prey vectors) were checked by streaking colonies that appeared on SC-Trp onto SC-His and SC-Leu plates. All PJ69-4α cells transformed either with pAS2.1-TEL2-, pAS2.1-TEL2ΔN-, or pAS2.1-TELΔRRM3- failed to grow in SC-Leu medium (medium without leucine) (Figure 4.6 B, E, H) but grew well in SC-Trp medium (Figure 4.6 A, D, G). PJ69-4α cells transformed with either pAS2.1-TEL2- and pAS-TEL2ΔRRM3 did not grow in SC-His medium, but PJ69-4α cells transformed with pAS2.1-TEL2ΔN did (Figure 4.6 C, F, I). Non-transformed PJ69-4α cells did not grow on any either SC-His or SC-Leu media (Figure 4.6).

The level of 3-AT required to suppress leaky *HIS3* expression was also determined. A Yeast culture was grown in the selective (SC-Trp) medium

overnight at 30°C, and 100μL of culture was plated onto different concentrations of 3-AT. The PJ69-4α cells transformed with pAS2.1-TEL2 grew on SC-His medium containing 0.2 mM 3-AT, but not 0.5 mM 3-AT. This indicated that 0.3 mM to 0.5 mM 3-AT was required to suppress leaky *HIS3* expression caused by transformation of pAS2.1-TEL2. PJ69-4α cells transformed with pAS2.1-TEL2ΔN showed growth on SC-His medium (3 colonies observed), but 0.2 mM 3-AT was enough to suppress any leaky *HIS3* expression.

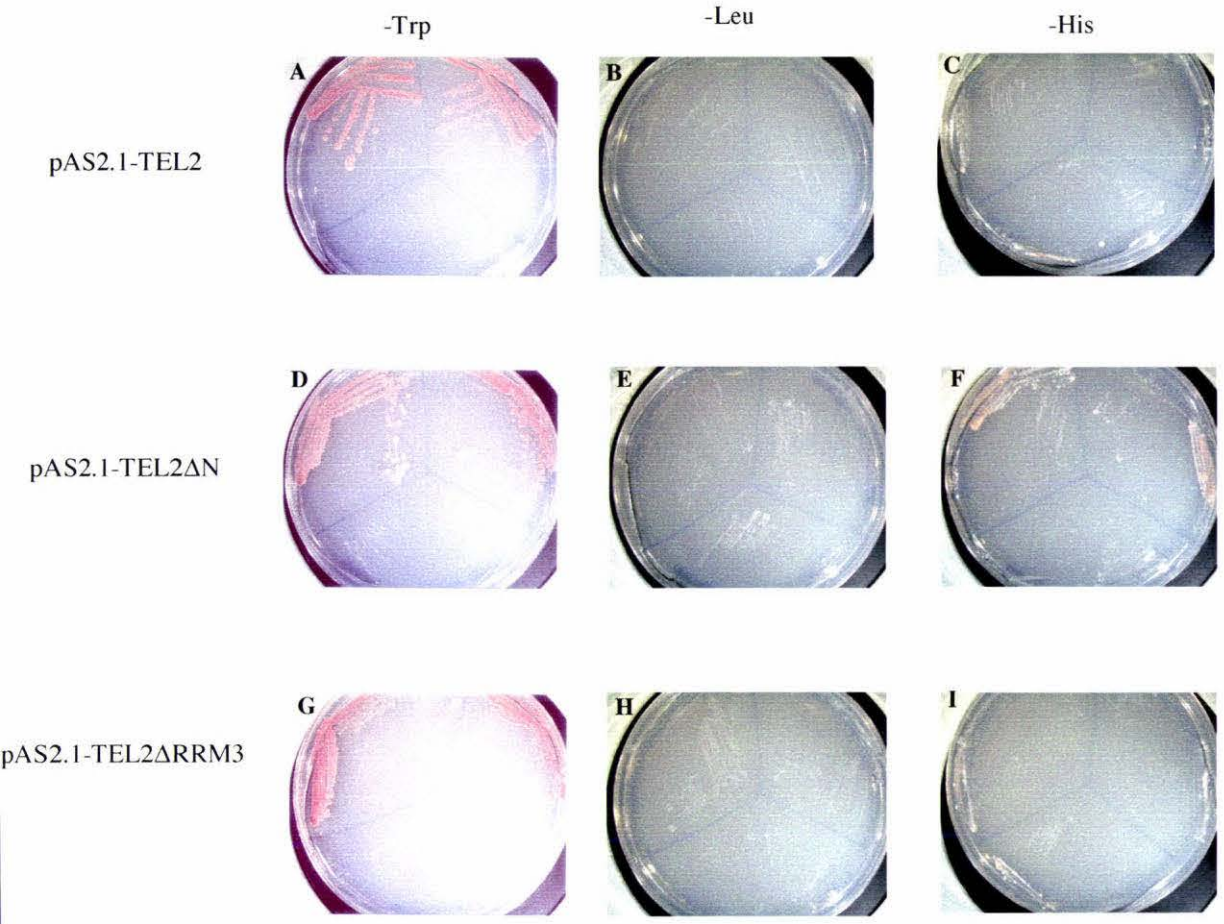

Figure 4.6 Growth of bait vector-transformed PJ69-4α cells on different selective media. PJ69-4α cells containing specified plasmids, pAS2.1-TEL2 (**A**, **B** and **C**), pAS2.1-TEL2ΔN (**D**, **E** and **F**) and pAS2.1-TEL2ΔRRM3 (**G**, **H** and **I**) were grown on SC-Trp (**A**, **D** and **G**), SC-Leu (**B**, **E** and **H**) and SC-His (**C**, **F** and **I**). *TRP1* is a selectable marker of the bait vector while *LEU2* is a selectable marker for the prey vector. *HIS3* is one of the reporter genes used in the yeast two-hybrid system. Colonies were picked and restreaked on the top two segments. Non-transformed PJ69-4α was restreaked on the bottom segment and showed that non-transformed PJ69-4α could not grow on the selective media. All the cells were grown at 30^0C for 2-4 days.

Table 4.1 Levels of 3-amino-1,2,4-triazol (3-AT) required to suppress leaky *HIS3* expression in PJ69-4α cells transformed with different bait vectors

		Number of colonies		
Vol. of 0.1M 3-AT stock added to the plate (μL)	**Conc. of 3-AT (mM)**	**pAS2.1-TEL2**	**pAS2.1-TEL2ΔN**	**pAS2.1-TEL2ΔRRM3**
0	**0.0**	2	3	0
60	**0.2**	1	0	0
150	**0.5**	0	0	0
240	**0.8**	0	0	0
300	**1.0**	0	0	0
360	**1.2**	0	0	0

PJ69-4α cells containing specified plasmids were grown in SC-Trp medium 30°C overnight. 100μL of culture was plated on each plate, and 0.1M 3-AT stock was added as indicated above. The concentration was calculated assuming that there was 30mL of medium in each plate. All the cells were incubated at 30°C for 2-4 days.

4.4.3 Transformation of CD4-22 cDNA library into bait-transformed PJ69-4α

Given that the truncated versions of *TEL2* did not effect yeast growth, these deletion derivatives were chosen as the bait vectors in the yeast two-hybrid system. To achieve the highest possible transformation efficiency, a number of small scale transformations were performed using different amounts of the CD4-22 cDNA library. The transformation efficiencies of the CD4-22 cDNA library on PJ69-4α with the two truncated versions of *TEL2*, designated as pAS2.1-TEL2ΔN and pAS2.1-TEL2ΔRRM3 were compared, and the best transformation results are summarised in Table 4.2. In general, a larger total number of transformants could be obtained when more CD4-22 cDNA library was used in each transformation reaction.

However, the transformation efficiency decreases when the amount of cDNA library used in a single reaction is increased (Table 4.2). The transformation efficiency of the CD4-22 cDNA library into pAS2.1-TEL2ΔRRM3-transformed PJ69-4α cells was higher than that observed for the pAS2.1-TEL2ΔN-transformed PJ69-4α cells (Table 4.2).

Table 4.2 Transformation efficiency of the CD4-22 cDNA library into bait vector-transformed PJ69-4α cells

	pAS2.1-TEL2ΔN		
Amount of CD4-22 cDNA (μg)	**Number of colonies**	**Number of transformants in total**	**Transformation Efficiency (/μg DNA)**
0.0	0	0	0
0.1	9	9.0×10^2	9.0×10^3
0.5	15	1.5×10^3	3.0×10^3
1.0	18	1.8×10^3	1.8×10^3
2.0	23	2.3×10^3	1.2×10^3

Table 4.2 (Continued)

	pAS2.1-TEL2ΔRRM3		
Amount of CD4-22 cDNA (μg)	**Number of colonies**	**Number of transformants in total**	**Transformation Efficiency (/μg DNA)**
0.0	0	0	0
0.1	19	1.9×10^3	1.9×10^4
0.5	27	2.7×10^3	5.4×10^3
1.0	58	5.8×10^3	5.8×10^3
2.0	79	7.9×10^3	4.0×10^3

For transformation of the CD4-22 cDNA library, the bait-containing PJ69-4α cells, were heat-shocked for 30 minutes at 42°C. After the CD4-22 cDNA library transformation, the cells were resuspended in 1mL of water, and one tenth of the volume (0.1mL) of a 10-fold dilution was plated on each plate. The cells were grown at 30°C for 2-4 days.

4.4.4 Yeast two-hybrid screen

In the yeast two-hybrid screen, the pAS2.1-TEL2ΔN truncation was chosen as the bait vector since the C-terminal region of TEL2 containing the RRM3 is the most conserved region with respect to Mei2p. Moreover, this N-terminal region of Mei2p is known to be essential for nuclear localisation and for the promotion of meiosis (Watanabe and Yamamoto, 1994; Yamashita *et al.*, 1998).

For the yeast two-hybrid screen, cDNA library transformation was set as a 30X scale, and 30μg of the CD4-22 cDNA library was used. One thirtieth of an undiluted cell suspension was plated on a SC-Trp-Leu plate to determine the transformation efficiency of the CD4-22 cDNA library into PJ69-4α cells transformed with pAS2.1-TELΔN.

Around 500 colonies appeared on this SC-Trp-Leu plate, and so the total number of transformants that contained both the bait and the prey was calculated as 1.5×10^4. Eight colonies were found on SC-Trp-Leu-His plates (*HIS3* is one of the reporter genes) after seven days of incubation. Those 8 *his*$^+$ colonies were picked and restreaked on the X-gal indication plates. Six yeast lines appeared 'blue' on X-gal indication plates while 2 lines (#1 and #4) appeared 'white' (Figure 4.7 A, B, C and D). The intensities of the blue colour of the transformed colonies of two-hybrid screen were compared with the positive control comprising murine p53 as the bait and SV40 large T antigen as a prey (Figure 4.7 E). The growth rate of the positive control was much higher than the *his*$^+$ transformants obtained in this two-hybrid screen, suggesting that the protein-protein interactions between the C-terminus of TEL2 and the prey proteins were not very strong.

The prey vectors were rescued from the PJ69-4α cells and were amplified in *E. coli* DH5α. Ten *E. coli* colonies were picked for each '*his*$^+$ transformant' line, the plasmid isolated and DNA samples then sequenced. BLASTn of TAIR and BLASTn of NCBI searches were performed with the resulting sequences, and the results are summarised in Table 4.3.

Table 4.3 Proteins identified in yeast two-hybrid screens

Lines (*his*$^+$ trans-formants)	Growth rate	Protein identified	Accession number at TAIR	References	E values (BLASTn search)	E values (BLASTx search)
#2	+	Cynase	At3g23490	Nil	0.0	3e-86
#3	+	KORRIGAN	At5g49720	Zuo *et al.*, 2000	0.0	1e-59
#5	++	Expressed protein	At1g52200	Nil	e-156	2e-44
#6	+	Ferredoxin precursor isolog	At1g10960	Nil	0.0	2e-41
#7	++	EF-hand Ca^{2+}-binding protein-like	At5g04170	Nil	e-151	3e-23
#8	++	Protein containing lipase domain	At1g28660	Brick *et al.*, 1995	0.0	e-121
Positive control	+++					

From the BLASTn search results, the following proteins were identified: KORRIGAN was identified in Line #3; a ferredoxin precursor isolog was identified in Line #6; an EF-hand Ca^{2+}-binding protein-like was identified in Line #7; a protein containing a lipase domain in Line #8, cyanase was identified in Line #2, and an expressed protein in Line #5 (Table 4.3). The BLASTx search was performed to confirm the results obtained in the BLASTn search, and the results from BLASTx were the same as those from the BLASTn search. The sequences of the prey cDNA were checked and were shown to be fused in-frame with the GAL4 AD. By replica plating, the *his*$^+$ phenotype of the PJ69-4α cells was shown to be dependent on the presence of both bait and prey plasmids, since if either bait or prey vector was lost from the host cells, PJ69-4α would be unable to grow on media lacking histidine

(data not shown).

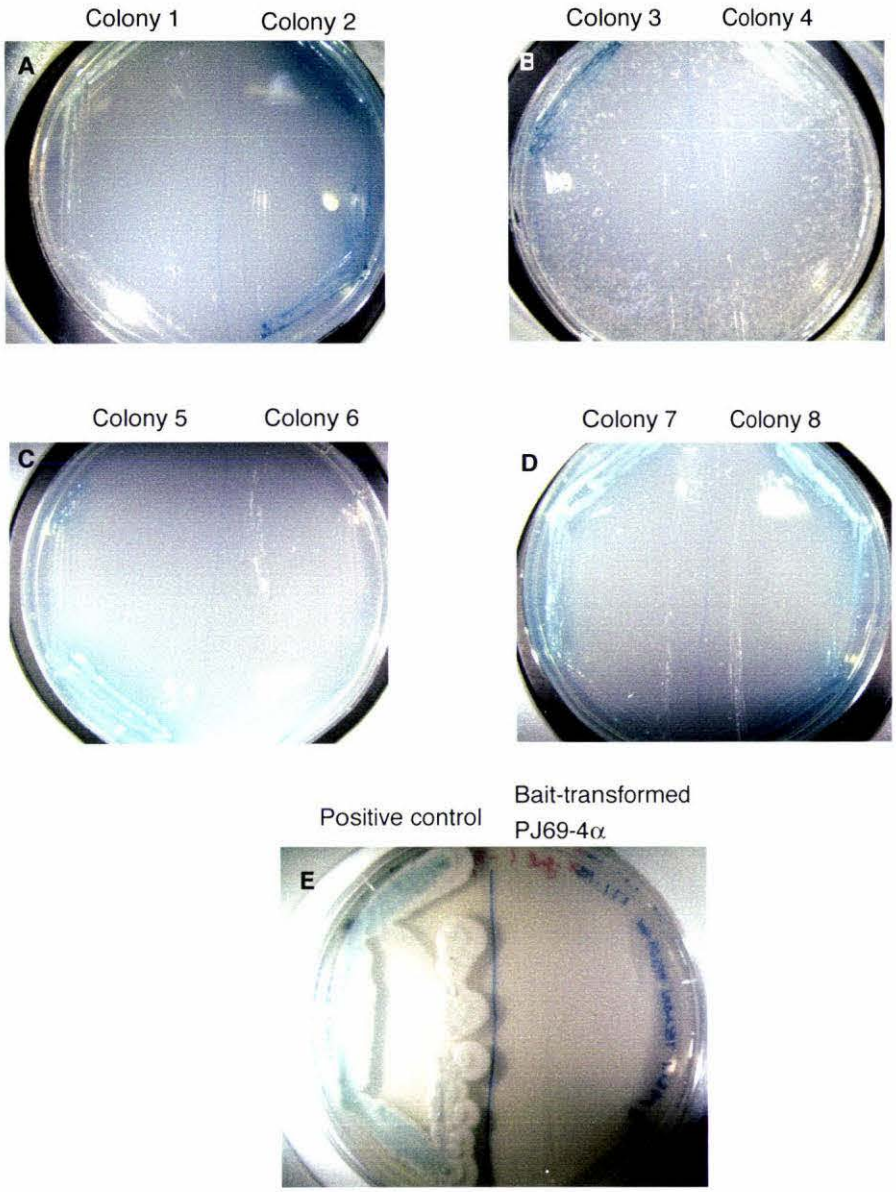

Figure 4.7 Colonies from the yeast two-hybrid screen grown on X-gal indication plates. Eight colonies were picked from SC-Trp-Leu-His plates, and restreaked on X-gal indication plates which were also selected on *trp*$^+$, *leu*$^+$ and *his*$^+$ transformants (**A**, **B**, **C** and **D**). Thus both the bait and the prey vectors were maintained and *HIS3* reporter remained active. The positive control (**E**, left hand side) was also restreaked to show that the *LacZ* gene was active. The positive control is murine p53 as the bait and SV40 large T antigen as a prey. The bait vector (pAS2.1-TEL2ΔN)-transformed PJ69-4α cells (**E**, right hand side) did not show any *LacZ* activity.

4.4.5 Factors affecting transformation of CD4-22 cDNA library into pAS2.1-TEL2ΔN transformed PJ69-4α

Since the total number of transformants obtained in the yeast two-hybrid screen was low, various factors that affect transformation efficiency (e.g. length of time for heat shock) were optimised in an attempt to achieve a higher transformation efficiency.

The optimal length of time for heat shock was tested on non-transformed PJ69-4α cells. The results suggested that ten minutes heat shock was sufficient to give a total number of 6.55 x 10^3 transformants. A longer heat shock time decreased the viability of cells, such that after 40 minutes of heat shock, the total number of transformants decreased to 1.35 x 10^3 (Table 4.4). Another yeast strain, 332, which is a yeast strain not normally used for the yeast two-hybrid system was used as comparison with PJ69-4α. In this strain, 40 minutes heat shock increased the number of transformants to 6.5 x 10^3, while only 5 x 10^2 transformants were obtained after 10 minutes of heat shock (Table 4.4).

Table 4.4 Length of heat shock time affecting transformation efficiency of two strains of yeast

	Strain 332			**Strain PJ69-4α**		
Time for heat shock (min)	Amount of plasmid DNA (μg)	Total No. of transformants	Transformation efficiency (/μg)	Amount of plasmid DNA (μg)	Total No. of transformants	Transformation efficiency (/μg)
10	0.78	5 x 10^2	6.4 x 10^2	0.195	6.5 x 10^3	3.3 x 10^4
20	0.78	2 x 10^3	2.6 x 10^3	0.195	2.9 x 10^3	1.5 x 10^4
40	0.78	6.5 x 10^3	8.3 x 10^3	0.195	1.4 x 10^3	7.2 x 10^3

Based on the heat shock optimisation results using non-transformed PJ69-4α cells, transformation of CD4-22 cDNA library into the bait (pAS2.1-TEL2ΔN) transformed PJ69-4α cells was also tested with different lengths of heat shock time. In these experiments, the total number of transformants from a 10-minute heat shock was lower than that observed from a 20- and 40-minute heat shock. Moreover, more colonies appeared on the SC-Leu medium when compared with the SC-Trp-Leu medium (Table 4.5). These results suggest that the bait vector might not be well maintained in the PJ69-4α cells.

Table 4.5 Length of heat shock time for transformation of CD4-22 cDNA library into PJ69-4α

		Total number of colonies	
Time for heat shock (min)	Amount of CD4-22 cDNA library (μg)	SC-Trp-Leu	SC-Leu
10	0.8	1.2×10^3	6.2×10^4
20	0.8	3.4×10^3	6.8×10^4
40	0.8		1.2×10^5

To test how well the bait vector was maintained in PJ69-4α, these cells were transformed with the bait vector, grown in the SC-Trp medium overnight, and then equivalent numbers of cells were plated on YPD and SC-Trp plates. If there is strong selection for maintenance of the *TRP1* marker and the plasmid is mitotically stable, the number of colonies on SC-Trp and YPD plates should be similar. However, despite the bait-vector transformed PJ69-4α cells being grown in the selective medium overnight, the number of colonies observed on SC-Trp plate was only one tenth of that observed on the YPD plate (Table 4.6). Similar results were obtained in PJ69-4α cells transformed with the

empty vector (Table 4.6), indicating that the insert, the C-terminal of *TEL2*, and the full length *TEL2*, might not contribute substantially to the loss of plasmid from the host cells.

The number of colonies of the PJ69-4α cells transformed with full length *TEL2* on the YPD plate was less than that of cells transformed with the empty vector or pAS2 1-TEL2ΔN, indicating that the growth rate of full length *TEL2*-transformed PJ69-4α cells was reduced. This agreed with the observations described in Section 4.4.1

Table 4.6 Maintenance of different bait vectors in PJ69-4α

	Cell titer (/mL)		
Vector	YPD	SC-Trp	**Cells maintaining bait vector**
pAS2 1	1.3×10^6	1.3×10^5	9.6%
pAS2.1-TEL2ΔN	9.0×10^5	9.1×10^4	10.1%
pAS2 1-TEL2	6.7×10^5	6.4×10^4	9.5%

The bait vector transformed PJ69-4α was grown at 30°C overnight in SC-Trp medium before plating on the plates.

Since the insert of *TEL2* did not affect the maintenance of the bait vector in the PJ69-4α cells, factors affecting the loss of the bait vector might come from the host cells. Another two yeast strains used for yeast two-hybrid assay, Y190 and CG-1945, and 332 (a yeast strain not normally used for two-hybrid assay), were transformed with the empty bait vector pAS2.1, and the results summarised in Table 4.7. In these experiments, maintenance of pAS2.1 in Y190 was better than that in PJ69-4α, but CG-1945 did not

maintain in pAS2.1 as well, with only 7.7% of cells containing the bait vector. However, pAS2.1 appears to be lost at a high frequency in all yeast strains trialed.

Table 4.7 Maintenance of the empty bait vector, pAS2.1, in various yeast strains

Yeast strain	Cell titer (/mL)		Cell maintaining bait vector
	YPD	SC-Trp	
PJ69-4α	7.52×10^5	7.50×10^4	10.0%
Y190	3.57×10^6	8.20×10^5	23.0%
CG-1945	2.98×10^6	2.30×10^5	7.7%
332	5.65×10^6	1.46×10^6	25.8%

4.5 Discussion

4.5.1 Full length and truncation of TEL2 affecting growth of PJ69-4α

Plant *Mei2-like* genes are expressed in the SAM. The expression patterns and mutant phenotypes of *Mei2-like* genes suggest that these genes may be involved in plant development, and possibly influence cell division and/or differentiation processes. However, the biochemical mechanisms and functions of *Mei2-like* genes remain unclear. The plant Mei2-like proteins contain three RRMs which are highly similar to those in *S. pombe* Mei2p (Veit *et al.*, 1998). Furthermore, RRM1 and RRM2 of Mei2p resemble those of splicesomal proteins, suggesting that Mei2-like proteins may be involved in RNA splicing (Yamamoto, 1996). To test this hypothesis, the yeast two-hybrid system was used to identify proteins which are capable of physically interacting with plant Mei2-like proteins.

Expression of full length TEL2 had a marked effect on the growth of the yeast PJ69-4α cells (Figure 4.3), and expression of full length *TEL2* in *E. coli* has also shown the same effect on growth (V. Trainor, unpublished data). These results suggest that overexprssion of RRM containing proteins can interfere with growth in other organisms. Moreover, the number of RRMs expressed in *S. cerevisiae* affected growth since truncation of *TEL2* (elimination of some RRMs) reduced the slow growth phenomenon in PJ69-4α (Figure 4.3).

Expression of full length *TEL2* might not lead to the death of yeast cells since cell number increased over time despite the fact that the lag phase was longer

in the *TEL2* transformed cells when compared with PJ69-4α cells transformed with the empty vector pAS2.1.

4.5.2 Protein interactions with the RRM3 domain of TEL2

The Mei2p of *S. pombe* binds to its ligand, meiRNA, *via* RRM3 (Yamashita *et al.*, 1998). In this thesis, pAS2.1-TEL2ΔN was chosen as the bait because the C-terminal region carries RRM3. This domain shows the highest similarity to RRM3 of Mei2p, and suggests that this unusual RRM is highly conserved between fission yeast and plants

Although only a small number of prey containing transformants were recovered from the yeast two-hybrid system, the following potential protein interactors with TEL2 were identified: a) KORRIGAN; b) an EF-hand Ca^{2+}-binding protein-like; c) a protein containing lipase domain; d) a ferredoxin precursor isolog; e) a cyanase and f) an expressed protein. Based on the biochemical properties of these proteins, speculation is offered on how they might contribute to *TEL2* function.

(a) KORRIGAN

KORRIGAN (*KOR*) encodes a putative endo-1,4-β-glucanase which is essential for cellulose synthesis during the formation of a cell plate (Zuo *et al.*, 2000; Sato, S. *et al.*, 2001). KOR localises from the plasma membrane (Nicol *et al.*, 1998) to the cell plate for cell wall assembly by polarisation (Zuo *et al.*, 2000). Mutation of the *KOR* gene results in aberrant cell plates, incomplete

cell walls and multinucleated cells. *kor* mutants also exhibit shorter seedlings and an irregular cell division pattern, suggesting that *KOR* is essential for cytokinesis (Zuo *et al.*, 2000).

KOR consists of a transmembrane domain and a cytosolic tail, and two polarised targeting motifs, LL and YXXΦ, are present in the cytosolic tail (Zuo *et al.*, 2000). The C-terminal half of TEL2 may interact with the cytosolic tail of KOR to prevent KOR from localising to the cell plate in the central zone of meristem causing a reduction of the rate of cell division in the central zone compared to other zones. In summary, expression of *TEL2* may limit *KOR* participation in cytokinesis.

(b) EF-hand calcium-binding protein-like

Another protein interactor identified in the yeast two-hybrid system is an EF-hand calcium-binding protein-like which is 37 kDa, contains 354 residues, and there are two EF-hand motifs found in the protein (Day *et al.*, 2002). Day *et al.* (2002) have analysed EF-hand-containing proteins of *A. thaliana*, and based on phylogenetic analysis, the EF-hand calcium-binding protein-like identified in this study is in "Group V", the same group as the Ca^{2+}-dependent protein kinases (CDPK) and the CDPK-related kinases (CRKs). Both CDPK and CRK contain the kinase domain, and CDPK carries four EF-hand motifs while CRK has one EF-hand motif. CDPK also contains an N-terminal variable domain, an autoinhibitory domain and a calmodulin-like domain (Cheng *et al.*, 2002). However, the EF-hand like protein identified in this

thesis only contains 2 EF-hand motifs and none of the other domains were identified (Day *et al.*, 2002). This EF-hand like protein can bind to two Ca^{2+}.

In low concentrations of free Ca^{2+}, the autoinhibitory domain of CDPK binds to the kinase domain and keeps substrate phosphorylation activity low. However, as the concentration of Ca^{2+} increases, binding of Ca^{2+} at the EF-hand causes a conformational change of CDPK and activates its kinase activity (Cheng *et al.*, 2002). Therefore, CDPK is a sensor of Ca^{2+} that modulates responses to various signals, such as hormones, light, growth and development, abiotic stress and pathogen defence (Cheng *et al.*, 2002).

The EF-hand motif is a helix-loop-helix structure and is highly conserved in prokaryotes and eukaryotes (Day *et al.*, 2002; Michiels *et al.*, 2001). In bacteria, a pair of EF-hand motifs binds two Ca^{2+} ions. One of the well known examples, calmodulin, contains four EF-hand motifs and forms two lobes at the N- and C-termini. A short antiparallel β-sheet links the two lobes (Michiels *et al.*, 2001). Calmodulins are also found in plants and the structure is well conserved (Day *et al.*, 2002; Luan *et al.*, 2002).

Since the EF-hand like protein identified in this thesis does not contain any special domains, besides the two EF-hand Ca^{2+} binding motifs, its specific function is unknown. The other question of interest is whether this protein is expressed in the meristems and is involved in controlling cell division. In bacteria, Ca^{2+} is a second messenger involved in a variety of cellular processes, including the cell cycle and cell division (Michiels *et al.*, 2001). There are no well-known Ca^{2+}-binding proteins that are involved in cell

division and the cell cycle in plants, but an interaction between TEL2 and this EF-hand like protein indicates that Ca^{2+} may regulate the function of TEL2 *via* mediation through this EF-hand like protein. If TEL2 controls cell division of the central zone of the apical meristem, a similar hormone-induced Ca^{2+} regulation of cell division may operate in plant cells as is observed in bacteria.

(c) the protein containing lipase domain

The lipase domain-containing protein is another protein identified by the yeast two-hybrid system. This protein contains a lipase domain and an aldehyde dehydrogenase domain. A family of lipolytic enzymes in plants has been described by Brick *et al.* (1995), and differential expression of the members in plant organs suggests that lipases play an important role in regulation of plant development (Brick *et al.*, 1995). However, no members of the lipase family have been identified that are expressed in meristems.

The protein identified in this thesis also contains the aldehyde dehydrogenase domain. Aldehyde dehydrogenase functions in salt stress and drought, and abscisic acid (ABA) upregulates expression of genes encoding aldehyde dehydrogenase (Ishitani *et al.*, 1995). Aldehyde dehydrogenase is a cytoplasmic protein (Li *et al.*, 2000), and so, this lipase protein could interact with TEL2 in the cytoplasm. However, as there is no evidence provided to suggest any function for theses lipase proteins, the biological significance of any interaction with TEL2 is only speculation.

The lipase also contains an active triad (Ser-His-Asp/Glu) with a nucleophilic serine at the end of a sharp turn between a β-strand and an α-helix (Upton and Buckley, 1995). As an antiparallel β-sheet and two α-helices are also found in RRMs of TEL2, it is possible that this lipase protein interacts with TEL2 *via* the β-strand and the α-helix.

(d) Ferredoxin precursor isolog

The ferredoxin protein is an electron carrier in the electron transport chain of the chloroplast. It contains 2Fe-2S clusters and is the terminal electron acceptor of the photosystem (PS) I (Lawlor, 2001). The ferredoxin precursor is synthesised in the cytoplasm and contains a transit sequence that allows importation of ferredoxin from the cytoplasm to the chloroplast. The transit sequence of the ferredoxin precursor isologue consists mostly of hydrophobic residues (Rensink *et al.*, 1998), and the hydrophobic residues might interact with TEL2 since TEL2 also contain stretches of hydrophobic amino acids in the C-terminal half. Therefore, TEL2 may interact with this ferredoxin precursor isolog in the cytoplasm *via* the hydrophobic region.

(e) Cyanase

Cyanase is an inducible enzyme which catalyses the reaction of cyanate with bicarbonate to produce ammonia and carbon dioxide (Taussig, 1960). It is found in *E. coli* and in plants. Cyanase is homodimer in which the two monomers interact with each other *via* the C-terminal domain. Cyanase can

also form a decamer which consists of five of these dimers. The active site is located between the dimers (Walsh *et al.*, 2000)

Each cyanase monomer consists of two domains, one at the N-terminus and the second at the C-terminus. The N-terminal domain is made up of a five-helix bundle, while the C-terminal domain has a "open fold" structure which interwinds in dimerisation. The C-terminal dimerisation domain consists of a two-stranded antiparallel β-sheet and a single α-helix. When two monomers dimerise, a four-stranded antiparallel β-sheet flanked by two α-helix is formed (Walsh *et al.*, 2000) In TEL2, the RRM consists of a four-stranded antiparallel β-sheet and two α helices, and so the structures of the C-terminal domain of cyanase and the RRM of TEL2 are similar. Thus TEL2 may interact with cyanase *via* these similar structures

TEL2 contains three RRMs, but there are no special structures or regions found outside those RRMs. The structure of each RRM is highly conserved, containing four β-strands and two α-helices that form an anti-parallel β-sheet (Burd and Drefuss, 1994). RNA binds into the platform of β-sheet and is buried in the crevice of the binding domain (Drefuss *et al.*, 1993).

TEL2 and Mei2p share high RRM similarity (Veit *et al.*, 1998) and the first two RRMs of Mei2p resemble those of splicesomal proteins (Yamamoto, 1996), hence, it is speculated that TEL2 is involved in RNA splicing. However, none of the proteins identified by the yeast two-hybrid assay were splicesomal proteins. Since only RRM3 of TEL2 was used as the bait, any TEL2-

splicesomal proteins associated *via* RRM1 and RRM2 were not detected. The RRM3 of TEL2, is common with Mei2p, binds to a specific mRNA ligand only. Binding of the RNA ligands may bring splicesomal proteins in proximity to TEL2, and so TEL2 is able to participate in RNA splicing. Some protein interactors could not be identified by the yeast two-hybrid system because the prey is constructed by fusing a cDNA library with the GAL4 activation domain (GAL4AD). Potential protein partner(s) may not be fused with the GAL4AD in-frame and may terminate prematurely or alter the original structure. In this situation, TEL2 cannot interact with its protein partners properly, and thus their identification by this screen would be unlikely.

4.5.3 Speculation of the function of TEL2

TEL2 is expressed in the central zone of the apical meristem. The cells in the central zone are undifferentiated and mitotic activity is extremely low (reviewed by Steeves and Sussex, 1989). The cytological differences of those stem cells in the central zone and expression of *TEL2* in this region led to speculation that *TEL2* may be involved in controlling cell division of stem cells. However, at present, there is no clear evidence to show that ectopic overexpression of *TEL* genes in *A. thaliana* induces meristematic characteristics in vegetative tissues and slows down growth of plants (V. Trainor, unpublished data).

Using the yeast two-hybrid assay, one of the proteins identified in this thesis is KOR, which is essential for cytokinesis. In the meristems, TEL2 may interact with KOR in the cytoplasm and limit localisation of KOR to the plasma

membrane, and so, cell division could be affected. Another protein identified is an EF-hand Ca^{2+}-binding protein-like. Calcium ions are a second messenger that mediates the signal from hormones. The EF-hand proteins are involved in controlling cell division and the cell cycle in bacteria (Michiels *et al.*, 2001), but have not been well defined in plants. In plants, EF-hand protein-like may function similarly in bacteria to control cell division. It is also suggested that calcium ions might mediate a signal pathway that controls cell division in the meristem. Further analysis, for example, *in situ* hybridisation, is required to show that the genes encoding these two proteins are expressed in the same region as *TEL*.

To address the question as to what is the biological significance of these protein interactions with TEL2 in plants, perturbation of expression of these genes identified by the two-hybrid assay should be performed. However, a single mutation of *TEL* genes and overexpression of one *TEL* gene do not show any obvious phenotype in *A. thaliana*. Hence, the actual biological function of *TEL2* may not be observed when the expression of its protein interactor has been perturbed.

Another approach to confirm the authenticity of interactions between those proteins with TEL2 may be provided by the use of tandem affinity purification (TAP) (Rigaut *et al.*, 1999). The TAP tag consists of the calmodulin binding peptide, a TEV protease cleavage site and an IgG binding domain. The TAP method involves the fusion of the TAP tag with TEL2 and introduction of the construct into *A. thaliana*. The construct is expressed at the same level of *TEL2*, and crude extracts containing the fusion protein and any interactors are

purified by an affinity column of IgG beads. After washing, the TEV protease is added to release the target protein complexes from the column. The second purification step allows the removal of the TEV protease and traces of contaminants by binding the target protein complexes to calmodulin matrix in the presence of Ca^{2+}. The bound protein complexes are eluted by EGTA that chelates Ca^{2+}. The TAP technique allows purification of the protein complexes from the crude extract without disrupting the conformation of proteins and protein-protein interactions. The protein complex can be analysed by mass spectrometry and sodium dodecyl sulphate-polyacrylamide gel electrophoresis (SDS-PAGE) (Rigaut *et al.*, 1999, http://www.embl-heidelberg.de/ExternalInfo/seraphin/TAP.html).

4.5.4 Problems and limitation of the yeast two-hybrid assay

The total number of transformants obtained in this yeast two-hybrid assay was very low, at about 1.5 x 10^4 cells. Compared to published data in which 1 x 10^6 transformants are obtained in a yeast two-hybrid screen, the total number of transformants in the yeast two-hybrid assay in this thesis was around 66-fold lower. The primary titre of CD4-22 cDNA library is 2 x 10^6. If only a small number of transformants are screened, only prey proteins which are highly expressed will be detected. It is difficult to detect the interaction between the bait and the prey proteins which are rarely expressed unless adequate numbers of prey molecules are screened.

Later experiments showed that the bait vector could not be well maintained in the PJ69-4α cell line. The total number of colonies on YPD plating was ten

times more than that in a SC-Trp plate, despite the cells being grown in the selective media. These results indicated that only 10% of cells contained the bait vector. Similar results were obtained using PJ69-4α cells transformed with the empty vector, suggesting that the insertion of the C-terminus of *TEL2* and the full length *TEL2*, did not contribute to the loss of vector from the host cells. Louvet *et al.* (1997) has pointed out that pAS2.1 is a very unstable plasmid. When a different two-hybrid yeast strain, HY, was transformed with the empty pAS2.1, only 20% of cells maintained the pAS2.1 vector even though yeast was grown in the selective (-Trp) medium (Louvet *et al.*, 1997). Based on the results from Louvet *et al.* (1997) and those presented in Table 4.7 in this thesis, one can conclude that pAS2.1 is not well maintained regardless of yeast strains. Thus using poor maintenance of pAS2.1-based bait vector leads to overall low transformation efficiency in two-hybrid screening.

To improve this problem, another bait vector should be used. pAS2.1 is used in the MATCHMAKER yeast two-hybrid system 2 (Clontech) while pGBKT7 is used in the new MATCHMAKER yeast two-hybrid. This may improve the transformation efficiency and increase the number of screens.

Another possible factor that may contribute to the small number of two-hybrid screens is "false negatives" which are caused by toxicity from protein-protein interactions between the bait and the prey. The interaction of the C-terminus of TEL2 and the prey proteins might be toxic to the cells, and ultimately, interfere with the viability of the host cells. Using single-copy number vectors (ARS/CEN based) instead of the high-copy number 2-micron-based vector

can reduce the toxicity since the protein expression levels are reduced (Robinson and Brasch, 1998)

Another limitation of the yeast two-hybrid assay is the failure of yeast cells to undergo various post-translational modifications which are required for protein-protein interactions in higher organisms, leading to false negatives. This problem can be solved by introducing a 'third' *trans*-acting partner. Several plasmids are designed to allow conditional expression of the third protein, and this protein can directly interact with two proteins of interest (X and Y) to form a trimeric complex with greater stability (Vidal and Legrain, 1999).

4.6 Conclusion

Full length *TEL2* affects the growth of the host strain, PJ69-4α, but truncation of *TEL2* reduced these effects. The transformation efficiency of the yeast two-hybrid assay is much lower than reported values in the literature, with only 10% of the bait vector-transformed PJ69-4α cells maintaining the plasmid vector due to the poor maintenance of pAS2.1 in the host yeast strain.

LacZ is one of the reporter genes used in yeast two-hybrid assay, and only six colonies appeared 'blue' on the X-gal indication plates. These were identified: KORRIGAN1 (KOR), the EF-hand Ca^{2+}-binding protein-like, the protein containing lipase domain and the ferredoxin precursor isologue were the four identified protein interactors from yeast two-hybrid system The two remaining proteins were cyanase and an expressed protein.

TEL genes are strongly expressed in the quiescent zone of the meristems and the mitotic activity of cells in this zone is low. Therefore, *TEL2* might be involved in controlling cell division in this zone. As *KOR* is essential for cytokinesis, in the meristem, TEL2 may interact with KOR in the cytoplasm and inhibit the localisation of KOR to plasma membrane, affecting cell division in the meristems.

The EF-hand protein-like is another potential protein interactor of TEL2. Calcium ions may also be involved in mediation of signal pathways that control cell division in the meristems. Of the other proteins identified, it was

difficult to make any meaningful speculations or their possible functions in the meristem, particularly if interacting with TEL2.

CHAPTER 5 SUMMARY

5.1 Summary of results

Molecular techniques were used to study Mei2-like proteins in plants which are a novel class of RNA-binding proteins, named by their similarity to the Mei2 protein (Mei2p) of *Schizosaccharomyces pombe*. All proteins in the Mei2-like family carry three RNA recognition motifs (RRMs). The first two RRMs are similar to those RRMs in splicing factors. The third RRM (RRM3) is unusual, since *S. pombe* Mei2p binds to a specific non-coding RNA, meiRNA, at the RRM3 (Watanabe and Yamamoto, 1994). The binding to meiRNA is essential for nuclear localisation and allows Mei2p to function in meiosis. This unusual RRM3 is highly conserved in the Mei2-like proteins, and provides a distinct hallmark in this family (Veit *et al.*, 1998, Jeffares, 2001).

However, the biochemical functions of the plant Mei2-like proteins remain unclear. The primary object of this study was to learn more about the biochemical mechanism by which this class of proteins operates in plants. The experimental strategies were largely based on observations related to Mei2p of *S. pombe* which is the founder member of this class of RNA-binding proteins. Two questions are addressed in this thesis: 1) whether the unusual pattern of cellular localisation of Mei2p in *S. pombe* also occurs in plants?, and 2) which specific *A. thaliana* proteins physically interact with the Mei2-like

proteins? Knowledge of these proteins may suggest some functions of the Mei2-like proteins.

To test the hypothesis that the mechanism of RNA-assisted accumulation of Mei2p observed in yeast is also conserved in plant cells, transient expression of GFP-tagged Mei2p and meiRNA in onion epidermal cells was utilised. Transient expression of *mei2::gfp* and *gfp::mei2* alone was observed, but only in the presence of meiRNA. The GFP-fused Mei2p appeared to preferentially localise in the nucleus with meiRNA, but the localisation pattern in onion epidermal cells was not as clear as it was in mammalian cells. The results suggest that in the absence of meiRNA, Mei2p-GFP might be uniformly distributed throughout the cell but be below the limit of detection. Alternatively, meiRNA might be required to prevent degradation of the GFP tagged Mei2p since GFP and Mei2p are foreign proteins in plants. For transient expression of GFP-tagged TEL2 in onion epidermal cells, the TEL2-GFP localised into the nucleus without co-expression of any special RNA species. The result suggests that either some RNA species assisting nuclear localisation of TEL2-GFP are already present in onion epidermal cells, or the mechanism of nuclear localisation of TEL2 is different from that of Mei2p of *S. pombe*. In stably transformed *A. thaliana* containing *35S::mei2::gfp*, no GFP signal was detected. Transcriptional analysis showed that *mei2::gfp* transcripts were present in two lines, Lines 1 and 6, by RT-PCR. However, western blot analysis did not detect the presence of Mei2::GFP in those lines. These results might be explained by inefficient translation of the foreign fusion protein or its relatively instability.

The RRMs of TEL resemble those found in splicing factors, suggesting that Mei2-like proteins may be involved in RNA processing To test this hypothesis, a yeast two-hybrid system was used to identify proteins of *A. thaliana* which physically interact with TEL2. Using the C-terminus of TEL2 containing the highly conserved RRM3 as a bait, six potential protein interactors were identified: 1) KORRIGAN (KOR), 2) an EF-hand Ca^{2+}-binding protein-like, 3) a protein containing lipase domain, 4) a ferredoxin precursor isologue, 5) cyanase and 6) an expressed protein. However, no clear examples of splicesomal proteins were identified in the yeast two-hybrid assay

Based on the known biochemical activities of the proteins that were identified by the yeast two-hybrid assay, speculation was offered on the possible function with TEL proteins. Since *TEL* genes are expressed in the central zone (CZ) of SAM and the mitotic activity of cells in CZ is low, *TEL* genes could be involved in controlling cell division in the CZ. Given this correlation, the observed interaction with KOR may have functional significance. Because KOR is essential for cytokinesis, it is conceivable that TEL2 may sequester KOR and limit cell division. Interaction of TEL2 and the EF-hand Ca^{2+}-binding protein-like suggests that Ca^{2+} ions may be involved in signal pathway to control cell division.

5.2 Future directions

This study attempted to analyse the functions of the *Mei2-like* genes in plants, and the following questions have been raised: 1) Since the expression of *TEL*

genes is in the central zone (CZ) of the meristems and mitotic activity of cells in the CZ is low, do *TEL* genes regulate cell division in the CZ? 2) Nuclear localisation of TEL2 suggests that TEL2 may function in the nucleus. Are the Mei2-like proteins involved in RNA processing? Is this process related to controlling cell division? 3) Since there are seven *Mei2-like* genes in *Arabidopsis*, do they interact with each other? Or, do they function in different stages during plant growth?

In recent studies by Shimada *et al.* (2003), Mei2p localises into the nucleus and associates at the *sme2* locus, which encodes meiRNA. This assembly may be required for promotion of meiosis in *S. pombe*. Based on this evidence and the results from the transient expression assays in this thesis, the following question on biochemical mechanism of the Mei2-like proteins is raised: 1) Is the mechanism of RNA-assisted nuclear localisation observed in yeast also conserved in plants? 2) If it is conserved in plants, TEL proteins may bind their special RNA ligand(s) to accumulate in the nucleus. What is/are the RNA ligand(s)? 3) Do the plant Mei2-like proteins act in the same way as the Mei2p of *S. pombe* that bind to locus encoding that RNA ligand?

Some experiments are in progress currently to study the biochemical function of TEL function. One approach is using tandem affinity purification (TAP) to identify protein interactors with TEL in plants. Studying the overexpression of *TEL* genes and *tel* mutants in *A. thaliana* can also provide information about *TEL* functions by observing the phenotypes.

REFERENCES

Agatep, R., Kirkpatrick, R. D., Parchaliuk, D. L., Woods, R. A. and Gietz, R. D., (1998). Transformation of *Saccharomyces cerevisiae* by the lithium acetate/single-stranded carrier DNA/polyethylene glycol (LiAc/ss-DNA/PEG) protocol. *Technical Tips Online* (http://tto.trends.com).

Agrobacterium-mediated transformation. http://www.plantsci.cam.ac.uk/Haseloff/microscopy/microscopyFrameset.html

Aida, M., Ishida, T. and Tasaka, M., (1999). Shoot apical meristem and cotyledon formation during *Arabidopsis* embryogenesis: interaction among the *CUP-SHAPED COTYLEDON* and *SHOOT MERISTEMLESS* genes. *Development* **126**, 1563 – 1570.

Aida, M., Vernoux, T., Furutani, M., Trass, J. and Tasaka, M., (2002). Roles of *PIN-FORMED1* and *MONOPTEROS* in pattern formation of the apical region of the *Arabidopsis* embryo. *Development* **129**, 3965 – 3974.

Allain, F. H.-T., Gilbert, D. E., Bouvet, P. and Feigon, J., (2000). Solution structure of the two N0terminal RNA-binding domians of nucleolin and NMR study of the interaction with its RNA target. *Journal of Molecular Biology* **303**, 227 – 241.

Alvarez, N. G., (2002). *Molecular genetic analysis of plant Mei2-like genes.* Massey University. New Zealand. PhD thesis.

Arabidopsis Genome Initiative, (2000). Analysis of the genome sequence of the flowering plant *Arabidopsis thaliana*. *Nature* **408**, 796 – 815.

Barton, M. K. and Poethig, R. S., (1993). Formation of the shoot apical meristem in *Arabidopsis thaliana*: an analysis of development in the wild type and in the *shoot meristemless* mutant. *Development* **119**, 823 – 831.

Biolistic PDS-1000/He particle delivery system. http://www.bio-rad.com/webmaster/pdfs/Bulltein_1700.pdf

Birney, E., Kumar, S. and Krainer, A. R., (1993). Analysis of the RNA-recognition motif and RS and RGG domains: conservation in metazoan pre-mRNA splicing factors. *Nucleic Acids Research* **21**, 5803 – 5816.

Bohmert, K., Camus, I., Bellini, C., Bouchez, D., Caboche, M. and Benning, C., (1998). *AGO1* defines a novel locus of *Arabidopsis* controlling leaf development. *EMBO Journal* **17**, 170 – 180.

Bollag, D. M., Bozycki, M. D. and Edelstein, S. J., (1996). Protein methods, 2nd ed. Wiley-Liss, A John Wiley and Sons, Inc., Publication, New York, pp 213.

Bowman, J. L. and Eshed, Y., (2000). Formation and maintenance of the shoot apical meristem. *Trends in Plant Science* **5**, 1360 – 1385.

Brand, U., Fletcher, J. C., Hobe, M., Meyerowitz, E. M. and Simon, R., (2000). Dependence of stem cell fate in *Arabidopsis* on a feedback loop regulated by *CLV3* activity. *Science* **289**, 617 – 619.

Brand, U., Grunewald, M., Hobe, M. and Simon, R., (2002). Regulation of *CLV3* expression by two homeobox genes in *Arabidopsis*. *Plant Physiology* **129**, 565 – 575.

Brick, D. J., Brumlik, M. J., Buckley, J. T., Cao, J.-X., Davies, P. C., Misra, S., Tranbarger, T. J. and Upton, C., (1995). A new family of lipolytic plant enzymes with members in rice, *Arabidopsis*, and maize. *FEBS Letters* **377**, 475 – 480.

Burd, C. G. and Dreyfuss, G., (1994). Conserved structures and diversity of functions of RNA-binding proteins. *Science* **265**, 615 – 621.

Cheng, S.-H., Willmann, M. R., Chen, H.-C. and Sheen, J., (2002). Calcium signaling through protein kinases. The *Arabidopsis* calcium-dependent protein kinase gene family. *Plant Physiology* **129**, 469 – 485.

Clark, S. E., Running, M. P. and Meyerowitz, E. M., (1995). *CLAVATA3* is a specific regulator of a shoot and floral meristem development affecting the same processes as *CLAVATA1*. *Development* **121**, 2057 – 2067.

Clark, S. E., Jacobsen, S. E., Levin, J. Z. and Meyerowitz, E. M., (1996). The *CLAVATA* and *SHOOT MERISTEMLESS* loci competitively regulate meristem activity in *Arabidopsis*. *Development* **122**, 1567 - 1575

Clark, S. E., (2001). Cell signalling at the shoot meristem. *Nature Reviews of Molecular Cell Biology* **2**, 276 – 284.

Clough, S. J. and Bent, A. F., (1998). Floral dip: a simplified method for *Agrobacterium*-mediated transformation of *Arabidopsis thaliana*. *Plant Journal* **16**, 735 - 743.

Day, I. S., Reddy, V. S., Ali, G. S. and Reddy, A. S. N., (2002). Analysis of EF-hand-containing proteins in Arabidopsis. *Genome Biology* **3**, research0056.1 – 0056.24

DeVoti, J., Seydoux, G., Beach, D. and McLeod, M., (1991). Interaction between *ran1*⁺ protein kinase and cAMP dependent protein kinase as negative regulators of fission yeast meiosis. *EMBO Journal* **10**, 3759 – 3768.

Dreyfuss, G., Matunis, M. J., Pinol-Roma, S. and Burd, C. G., (1993). hnRNP proteins and the biogenesis of mRNA. *Annual Reviews of Biochemistry* **62**, 289 - 321.

Elliott, R. C., Betzner, A. S., Huttner, E., Oakes, M. P., Tucker, W. Q., Gerentes, D., Perez, P., and Smyth, D.R., (1996). *AINTEGUMENTA*, an

APETALA2-like gene of *Arabidopsis* with pleiotropic roles in ovule development and floral organ growth. *Plant Cell* **8**, 155 – 168.

Endrizzi, K., Moussian, B., Haecker, A., Levin, J. Z. and Laux, T., (1996). The *SHOOT MERISTEMLESS* gene is required for maintenance of undifferentiated cells in *Arabidopsis* shoot and floral meristems and acts at a different regulatory level than the meristem genes *WUSCHEL* and *ZWILLE*. *Plant Journal* **10**, 967 – 979.

Fagard, M., Boutet, S., Morel, J.-B., Bellini, C. and Vaucheret, H., (2000). AGO1, QDE-2, and RDE-1 are related proteins required for post-transcriptional gene silencing in plants, quelling in fungi, and RNA interference in animals. *Proc. Natl. Acad. Sci. USA* **97**, 11650 – 11654.

Fields, S. and Song, O.-k., (1989). A novel genetic system to detect protein-protein interactions. *Nature* **340**, 245 – 246.

Fletcher, J. C., Bramd, U., Running, M. P., Simon, R. and Meyerowitz, E. M., (1999). Signaling of cell fate decisions by *CLAVATA3* in *Arabidopsis* shoot meristems. *Science* **283**, 1911 – 1914.

Gallois, J.-L., Woodward, C., Reddy, G. V. and Sablowski, R., (2002). Combined SHOOT MERISTEMLESS and WUSCHEL trigger ectopic organogenesis in *Arabidopsis*. *Development* **129**, 3207 – 3217.

Gerdes, H. H. and Kaether, C., (1996). Green fluorescent protein: applications in cell biology *FEBS Letters* **389**, 44 - 47

Gleave, A P., (1992). A versatile binary vector system with a T-DNA organisational structure conducive to efficient integration of cloned DNA into the plant genome. *Plant Molecular Biology* **20**, 1203 – 1207.

Handa, N., Nureki, O., Kurimoto, K., Kim, I., Sakamoto, H., Shimura, Y, Muto, Y. and Yokoyama, S., (1999). Structural basis for recognition of the *tra* mRNA precursor by the Sex-lethal protein. *Nature* **398**, 579 – 585.

Haseloff, J., Siemering, K. R., Prasher, D. C and Hodge, S., (1997). Removal of a cryptic intron and subcellular localization of green fluorescent protein are required to mark transgenic *Arabidopsis* plants brightly *Proc Natl. Acad. Sci. USA* **94**, 2122 – 2127.

Heim, R., Cubitt, A. B. and Tsien, R. Y , (1995). Improved green fluorescence *Nature* **373**, 663 – 664.

Hoffman, D. W., Query, C. C., Golden, B. L., White, S. w. amd Keene, J. D., (1991). RNA-binding domain of the A protein component of the U1 small nuclear ribonucleoprotein analyzed by NMR spectroscopy is structurally similar to ribosomal proteins. *Proc. Natl. Acad. Sci. USA* **88**, 2495 – 2499.

Howe, C., (1995). *Gene cloning and manipulation*, 1st ed. Cambridge University Press, Cambridge, pp 160 – 164.

Hirayama, T., Ishida, C., Kuromori, T., Obata, S., Shimoda, C., Yamamoto, M., Shinozaki, K. and Ohto, C., (1997). Functional cloning of a cDNA encoding Mei2-like protein from *Arabidopsis thaliana* using a fission yeast pheromone receptor deficient mutant. *FEBS Letters* **413**, 16 – 20.

Intracellular localisation of GFP. http://www.plantsci.cam.ac.uk/Haseloff/microscopy/gfpFrameset.html

Ishiguro, S., Watanabe, Y., Ito, N., Nonaka, H., Takeda, N., Sakai, T., Kanaya, H and Okada, K., (2002). *SHEPHERD* is the *Arabidopsis* GRP94 responsible for the formation of function CLAVATA proteins. *EMBO Journal* **21**, 898 – 908.

Ishitani, M., Nakamura, T., Han, S. Y., and Takabe, T., (1995). Expression of the betaine aldehyde dehydrogenase gene in barley in response to osmotic stress and abscisic acid *Plant Molecular Biology* **27**, 307 – 315.

Jackson, D., Veit, B. and Hake, S., (1994). Expression of maize *KNOTTED1* related homeobox genes in the shoot apical meristem predicts patterns of morphogenesis in the vegetative shoot. *Development* **120**, 405 – 413.

Jeffares, D., (2001). *Molecular genetic ana;ysis of maize terminal ear 1 gene and in silico analysis of related genes.* Massey University. New Zealand. PhD thesis.

Kaya, H., Scibahara, K.-i., Taoka, K.-i., Iwabuchi, M., Stillman, B. and Araki, T., (2001) *FASCIATA* genes for chromatin assembly factor-1 in *Arabidopsis* maintain the cellular organization of apical meristems. *Cell* **104**, 131 –142.

Kerstetter, R. A., Laudencia-Chingcuanco, D., Smith, L. G. and Hake, S., (1997). Loss-of-function mutations in the maize homeobox gene, *knotted1*, are defective in shoot meristem maintenance. *Development* **124**, 3045 – 3054

Kiledjian, M., and Dreyfuss, G., (1992) Primary structure and binding activity of the hnRNP U protein: binding RNA through RGG box *EMBO Journal* **11**, 2655 – 2664.

Kim, J., Harter, K., and Theologis, A., (1997). Protein-protein interactions among the Aux/IAA proteins *Proc Natl Acad Sci U S A* **94**, 11786 – 11791.

Kitamura, K., Katayama, S., Dhut, S., Sato, M., Watanabe, Y., Yamamoto, M. and Toda, T., (2001). Phosphorylation of Mei2 and Ste11 by Pat1 kinase inhibits sexual differentiation via ubiquitin proteolysis and 14-3-3 protein in fission yeast. *Developmental Cell* **1**, 389 – 399.

Kranz, J. K. and Hall, K. B., (1999). RNA recognition by the human U1A protein is mediated by a network of local cooperative interactions that create the optimal binding surface. *Journal of Molecular Biology* **285**, 215 – 231.

Laufs, P., Dockx, J., Kronenberger, J. and Trass, J., (1998). *MGOUN1* and *MGOUN2*: two genes required for primordium initiation at the shoot apical and floral meristems in *Arabidopsis thaliana*. *Development* **125**, 1253 – 1260.

Laux, T., Mayer, K. F. X., Berger, J. and Jurgen, G., (1996). The *WUSCHEL* gene is required for shoot and floral meristem integrity in *Arabidopsis*. *Development* **122**, 87 – 96.

Leffel, S. M., Mabon, S. A. and Stewart, C.N. Jr., (1997). Applications of green fluorescent protein in plants. *BioTechniques* **23**, 912 – 918.

Lenhard, M., Bohnert, A. Jurgen, G. and Laux, T., (2001). Termination of stem cell maintenance in *Arabidopsis* floral meristems by interactions between *WUSCHEL* and *AGAMOUS*. *Cell* **105**, 805 – 814.

Lenhard, M., Jurgen, G. and Laux, T., (2002). The *WUSCHEL* and *SHOOTMERISTEMLESS* genes fulfil complementary roles in *Arabidopsis* shoot meristem regulation. *Development* **129**, 3195 – 3206.

Li, Y., Nakazono, M., Tsutsumi, N. and Hirai, A., (2000). Molecular and cellular characterizations of a cDNA clone encoding a novel isozyme of aldehyde dehydrogenase from rice. *Gene* **249**, 67 – 74.

Lohmann, J. U., Hong, R. L., Hobe, M., Busch, M. A., Parcy, F., Simon, R. and Weigel, D., (2001). A molecular link between stem cell regulation and floral patterning in *Arabidopsis*. *Cell* **105**, 793 – 803.

Long, J. A., Moan, E. I., Medford, J. I. and Barton, M. K., (1996). A member of the KNOTTED class of homeodomain proteins encoded by the *STM* gene of *Arabidopsis*. *Nature* **379**, 66 - 69.

Lorkovic, Z. J. and Barta, A., (2002). Genome analysis: RNA recognition motif (RRM) and K homology (KH) domain RNA-binding proteins from the flowering plant *Arabidopsis thaliana*. *Nucleic Acids Research* **30**, 623 – 635.

Louvet, O., Doignon, F and Crouzet, M., (1997). Stable DNA-binding yeast vector allowing high-bait expression for use in the two-hybrid system. *BioTechniques* **23**, 816 - 818, 820.

Luan, S., Kudla, J., Rodriguez-Concepcion, M., Yalovsky, S. and Gruissem, W., (2002). Calmodulins and calcineruin B-like proteins: Calcium sensors for specific signal response coupling in plants. *Plant Cell Supplement*, S389 – S400

Lynn, K., Fernandez, A., Aida, M., Sedbrook, J., Tasaka, M., Masson, P. and Barton, M K., (1999). The *PINHEAD/ZWILLE* gene acts pleiotropically in *Arabidopsis* development and has overlapping function with the *ARGONAUTE1* gene. *Development* **126**, 469 – 481.

Macknight, R., Bancroft, I., Page, T., Lister, C., Schmidt, R., Love, K., Westphal, L., Murphy, G., Sherson, S., Cobbett, C. and Dean, C., (1997). *FCA*, a gene controlling flowering time in *Arabidopsis*, encodes protein containing RNA-binding domains. *Cell* **89**, 737 – 745.

Malim, M. H., Hauber, J., Le, S.-Y., Maizel, J. V. and Cullen, B. R., (1989). The HIV-1 *rev trans*-activator acts through a structured target sequence to activate nuclear export of unspliced viral mRNA. *Nature* **338**, 254 – 257.

MATHCHMAKER GAL4 two-hybrid vectors handbook. CLONTECH Laboratories (1997).

Matthews, D. L., Grogan, C. O. and Manchester, C. E., (1974). Terminal ear mutant of maize (*Zea mays* L.). *J. Agric. Sci. Camb.* **82**, 433 – 435.

Mayer, K. F. X., Schoof, H., Haecker, A., Lenhard, M., Jurgen, G. and Laux, T., (1998). Role of *WUSCHEL* in regulation stem cell fate in the *Arabidopsis* shoot meristem. *Cell* **95**, 805 – 815.

McDaniel, C. N. and Poethig, R. S., (1988). Cell-lineage patterns in the shoot apical meristem of the germination maize embryo. *Planta* **175**, 13 – 22.

Michiels, J., Xi, C., Verhaert, J. and Vanderleyden, J., (2002). The functions of $Ca2^{+}$ in bacteria: a role for EF-hand proteins? *Trends in Microbiology* **10**, 87 – 93.

McLean, B. G., Eubanks, S. and Meagher, R. B., (1990). Tissue-specific expression of divergent actins in soybean root. *Plant Cell* **2**, 335 – 344.

Mizukami, Y. and Fischer, R. L., (2000). Plant organ size control: *AINTEGUMENTA* regulates growth and cell numbers during organogenesis. *Proc. Natl. Acad. Sci. USA* **97**, 942 – 947.

Modified *gfp* gene cassettes. http://www.plantsci.cam.ac.uk/Haseloff/microscopy/microscopyFrameset.html

Moussian, B., Schoof, H., Haecker, A., Jurgen, G. and Laux, T., (1998). Role of the *ZWILLE* gene in the regulation of central shoot meristem cell fate during *Arabidopsis* embryogenesis. *EMBO Journal* **17**, 1799 – 1809.

Murphy, K. G. K. and Manley, J. L., (1992). Characterization of the multisubunit cleavage-polysdenylation specificty factor from calf thymus. *Journal of Biological Chemistry* **267**, 14804 – 14811.

Nagai, K., Oubridge, C., Jessen, T. H., Li, J. and Evans, P. R., (1990). Crystal structure of the RNA-binding domain of the U1 small nuclear ribonucleoprotein A. *Nature* **348**, 515 – 520.

Nagata, T., Kanno, R., Kurihara, Y., Uesugi, S., Imai, T., Sakakibara, S., Okano, H., and Katahira, M., (1999). Structure, backbone dynamics and interactions with RNA of the C-terminal RNA-binding domain of a mouse neural RNA-binding protein, Musashi1. *Journal of Molecular Biology* **287**, 315 – 330.

Newman, K. L., Fernandez, A. G. and Barton, M. K., (2002). Regulation of axis determinacy by the *Arabidopsis PINHEAD* gene. *Plant Cell* **14**, 3029 – 3042.

Nicol, F., His, I., Jauneau, A., Vernhettes, S., Canut, H., and Hofte, H., (1998). A plasma membrane-bound putative endo-1,4-beta-D-glucanase is required for normal wall assembly and cell elongation in *Arabidopsis*. EMBO Journal 17, 5563 – 5576.

Ohno, M. and Mattaj, I. W., (1999). Meiosis: MeiRNA hits the spot. *Current Biology* **9**, R66 – R69.

Oubridge, C., Ito, N., Evans, P. R., Teo, C.-H. and Nagai, K., (1994). Crystal structure at 1.92 Å resolution of the RNA-binding domain of the U1A splicesomal protein complexed with an RNA hairpin. *Nature* **372**, 432 – 438.

Prasher, D. C., Eckenrode, V. K., Ward, W. W., Prendergast, F.G. and Cormier, M. J., (1992). Primary structure of the *Aequorea victoria* green-fluorescent protein. *Gene* **111**, 229 – 233.

Poethig, R. S., Coe, Jr., E. H. and Johri, M. M., (1986). Cell lineage patterns in maize embryogenesis: a clonal analysis. *Developmental Biology* **117**, 392 – 404.

Quick and easy TRAFO protocol.
http://www.umanitoba.ca/faculties/medicine/biochem/gietz/Quick.html

Rensink, W. A., Pilon, M. and Weisbeek, P., (1998). Domains of a transit sequence required for *in vivo* import in *Arabidopsis* chloroplasts. *Plant Physiology* **118**, 691 – 699.

Rigaut, G., Shevchenko, A., Rutz, B., Wilm, M., Mann, M., and Seraphin, B., (1999). A generic protein purification method for protein complex characterization and proteome exploration. *Nature Biotechnology* **17**, 1030 – 1032.

Robinson, L. L. and Brasch, M. A., (1998) Identification of interacting proteins with the ProQuest™ two-hybrid system. *Focus* **20**, 19 – 23.

Sachs, A., and Wahle, E., (1993). Poly(A) tail metabolism and function in eucaryotes. *Journal of Biological Chemistry* **5**, 22955 – 22958.

Sambrook, J., Fritsch, E F. and Maniatis, T., (1989). *Molecular Cloning: a laboratory manual*. Cold Spring Harbour Laboratory Press, New York.

Samuels, M., Deshpande, G. and Schedl, P., (1998). Activities of the Sex-lethal proteins in RNA binding and protein.protein interactions. *Nucleic Acids Research* **26**, 2625 – 2637.

Sanford, J. C., Smith, F. D. and Russell, J. A., (1993). Optimizing the biolistic process for different biological applications. *Methods of Enzymology* **217**, 483 – 509.

Sato, M., Shinozaki-Yabana, S., Yamashita, A., Watanabe, Y. and Yamamoto, M., (2001). The fission yeast meiotic regulator Mei2p undergoes nucleocytoplasmic shuttling. *FEBS Letters* **499**, 251 – 255.

Sato, S., Kato, T., Kakegawa, K., Ishii, T., Liu, Y.-G., Awano, T., Takabe, K., Nishiyama, Y., Kuge, S., Sato, S., Nakamura, Y., Tabata, S. and Shibata, D., (2001). Role of the putative membrane-bound endo-1,4-β-glucanase KORRIGAN in cell elongation and cellulose synthesis in *Arabidopsis thaliana*. *Plant Cell Physiology* **42**, 251 – 263.

Schoof, H., Lenhard, M., Haecker, A., Mayer, K. F. X., Jurgen, G. and Laux, T., (2000). The stem cell population of *Arabidopsis* shoot meristems is maintained by a regulatory loop between the *CLAVATA* and *WUSCHEL* genes. *Cell* **100**, 635 – 644.

Scott, A., Wyatt, S., Tsou, P.-L., Robertson, D. and Stromgren Allen, N., (1999). Model system for plant cell biology: GFP imaging in living onion epidermal cells. *BioTechniques* **26**, 1125 – 1132.

Shabde, M. and Murshige, T., (1977). Hormonal requirements of excised *Dianthus caryophyllus* L. shoot apical meristem *in vitro*. *American Journal of Botany* **64**, 443 – 448.

Shamoo, Y., Abdul-Manan, N. and Williams, K. R., (1995). Multiple RNA binding domains (RBDs) just don't add up. *Nucleic Acids Research* **23**, 725 – 728.

Sheen, J., Hwang, S., Niwa, Y., Kobayashi, H. and Galbraith, D W., (1995). Green-fluorescent protein as a new vital marker in plant cells. *Plant Journal* **8**, 777 – 784.

Shimoda, C., Uehira, M., Kishida, M., Fujioka, H., Iino, Y., Watanabe, Y and Yamamoto, M., (1987). Cloning and analysis of transcription of the *mei2* gene responsible for initiation of meiosis in the fission yeast *Schizosaccharomyces pombe*. *Journal of Bacteriology* **69**, 93 – 96.

Shimada, T, Yamashita, A. and Yamamoto, M., (2003). The fission yeast meiotic regulator Mei2p forms a dot structure in the horse-tail nucleus in association with the *sme2* locus on chromosome II. *Molecular Biology and Cells* **14**, 2461 – 2469.

Shinozaki-Yabana, S., Watanabe, Y. and Yamamoto, M., (2000) Novel WD-repeat protein Mip1p facilitates function of the meiotic regulator Mei2p in fission yeast. *Molecular and Cellular Biology* **20**, 1234 – 1242.

Smith, L. G., Greene, B., Veit, B. and Hake, S., (1992). A dominat mutation in the maize homeobox gene, *Knotted-1*, causes its ectopic expression in leaf cells with altered fates. *Development* **116**, 21 – 30.

Smith, R. H. and Murashige, T., (1970). *In vitro* development of the isolated shoot apical meristem of angiosperms. *American Journal of Botany* **57**, 562 – 568.

Steeves, T. A. and Sussex, I. M., (1989). *Patterns in Plant Development*, 2nd ed. Cambridge University Press, Cambridge

Taussig, A., (1960). The syhtheis of the induced enzyme, 'cyanase', in *E. coli*. *Biochim Biophys. Acta* **44**, 510 - 519

Tsien, R Y (1998). The green fluorescent protein *Annual Reviews of Biochemistry* **67**, 509 - 544.

Upton, C., and Buckley, J. T., (1995). A new family of lipolytic enzymes? *Trends in Biochemical Sciences* **20**, 178 – 179.

Varagona, M. J., Schmidt, R. J and Raikhel, N. V . (1992). Nuclear localisation signal(s) required for nuclear targeting of the maize regulatory protein Opaque-2. *Plant Cell* **4**, 1213 - 1227

Veit, B., Briggs, S. P., Schmidt, R J., Yanofsky, M F and Hake, S., (1998). Regulation of leaf initiation by the *terminal ear 1* gene of maize. *Nature* **393**, 166 - 168.

Vidal, M., Brachmann, R. K., Fattaey, A., Harlow, E. and Boeke, J. D., (1996a). Reverse two-hybrid and one-hybrid systems to detect dissociation of protein-protein and DNA-protein interactions. *Proc Natl. Acad. Sci. USA* **93**, 10315 – 10320.

Vidal, M., Braun, P., Chen, E., Boeke, J. D. and Harlow, E., (1996b). Genetic characterization of a mammalian protein-protein interaction domain by using a yeast reverse two-hybrid system. *Proc Natl Acad Sci. USA* **93**, 10321 – 10326.

Vidal, M. and Legrain, P., (1999). Yeast forward and revese 'n'-hybrid systems. *Nucleic Acid Research* **27**, 919 - 929.

Vollbrecht, E., Veit, B., Sinha, N. and Hake, S., (1991). The developmental gene *Knotted-1* is a member of a maize homeobox gene family. *Nature* **350**, 241 – 243.

Vollbrecht, E., Reiser, L and Hake, S., (2000). Shoot meristem size is dependent on inbred background and presence of the maize homeobox gene, *knotted1*. *Development* **127**, 3161 – 3172.

von Arnim, A. G., Deng, X.-W. and Stacey, M. G., (1998). Clonign vectors for the expression of green fluorescent protein fusion proteins in transgenic plants. *Gene* **221**, 35 – 43.

Walsh, M., Otwinowski Z., Perrakis, A., Anderson, P. M. and Loachimiak, A., (2000). Structure of cyanase reveals that a novel dimeric and decameric arrangement of subunits is required for formation of the enzyme active site. *Structure* **8**, 505 – 514.

Watanabe, Y., Lino, Y., Furuhata, K., Shimoda, C., and Yamamoto, M., (1988). The *S. pombe mei2* gene encoding a crucial molecule for commitment to meiosis is under the regulation of cAMP. *EMBO Journal* **7**, 761 – 767.

Watanabe, Y. and Yamamoto, M., (1994). *S. pombe mei2*$^{+}$ encodes an RNA-binding protein essential for premeiotic DNA synthesis and meiosis I, which cooperates with a novel RNA species meiRNA. *Cell* **78**, 487 – 498.

Watanabe, Y., Shinozaki-Yabana, S., Chikashige, Y., Hiraoka, Y. and Yamamoto, M., (1997). Phosphorylation of RNA-binding protein controls cell cycle switch from mitotic to meiosis in fission yeast. *Nature* **386**, 187 – 190.

Welcome to the TAP method home page. http://www-db.embl-heidelberg.de/jss/servlet/de.embl.bk.wwwTools.GroupLeftEMBL/ExternalInfo/seraphin/TAP.html

Yamamoto, M., (1996). The molecular control mechanisms of meiosis in fission yeast. *Trends in Biochemical Sciences* **21**, 18 – 22.

Yamashita, A., Watanabe, Y., Nukina, N. and Yamamoto, M., (1998). RNA-assisted nuclear transport of the meiotic regulator Mei2p in fission yeast. *Cell* **95**, 115 – 123.

Yu, L. P., Simon, E. J., Trotochaud, A. E. and Clark, S. E., (2000). *POLTERGEIST* functions to regulate meristem development downstream of the *CLAVATA* loci. *Development* **127**, 1661 – 1670.

Zuo, J., Niu, Q.-W., Nishizawa, N., Wu, Y., Kost, B. and Chua, N.-H., (2000). KORRIGAN, an *Arabidopsis* endo-1,4-β-glucanase, localizes to the cell plate by polarized targeting and is essential for cytokinesis. *Plant Cell* **12**, 1137 – 1152.

APPENDIX 1 GENOTYPES OF YEAST STRAINS

PJ69-4a: ***MATa***, *trp1-90, leu2-3, 112, ura 3-52, his3-200, gal4Δ, gal80Δ, GAL-ADE2, LYS2::GAL1-HIS3, met2::GAL1-lacZ*

PJ69-4α: ***MATα***, *trp1-901, leu2-3,112, ura 3-52, his3-200, gal4Δ, gal80Δ, GAL-ADE2, LYS2::GAL1-HIS3, met2::GAL1-lacZ*

Y190: ***MATa***, *ura3-52, his3-200, lys2-801, ade2-101, trp1-901, leu2-3, 112, gal4D, gal80D, cyh^{r}2, LYS2::GAL1$_{UAS}$-HIS3$_{TATA}$-HIS3, URA3::GAL1$_{UAS}$-GAL1$_{TATA}$-lacZ*

CG-1945: ***MATa***, *ura3-52, his3-200, lys2-801, ade2-101, trp1-901, leu2-3, 112, gal4-542, gal80-538, cyh^{r}2, LYS2::GAL1$_{UAS}$-GAL1$_{TATA}$-HIS3, URA3::GAL4$_{17\text{-}mers(x3)}$-Cyc1$_{TATA}$-lacZ*

332: ***MATa***, *leu2-3, 112, gal1, trp1-289, ura3-52, his7 pep4-3 prb1-1122*

APPENDIX 2 SOLUTION PAGES

Media and Solutions for *E. coli*

Luria broth (LB)

Tryptone (1%, w/v)	10 g
Bacto-yeast extract (0.5%, w/v)	5 g
Sodium chloride (1%, w/v)	10 g
Bacto-agar (1.5%, w/v)	15 g
MilliQ water	1 L

Adjust pH to 7.0 with 10 N NaOH.

Autoclave for 15 minutes at 121^{0}C and 15 lb/sq.

SOC medium

Tryptone (2%, w/v)	5 g
Bacto-yeast extract (0.5%, w/v)	2.5 g
Sodium chloride (10 mM)	0.29 g
Potassium chloride (2.5 mM)	0.093 g
MilliQ water	0.5 L

Adjust pH to 6.8 – 7.0 with NaOH

Autoclave for 15 minutes at 121^{0}C and 15 lb/sq.

Cool down the medium to room temperature, then add 5 mL of 1M $MgCl_2$ and 1M $MgSO_4$ solution and 5 mL of 2M glucose solution. Filter-sterilise using a 0.2-μm filter

Terrific Broth (TB) medium

Tryptone	9.6 g
Bacto-yeast extract	19.2 g
Glycerol	3.2 mL

Make up to 720 mL with MilliQ water. Add 80 mL of sterile 0.17 M potassium phosphate buffer (Make 1.85 g KH_2PO_4 and 10 g K_2HPO_4 up to 80 mL MilliQ water. Autoclave for 15 minutes at 121°C and 15 lb/sq.) Autoclave TB medium for 15 minutes at 121°C and 15 lb/sq.

RF1 solution

Potassium chloride (100 mM)	1.86 g
Calcium chloride (10 mM)	0.37 g
Manganese chloride (50 mM)	2.47 g
Potassium acetate (30 mM)	0.74 g
Glycerol (15%, v/v)	37.5 mL
MilliQ water	250 mL

Adjust pH to 5.8 with glacial acetic acid. Filter-sterilise using a 0.2-μm filter.

RF2 solution

MOPS (10 mM)	0.52 g
Potassium chloride (10 mM)	0.19 g

Calcium chloride (75 mM)	2.76 g
Glycerol (15%, v/v)	37.5 mL
MilliQ water	250 mL

Adjust pH to 6.5 with NaOH. Filter-sterilise using a 0.2-μm filter.

STE (sodium chloride and TE) solution, pH 8.0

10 mM Tris.HCl (pH 8.0)

1 mM EDTA (pH 8.0)

100 mM sodium chloride

Autoclave for 15 minutes at 121^{0}C and 15 lb/sq.

STET buffer

100 mM sodium chloride

10 mM Tris.HCl (pH 8.0)

1 mM EDTA (pH 8.0)

0.25% (v/v) Trition X-100

Media and Solutions for *S. cerevisiae*

YPD (YEPD)

Bacto-yeast extract (1%, w/v)	10 g
Bacto-peptone (2%, w/v)	20 g
Bacto-agar (2%, w/v)	20 g
MilliQ water	900 mL

Autoclave for 15 minutes at 121°C and 15 lb/sq.

Add 100 mL of 20% (w/v) glucose solution (2%, w/v) to the sterile the medium.

YPAD

Bacto-yeast extract (1%, w/v)	10 g
Bacto-peptone (2%, w/v)	20 g
Bacto-agar (2%, w/v)	20 g
Adenine hemisulphate (0.004%, w/v, Sigma-Aldrich)	40 mg
MilliQ water	900 mL

Autoclave for 15 minutes at 121°C and 15 lb/sq.

Add 100 mL of 20% (w/v) glucose solution (2%, w/v) to the sterile medium.

Synthetic complete (SC) and drop-out media

Difco yeast nitrogen base without amino acids (0.67%, w/v)	6.7 g
Yeast synthetic drop-out meedia supplement without histidine, leucine, tryptophan and uracil (0.14%, w/v, Sigma-Aldrich)	1.4 g

Bacto-agar (2%, w/v)	20 g
MilliQ water	900 mL

Adjust the pH value to 5.6 with 10 N NaOH.

Autoclave for 15 minutes at 121^{0}C and 15 lb/sq.

Add 100 mL of 20% (w/v) glucose solution (2%, w/v) to the sterile medium.

X-gal (5-bromo-4-chloro-3-indolyl-β-D-galactose) indicator plates

Solution I:	10 x Phosphate-buffer stock solution	100 mL
	1000 x Mineral stock solution	1 mL
	Yeast synthetic drop-out meedia supplement without histidine, leucine, tryptophan and uracil (0.14%, w/v, Sigma-Aldrich)	1.4 g
	MilliQ water	450 mL
Solution II:	Bacto-agar	20 g
	MilliQ water	450 mL

Autoclave the solutions separately. Cool the solutions to 65^{0}C and add the following to Solution I:

20% (w/v) Glucose solution (2%, w/v)	10 mL
X-gal (20 mg/mL dissolved in dimethylformamide)	2 mL
100 x Vitamin stock solution	10 mL

10x Phosphate-buffer stock solution:	KH_2PO_4 (1 M)	136.1 g
	$(NH_4)_2SO_4$ (0.15 M)	19.8 g
	KOH (0.75 N)	42.1 g
	MilliQ water	1000 mL
	Adjust pH to 7 and autoclave.	
1000x Mineral stock solution:	$FeCl_3$ (2 mM)	32 mg

	$MgSO_4 7H_2O$ (0.8 M)	19.72 g
	MilliQ water	100 mL
	Autoclave for 15 minutes. Resuspend a fine yellow precipitate before use.	
100x Vitamin stock solution:	Thiamine (0.04 mg/mL)	4 mg
	Biotin (2 μg/mL)	0.2 mg
	Pyridoxine (0.04 mg/mL)	4 mg
	Inositol (0.2 mg/mL)	20 mg
	Pantothenic acid (0.04 mg/mL)	4 mg
	MilliQ water	100 mL
	Filter-sterilise using a 0.2-μm filter.	

Single-stranded carrier DNA (2 mg/mL)

Deoxyribonucleic acid sodium salt type III from salmon testes (Sigma-Aldrich)	200 mg
TE buffer (10 mM Tris.HCl, pH 8.0; 1.0 mM EDTA, pH 8.0)	100 mL

Dissolve DNA in TE buffer by mixing vigorously at 4°C overnight. Aliquot the DNA and store at –20°C. Boil DNA for 5 minutes and chill on ice before use.

1.0 M Lithium acetate stock solution

LiAc	10.2 g
MilliQ water	100 mL

Filter sterilise by using a 0.2-μm filter.

SCE solution

Sorbitol	182 g
Sodium citrate	29.4 g
di-Sodium EDTA	22.3 g

Adjust pH to 8.0 with sodium hydroxide pellets

Autoclave for 15 minutes at 121^{0}C and 15 lb/sq.

Media for *A. tumefaciens* and plants

YEB broth

Beef extract	5 g
Bacto-yeast extract	1 g
Bacto-peptone	5 g
$MgSO_4.7H_2O$	0.5 g
Sucrose	5 g
MilliQ water	1000 mL

Adjust pH to 7.3 with 10 N NaOH. Autoclave for 15 minutes.

Murashige and Skoog (1X) Medium

Micro elements:	$CoCl.6H_2O$	0.025 mg/L
	$CuSO_4.5H_2O$	0.025 mg/L
	FeNaEDTA	36.70 mg/L
	H_3BO_3	6.20 mg/L
	KI	0.83 mg/L

	$MnSO_4.H_2O$	16.90 mg/L
	$Na_2MoO_4.2H_2O$	0.25 mg/L
	$ZnSO_4.7H_2O$	8.60 mg/L
Macro elements:	$CaCl_2$	332.02 mg/L
	KH_2PO_4	170.00 mg/L
	KNO_3	1900.00 mg/L
	$MgSO_4$	180.54 mg/L
	NH_4NO_3	4302.09 mg/L
Vitamins:	Glucine	2 mg/L
	myo-inositol	100.00 mg/L
	Nicotinic acid	0.50 mg/L
	Pyridoxine HCl	0.50 mg/L
	Thiamine HCl	0.10 mg/L

APPENDIX 3 LISTS OF SUPPLIERS

Amersham Biosciences AB

SE-751 84 Uppsala

Sweden

Applied Biosystems

850 Lincoln Centre Drive

Foster City, CA 94494

USA

BD Biosciences Clontech

1020 East Meadow Circle

Palo Alto, CA 94303

USA

Bio-Rad Laboratories

1000 Alfred Nobel Crive

Hercules, CA 94547

USA

Invitrogen Life Technologies

Invitrogen Corporation

1600 Faraday Avenue

PO Box 6482

Calsbad, California 92008

USA

Qiagen GmbH

Max-Volmer-Straβe-4

40724 Hilden

Gemany

Roche Applied Science

Roche Diagnostics GmbH

Dept. GD-M

Sandhofer Str. 116

68298 Mannheim

Gemany

Sigma-Aldrich Co.

PO Box 14508

St Louis MO 63178

USA